UNIVERSITY OF CALIFORNIA, SAN DIEGO

Dynamics of nuclear envelope and nuclear pore complex formation

A dissertation submitted in partial satisfaction of the

requirements for the degree Doctor of Philosophy

in

Biology

by

Daniel J Anderson

Committee in charge:

Professor Martin Hetzer, Chair
Professor Donald Cleveland
Professor William McGinnis
Professor Kit Pogliano
Professor John Young

2008

The Dissertation of Daniel J Anderson is approved, and it is acceptable in quality and form for publication on microfilm and electronically:

_____

_____

_____

_____

_____
Chair

University of California, San Diego

2008

DEDICATION

I dedicate this thesis to my parent Emily and Glenn Vasey, who instilled a love of science in me from a young age, my brother Charlie Vesey, who has been a shining example of how to be an excellent biologist, and my girlfriend Anne Ruminski, who has been a constant supportive and loving presence through out my PhD education.

TABLE OF CONTENTS

LIST OF FIGURES

Chapter I

Chapter II

Chapter III

Chapter IV

Chapter V

LIST OF TABLES

Chapter III

ABBREVIATIONS IN USE

Abbreviation	Definition
~	approximately
>	greater than
<	less than
ATP	adenosine-5'-triphosphate
ATPγS	adenosine 5'-O-(3-thio)triphosphate
BAF	barrier to autointegration factor
DNA	Deoxyribonucleic acid
EM	electron microscopy
ER	endoplasmic reticulum
GFP	green fluorescent protein
GTP	guanosine-5'-triphosphate
GTPγS	guanosine 5'-(3-O-thio)triphosphate
HeLa	cell line derived from cervical cancer
HP1	heterochromatin Protein 1
INM	inner nuclear membrane
NE	nuclear envelope
NEBD	nuclear envelope breakdown
NLS	nuclear localization signal
NPC	nuclear pore complex
Nap	nucleoporin
ONM	outer nuclear membrane
PCR	polymerase chain reaction
RNA	ribonucleic acid
Rtn	Reticulon
siRNA	small interfering RNA
tdTomato	tandem-dimer Tomato
U2OS	human osteosarcoma cell line
WGA	wheat germ agglutinin

ACKNOWLEDGEMENTS

I've had the great fortune of being Martin Hetzer's first graduate student, giving me the chance to learn many aspects of being a biologist first-hand. Martin is a brilliant scientist who is always willing to discuss new ideas or confusing data. He taught me first had how to exploit the *Xenopus* egg extract nuclear reconstitution system in ways which have not previously been attempted. Martin has enduring patients with my dislecsic writing and constant questions. I feel true honored to have spent the last four years working in Martin's lab. My committee: Bill McGinnis, John Young, Kit Poliano, and Don Cleveland have all been supportive throughout me PhD education, pushing me to strive for excellence.

The members of the Hetzer labs have been friendly and supportive, always willing to discuss scientific ideas and methods as well as very giving with reagents. I want to specifically thank all the lab members for the very necessary proofreading and editing. Members of the Hetzer lab have also been great friends, I'm sure that I will miss the camaraderie that we all shared.

I want to acknowledge my parent: Emily Vesey, Glenn Vasey, Tom Anderson and Bernadette Anderson, who have truly supported my education. They have always encouraged my love of science and been a constant loving presence in my life. My brother, Charles Anderson, has always been my role model. He has always excelled to the highest lest in every academic endeavor, making me strive to emulate his success.

I met Anne Ruminski soon after starting my graduate education. Anne is a talented chemist who works with great diligence and passion. Our time together has

been a true highlight of the past four years. Anne is extremely supportive of my education and the love of my life. Other fiends I have made during my time at UCSD including members of the nacl running team and the UCSD triathlon team have allowed me to keep balance in my life. They are a great bunch of people who I am sure will remain life-long friends.

Chapter 1 is modified from the following publications.

Anderson DJ, Hetzer MW. 2008. Shaping the endoplasmic reticulum into the nuclear envelope (review). J Cell Sci.121(Pt 2):137-42.

Anderson DJ, Hetzer MW. 2008. The life cycle of the metazoan nuclear envelope (review) Curr Opin Cell Biol. doi:10.1016/j.ceb.2008.03.016

Both of these reviews were co-written by Marin Hetzer and myself.

Chapter 2, in full, consists of the following publication.

Anderson DJ, Hetzer MW. 2007. Nuclear envelope formation by chromatin-mediated reorganization of the endoplasmic reticulum. Nat Cell Biol. 10, 1160-6.

I was the primary researcher of these studies under the supervision and direction of Martin Hetzer. The manuscript was co-written by Martin Hetzer and myself.

Chapter 3, in full, consists of the following publication.

Anderson DJ, Hetzer MW. 2008. Morphological reshaping of the endoplasmic reticulum limits the rate for nuclear envelope formation in vivo. J Cell Biol. in press.

I was the primary researcher and author of these studies under the supervision and direction of Martin Hetzer.

Chapter 4, in full, consists of the following manuscript submitted for publication in *Science*

Jesse Vargas and I were the primary researchers and authors for these studies under the supervision and direction of Martin Hetzer. Joshua Hsia contributed the cloning of constructs used in this study.

Chapter 5 is modified from the following publication.

D'Angelo MA*, Anderson DJ*, Richard E, Hetzer MW. 2006. Nuclear pores form de novo from both sides of the nuclear envelope. Science 312, 440-3 (*co-first authors)

Maxi D'Angelo, Martin Hetzer and I were the primary researchers of these studies. Martin Hetzer was the primary author of this manuscript. Erin Richard was involved in cloning and protein purification for these studies.

VITA

EDUCATION

2008	Ph.D., Biology, University of California, San Diego
2004	B.S., Biology, University of Pittsburgh
2000	High school diploma, JP McCaskey High School Lancaster, PA

WORK EXPERIENCE

1999-2000	Research Assistant, University of Pennsylvania
2000-2004	Research Assistant, University of Pittsburgh

PUBLICATIONS

Sproul LR**, Anderson DJ**, Mackey AT, Saunders WS, Gilbert SP. 2005. Cik1 targets the minus-end kinesin depolymerase kar3 to microtubule plus ends. Curr Biol 15, 1420-7.

D'Angelo MA*, **Anderson DJ***, Richard E, Hetzer MW. 2006. Nuclear pores form de novo from both sides of the nuclear envelope. Science 312, 440-3 (* co-first authors)

Anderson DJ, Hetzer MW. 2007. Nuclear envelope formation by chromatin-mediated reorganization of the endoplasmic reticulum. Nat Cell Biol. 10, 1160-6.

Anderson DJ, Hetzer MW. 2008. Shaping the endoplasmic reticulum into the nuclear envelope (review). J Cell Sci.121(Pt 2):137-42.

Anderson DJ, Hetzer MW. 2008. The life cycle of the metazoan nuclear envelope (review) Curr Opin Cell Biol. doi:10.1016/j.ceb.2008.03.016

Anderson DJ, Hetzer MW. 2008. Morphological reshaping of the endoplasmic reticulum limits the rate for nuclear envelope formation *in vivo*. J Cell Biol. 182(5):911-24.

Anderson DJ*, Vargas, JA*, Hsiao JP, Hetzer MW. 2008 Nuclear envelope proteins act redundantly to promote nuclear membrane formation. in preparation. (*co-first authors)

TEACHING AND MENTORSHIP

Teaching assistant to Dr Lara Sowal, Biochemical Techniques Laboratory, University of California San Diego, Winter 2006.

Teaching assistant to Dr Yemen Zou, Cellular Biology Lecture, University of California San Diego, Spring 2007.

Mentor to Joshua Hsiao as part of the Salk High School Summer Enrichment Program, Summer 2007 and Summer 2008.

Mentor to rotation student Mira Chaurushiya, Winter 2006.

Mentor to rotation student Jesse Vargas, Spring 2008.

Mentor to rotation student Russel DeKelver, Fall 2008.

FIELDS OF STUDY

Major Field: Biology

Studies in Cellular and Molecular Biology
Professor Martin Hetzer
The Salk Institute for Biological Studies

Studies in Biophysics and Cellular Biology
Professor Susan Gilbert
University of Pittsburgh

Studies in Developmental and Molecular Biology
Professor Peter Klein
University of Pennsylvania

ABSTRACT OF THE DISSERTATION

Dynamics of nuclear envelope of nuclear pore complex formation

by

Daniel J Anderson

Doctor of Philosophy in Biology

University of California, San Diego, 2008

Professor Martin Hetzer, Chair

The nucleus is in many ways the centerpiece of the eukaryotic cell, as it houses the genome and is the primary site of gene regulation. Nuclear enclosure is achieved by the double lipid bilayer named the nuclear envelope (NE). The outer membrane of the NE is connected and continuous with the endoplasmic reticulum (ER). The inner membrane of the NE attaches to chromatin and a meshwork of intermediate filaments called the nuclear lamina though NE-specific integral membrane proteins. Transport between the cytoplasm and nucleoplasm is mediated by nuclear pore complexes, multi-protein assemblies that are present where of the NE where the outer and inner membranes are connected. In metazoans, the nuclear envelope is broken down during mitosis to allow for cytoplasm spindle formation and segregation the NE materials into the daughter cells. At the beginning of my thesis the fate of NE components

during cell division and the mechanism of nuclear reformation have been controversial, and it was unclear whether the NE is broken into vesicles or absorbed into the ER during mitosis.

The main focus of this thesis was to characterize NE formation at the end of open mitosis. We determine that the network of ER tubules directly contributes to nuclear membrane formation in a fusion independent mechanism. A role for the ER shaping protein family of Reticulons as a negative regulator of NE formation was also characterized. A model was developed where transmembrane proteins of the NE target and reshape ER membranes around chromatin during nuclear assembly. This model was supported be a detailed kinetic analysis of nuclear assembly in cells where protein expression levels of candidate proteins were changed. Together these studies clarify the mechanism of how the nuclear membrane encloses the chromatin mass at the end of cell division.

CHAPTER I

Introduction

Introduction

A central trait of eukaryotic cells is the physical separation of the nuclear genome from the cytoplasm by the nuclear envelope (NE). This barrier is composed of two spheroid membrane sheets, the inner and outer nuclear membranes (INM and ONM), which are evenly separated by ~ 50 nm, generating the pronuclear space [1, 2]. The INM and ONM are connected at numerous sites, where aqueous channels form between the nucleoplasm and the cytoplasm. These channels are occupied by nuclear pore complexes (NPCs), large protein assemblies that mediate all transport across the NE [3-7].

NPCs are made up of multiple copies of ~30 unique proteins called nucleoporins. This aqueous channels are the exclusive sites of nucleo-cytoplamsic transport [8]. NPCs form a hollow cylinder with nucleoplasmic and cytoplamsic filamentous attachments that together form a transport channel across the NE. Although NPCs are membrane embedded, only three transmembrane nucleoporins have been identified [9] [10] [11].

The NE forms a continuous membrane system with the ER network (Fig. 1, prophase), which allows molecules to diffuse freely between the pronuclear space and the ER lumen [12]. The functional relationship between the ONM and the rough ER becomes obvious when visualized at the ultra structural level, ribosomes covering both membranes [13, 14]. Despite the lipid continuity between the NE and ER, both the ONM and INM are specialized domains that contain specific integral membrane proteins that are not abundant in ER cisternae. For instance, proteins of the nesprin

family specifically localize to the ONM and interact with components of the cytoskeleton and Sun-domain containing INM proteins [15-17]. The INM contains many integral membrane proteins that provide binding sites for chromatin or the lamina, a protein meshwork that provides structural integrity to the nucleus [18, 19] [20-22]. A recent study identified >60 NE transmembrane proteins [23]. Although most of these remain uncharacterized, many of those analyzed have been shown to interact with chromatin and/or the nuclear lamina [24]. This suggests NE transmembrane proteins may play a vital role in chromatin organization. Furthermore, recent studies suggest that the interactions between the NE and chromatin might regulate gene expression [25, 26]. The importance of the NE for cell function is further highlighted by numerous human diseases [18], caused by mutations in NE proteins or lamins [27-31]. This novel class of genetic disorders, referred to as laminopathies or 'nuclear envelopathies', include muscular dystrophies, neurodegenerative diseases and progeria [19, 32-34].

The overall topology of the NE is evolutionarily conserved; however, different mechanisms have evolved to propagate the nucleus to the daughter cells. In yeasts, the NE is preserved during cell division, and the mitotic spindle forms within the nucleus. After chromosome segregation, the nucleus is divided into two daughter nuclei by a poorly understood fission process [35]. In striking contrast, the nuclear membrane of metazoa completely disassembles at the prophase-metaphase transition to allow cytoplasmic microtubules of the mitotic spindle to gain access to condensing chromosomes. Such 'open' mitoses require NE reformation after chromosome

segregation [35]. This structural change of nuclear membrane is contrasted by the ER network, which remains intact throughout mitosis. Between these extreme cases of open and closed mitosis lies a continuum of mechanisms in which the NE becomes partially permeable [36, 37].

Nuclear envelope breakdown

Nuclear envelope breakdown (NEBD) marks the entry into mitosis and precedes the formation of the mitotic spindle apparatus. NEBD appears to be regulated at several levels (Figure 1, pro-metaphase). In Drosophila embryos and starfish acolytes, NEBD is triggered by NPC disassembly [38]. A crucial event in the disassembly is phosphorylation of NE components by several kinases such as Cdk1, PKC, NIMA and Aurora A [39]. These kinases might be involved in disrupting protein-protein interactions and/or in the activation of factors involved in NEBD. Recently, RanGTP, a small GTPase known for its functions in nuclear transport, nuclear formation and spindle assembly [40], has been shown to be involved in NEBD, presumably by either sequestering NE components through Importin β or by regulating microtubule dynamics. The latter view would be consistent with dynein-dependent processes known to rupture the NE by mechanical forces generated by interactions of microtubules with the NE and lamina [41].

Several nucleoporins are actively involved in NEBD. For example, recent data in C. elegans and egg extracts point to a strong, yet non-essential, role of the trans-membrane nucleoporin gp210, which is enriched in its phosphorylated form at the NE

just before NEBD occurs [42]. The mechanism of how gp210 triggers disassembly of NPCs the lamina remains to be analyzed.

Additionally, depletion of Nup153 from extracts inhibits nuclear envelope breakdown (NEBD) during mitosis. Nup153 was shown to recruit the COPI complex, which mediates retrograde transport from the Golgi to the ER, to the nuclear envelope [43]. A direct role of the COPI complex in this process was further supported by antibodies against β-COP which inhibited NEBD [43]. What role the COPI complex plays in this process remains to be analyzed.

Similar to other NE components, the lamina is disassembled by Cdk1 mediated hyper-phosphorylation [44-46]. While the majority of lamin B is dispersed in the mitotic cytosol, a fraction is associated with the mitotic spindle matrix. Together with the relocation of Nup358 and the Nup107/160 to kinetochores [47, 48], these findings support the emerging theme that many NE proteins have dual functions in interphase and mitosis. Although the several mechanisms of NEBD are now well characterize, less in know about the fate of nuclear membranes after NEBD and the process of NE reformation at the end of cell division.

Models of open mitosis

At the onset of my thesis research two conflicting models were present to explain the fate of membrane components of the NE during metazoan open mitosis. In one model, it was suggested that the NE breaks down into distinct vesicles, separate from the mitotic ER [49]. These vesicles were proposed to target to chromatin during

anaphase and fuse via an uncharacterized process. In an alternative model, the NE retracts into the connected mitotic ER, which must then be targeted and transformed in shape to generate daughter Nest [50].

Vesicle model

Evidence for the "vesicle" model was compelling, mainly being drawn from biochemical analysis of in vitro nuclear reconstitution and electron microscopic analyses. *Xenopus* eggs are massive cells with stockpiles of materials required for the large number of nuclei formed during the proliferative stage of embryogenesis. For this reason, when *Xenopus* eggs are fractionated, isolated membrane and cytosol are well suited for *in vitro* nuclear reconstitution [51, 52]. In biochemical characterization of membrane vesicles isolated from miotically arrested Xenopus eggs were separated based on density. Certain density fractions of vesicles were enriched in NE components and specifically promoted *in vitro* nuclear assembly [53-55]. Importantly, a different population of membrane vesicles was found to contribute to the cytoplasmic ER. These biochemical characterizations of membranes fractionated from mitotically arrested eggs provided strong evidence supporting the vesicle model of NE formation. Further evidence supporting this model was gathered by microscopic analysis of intermediates of *in vitro* reconstituted nuclei. Membrane vesicles were observed to target and fuse on the surface of chromatin during nuclear assembly [56]. This vesicle fusion, and therefore nuclear assembly, was inhibited by the addition of either GTPγS or ATPγS, non-hydrolysable NTP analogs [57].

Additionally, the AAA-ATPase p97 was implicated in the process, suggesting that nuclear formation might involve a complex set of membrane fusion and reshaping steps [58].

A third line of evidence supporting the vesicle model came from electron microscopic analysis [59] [60]. During NE formation membrane vesicles were often found bound to the surface of chromatin. These imaging experiments provided *in vivo* evidence for the model where vesicle fusion mediates NE formation at the end of cell division.

ER absorption Model

Although compelling data supported the model where the NE resides in vesicles during cell division, several lines of evidence pointed to a different scenario where the nuclear membrane is absorbed into the ER during NEBD. In such a model ER tubules would then target to the segregated chromosomes and expand to enclose the daughter nuclei. Such a model was first suggested when integral membrane proteins of the INM were found to co localize with protein of the ER in mitotic cells as judged by immunofluorescence [61]. Addition support for the ER absorption model was generated when INM proteins such as lamin B receptor was fused to green fluorescent protein and imaged live in cells undergoing cell division [50]. Such analyses lead to the observation that the localization pattern of such INM proteins was very similar to that of membrane proteins of the ER, suggesting that these NE-components freely diffuse throughout the mitotic ER.

When intermediate structures of the forming NE were analyzed using the *Xenopus* nuclear reconstitution system a dense network of tubules form prior to full membrane enclosure [58]. This network is similar in conformation to that of tubular components of the peripheral interphase ER. These data suggest that the vesicle fusion that is required for *in vitro* nuclear reconstitution might simply be a consequence of the need to reassemble the tubular ER, which is heavily fragmented during cell fractionation. Testing these hypotheses is a main focus of chapter 1 of this thesis.

The NE between metaphase and telophase

Between prophase and early anaphase, during which time chromosomes condense, align in the metaphase plate and segregate, chromatin is essentially free of membranes (Figure 1, Metaphase) [50, 62]. Also, the majority of soluble nucleoporins are thought to be distributed throughout the cytoplasm. In late anaphase, membranes start to associate with chromatin by a poorly understood mechanism (Figure 1, anaphase).

How are the membranes targeted to chromatin? A model that we developed during my thesis proposes predicts that integral membrane proteins with DNA-binding capacity are recruited to chromatin. This notion is consistent with recent findings that DNA-binding activity of some INM proteins is required for NE formation in vitro [63]. Furthermore, membrane sheets formed efficiently on protein-free immobilized DNA isolated membranes [62]. Additionally, several INM proteins bind to chromatin

constituents such as heterochromatin protein 1 (HP1) or barrier-to-autointegration factor (BAF) [64] and these interactions have been indirectly implicated in NE assembly. For example, two studies have demonstrated that the integral INM protein LBR, that binds to HP1, is required for targeting and anchoring NE membranes to chromatin *in vitro* [65, 66]. Adding excess BAF to an in vitro nuclear assembly reaction leads to chromatin condensation and inhibition of NE formation [64]. Recent analysis of BAF and it's kinase Vrk suggest that BAF plays a direct role in NE formation by recruiting LEM domain proteins to chromatin [67]. BAF phosphorylation reduces chromatin binding and interactions with LEM domain proteins such as emerin [68, 69]. In summary, NE formation is likely to involve a complex interplay of trans-membrane NE proteins with decondensing chromatin.

While the above studies are consistent with the idea that NE formation occurs by chromatin-mediated reshaping of the ER, a different set of experimental data suggest that the NE forms by the fusion of vesicles. Early results in *Xenopus* have shown that in vitro nuclear assembly initiated from fragmented ER vesicles is blocked by GTPγS [57] [70]. However, these findings did not discriminate between fusion events that are involved in ER reconstitution or NE assembly. When ER is preformed, NE formation occurs in the presence of GTPγS and ATPγS, suggesting that membrane fusion is not required to form flat sheets [62]. Similarly, a recently observed role of SNARE proteins in NE formation could be an indirect effect of blocked ER reconstitution [71].

Simultaneously with membrane coating of chromatin, NPCs are reassembled from disassembled precursors in late anaphase/telophase. Several nucleoporins have been shown to be essential for pore assembly [3]. Most notably, depletion of the Nup107/160 complex, results in NPC-free nuclear membranes. In vertebrates only two out of the three transmembrane nucleoporins seem to be involved in NE formation, Ndc1 and Pom121 [9]. Their exact role is unknown, but an interesting link between Pom121 and the Nup107/160 complex has been made. Nuclear membrane formation might actually be linked to pore assembly by a poorly understood POM121-Nup107/160 complex membrane assembly checkpoint [72]. Interestingly, Nup133 a member of the Nup107/160 complex has been identified as containing an ALPS-like motif, which contains amphipathic alpha-helical domains that have been shown to act as a membrane curvature sensor in vitro [73] it is likely that this domain is required for targeting of the Nup107/160 complex to membranes during NE formation.

While the targeting of soluble nucleoporins to membranes and chromatin during NE formation is still not fully understood, some progress has been made in determining how the Nup107/160 complex is recruited to chromatin. Mel-28/ELYS was identified in a screen in C. elegans for factors involved in pronuclear formation. In the absence of Mel-28/ELYS, the Nup107/160 complex is no longer recruited to chromatin [74, 75]. Mel-28/ELYS contains an AT-hook domain and the simplest model is that Mel-28/ELYS binds directly to DNA and recruits Nup107/160. RanGTP stimulates Mel-28/ELYS recruitment, re-emphasizing the crucial role of Ran in NE formation. Other nucleoporins have been implicated in pore assembly, but their exact

role remains to be determined. For instance, a complex of Nup53 and Nup155 has recently been shown to be essential for NE formation in nematodes and vertebrates [76, 77], however, how Nup53 coordinates interactions between chromatin, membranes and soluble Nup155 remains unclear.

The interphase nucleus

The NE is established as a closed membrane barrier at the end of cell division, re-establishing the nuclear compartment by selective nuclear transport, i.e. unmixing of cytosolic and nucleoplasmic components that were distributed during mitosis. Relatively little is known about this transition and questions such as when do pores become active for transport remain to be analyzed. However, it is clear that even after its formation, the NE undergoes a series of changes necessary for cell cycle progression and transcription. These steps include the assembly of a lamina, duplication of pore number, and NE expansion. A recently uncovered interaction between the nucleoporins ELYS and Mcm2-7 replication licensing proteins suggest a direct link between pore assembly and DNA metabolism [78].

A-type lamins are present only in a subset of cell types and the majority of these lamins are imported into the nucleus in G1 [79, 80]. Nuclei lacking lamins also mislocalize some INM proteins [81] and exhibit NPC clustering [82]. In cells where assembly of B-type lamins was inhibited NE formation still occurred but, interestingly, apoptosis rates increased dramatically [83, 84]. The lack of effect on NE assembly observed in these studies is consistent with the finding that B-type lamins

accumulate at the nuclear periphery after a closed NE is formed [85, 86]. It is therefore clear that lamins are important for nuclear integrity and function, most directly demonstrated by the repression of artificially repositioned genes to the lamina [87].

As cells grow and prepare to divide, the number of NPCs doubles and the NE surface increases substantially [88]. How membranes feed into the expanding NE had not been previously addressed and is characterized in chapters 2 and 3 of this thesis. The insertion of existing pores during interphase was proposed to occur via budding from existing NPCs [89], however our investigation into interphase NPC formation reveals *de novo* assembly into the intact NE (Chapter 5).

Growth of the INM requires passage of membrane components through the fusion sites with the ONM at the NPCs. The current view is that INM proteins are retained once they reach the INM by interactions with either the lamina or chromatin. How INM proteins are targeted in metazoa is less clear. One model suggested that ATP-driven changes in nucleoporin interactions might allow membrane proteins to travel across the NPC [90]. In yeast, integral INM proteins have been shown to directly interact with specific nucleoporins and importin α and β to promote their movement past the NPC [91].

Summary

In this thesis I examined several aspects related to the dynamics of the NE and NPCs during cell cycle progression. Chapters 2 through 4 cover various aspects of NE formation at the end of cell division, including fate of the nuclear membranes during

mitosis, the structural changes required for closure of daughter nuclei, and identification of proteins that involved to targeting and reshaping of membranes during nuclear assembly. Additionally, an intimate connection between the peripheral ER and nuclear expansion is uncovered in chapters 2 and 3. Chapter 4 characterizes how NPCs are inserted into the enclosed NE during interphase. Organelle homeostasis is a vital regulatory process, which is exemplified in proliferative cells. The nucleus is a central example of such processes, better understanding the mechanisms of nuclear homeostasis and mitotic dynamics will provide advancement in our general knowledge of cell function.

Acknowledgements

Chapter 1 is modified from the following publications.

Anderson DJ, Hetzer MW. 2008. Shaping the endoplasmic reticulum into the nuclear envelope (review). J Cell Sci.121(Pt 2):137-42.

Anderson DJ, Hetzer MW. 2008. The life cycle of the metazoan nuclear envelope (review) Curr Opin Cell Biol. doi:10.1016/j.ceb.2008.03.016

Both of these reviews were co-written by Marin Hetzer and myself.

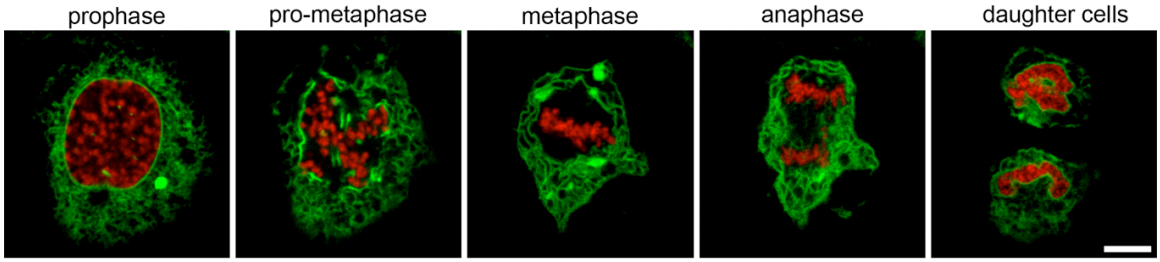

Chapter I Figure 1
Metazoan cells undergo open mitosis. U2OS cells were transfected with GFP-Sec61(first 65 aa) and H2B-tdTomato and imaged in real time using spinning disk confocal microscopy throughout mitosis. Following chromatin condensation (prophase) the NE is torn apart and absorbed into the ER (pro-metaphase). When the chromosomes align on the metaphase plate there is little or no contact between chromosomes and the membranes of the ER (metaphase). The tubule tips of the ER first contact the chromatin during chromosome segregation (anaphase). The NE is reformed during cytokenisis (daughter cells). Scale bar, 10 μm.

CHAPTER II

Nuclear Envelope Formation by Chromatin-mediated Reorganization of the Endoplasmic Reticulum

Abstract

The formation of the nuclear envelope (NE) around chromatin is a major membrane-remodeling event occurring during cell division of metazoa. It is unclear whether the nuclear membrane reforms by the fusion of NE fragments or if it re-emerges from an intact tubular network of the endoplasmic reticulum (ER). Here we show that NE formation and expansion requires a tubular ER network and occurs efficiently in the presence of the membrane fusion inhibitor GTPγS. Chromatin recruitment of membranes, which is initiated by tubule end binding followed by the formation, expansion and sealing of flat membrane sheets is mediated by DNA-binding proteins residing in the ER. Thus, chromatin plays an active role in the reshaping of the ER during NE formation.

Introduction

The nuclear envelope (NE) is a double membrane that compartmentalizes eukaryotic cells into nucleoplasm and cytoplasm. The outer (ONM) and the inner nuclear membranes (INM), which are fused at sites of nuclear pore insertion, form a continuous membrane system with the endoplasmic reticulum (ER) [3, 92, 93]. In metazoa, the NE undergoes a cycle of disassembly and reformation during cell division while the ER network remains intact [3, 50, 93-96]. Evidence from live cell imaging suggests that NE components are redistributed into the ER implying that ER tubules might be the precursor membrane to rebuild the NE [50]. However, the

mechanisms that would target the ER to chromatin and reorganize membrane tubules into the flat NE sheets are unknown.

Nuclear Assembly requires an intact ER network and is insensitive to GTPγS or ATPγS

Most of our knowledge about NE formation is derived from cell-free reconstitution systems [49]. We chose to study the reorganization of the ER into the NE on the surface of chromatin using fractionated Xenopus eggs [97], which have been shown to faithfully recapitulate various steps of nuclear assembly [3, 5, 98]. During cell fractionation into cytosol and ER membranes[70] the fragile ER network was heavily fragmented (Fig. 1a), which made it difficult to discriminate between the molecular requirements of ER reconstitution and NE formation. To overcome this limitation, we preformed an intact ER by incubating cytosol with fluorescently labeled membranes for *20* min and then added sperm chromatin to initiate nuclear assembly (Fig. 1a and ref. 10). We found that membrane tubules rapidly covered the chromatin surface (Fig. 1a) and that the chromatin-associated network stained with an antibody against reticulon 4a (Rtn4a), a characteristic protein of tubular ER (Fig. 2a). After 60 min incubation, intact nuclei with a closed NE formed (Fig. 1a). This demonstrates that NE formation from intact ER can be recapitulated in vitro.

Using this experimental strategy we first asked if NE formation is sensitive to the non-hydrolysable NTP analogs GTPγS and ATPγS. While GTPγS has been shown to prevent ER reconstitution in vitro by blocking membrane fusion (Fig. 2b), ATPγS

specifically inhibits ER tubule formation [70]. When sperm chromatin was added to reconstituted ER, nuclear assembly occurred with similar efficiency in the absence or presence of 4 mM GTPγS and ATPγS. We noticed that GTPγS nuclei were smaller due to a block in nuclear transport, which is required for nuclear expansion[99] (Fig. 1b, c). Importantly, the nuclei formed in the presence of GTPγS and ATPγS were intact, i.e. they had acquired a closed NE, because they excluded fluorescently labeled streptavidin, an inert protein that cannot diffuse across an intact NE [75] (Fig. 1c). These results were surprising since it had been shown that NE formation in vitro is strongly inhibited by GTPγS and ATPγS [57, 70, 100]. However, our results suggest that the inhibition observed in previous studies was due to a block in reconstituting a tubular network from fragmented ER membranes. Consistent with this idea, we found that both 4 mM GTPγS and ATPγS efficiently blocked NE formation when initiated from fragmented membranes, as judged by the failure to exclude streptavidin (Fig. 1c, Fig. 2b). Unfused membrane fragments were visible on the chromatin surface, which did not stain with wheat germ agglutinin, a lectin that binds to nuclear pores (Fig. 1b). We therefore conclude that NE formation in vitro requires the generation of an intact ER, which involves homotypic membrane fusion. However, the formation of the NE from an intact ER is insensitive to GTPγS and ATPγS.

It was possible that in contrast to vesicle fusion, ER tubules/sheets could still fuse [101] in the presence of GTPγS, explaining why NE formation from the ER was insensitive to GTPγS. To test this, we assembled ER, labeled separately either with green ($DiOC_{16}$) or red ($DiIC_{18}$) lipophilic dyes, and combined the two reactions in the

absence or presence of 4 mM GTPγS and ATPγS. The fusion of the two ER populations was specifically blocked by GTPγS but not ATPγS (Fig. 2c). Thus, under these experimental conditions GTPγS acts as a general inhibitor of ER membrane fusion. Taken together these results suggest that NE formation occurs either by GTPγS-insensitive fusion events or by fusion independent reorganization of the ER.

Reticulons are present in membranes that mediate nuclear assembly

One prediction from the latter hypothesis is that the topology of the tubular ER network is required for NE formation. Recently it was shown that the formation of the ER is mediated by reticulon Rtn4a [102]. Consistent with this report we found that antibodies against Rtn4a, but not Rtn2, blocked ER network formation (Fig. 2d). We incubated cytosol in the presence of anti-Rtn4a or anti-Rtn2, and added sperm chromatin. Closed NE formation was specifically inhibited by anti-Rtn4a. When anti-Rtn4 was added to preformed ER, NE formation occurred efficiently (Fig. 1d). Importantly, ER membranes could still fuse in the presence of anti-Rtn4 resulting in the formation of large vesicles[17, 23, 28]. Similar results were obtained by adding 4 mM ATPγS, which also blocks tubule formation [58, 70] but not membrane fusion (Fig. 1c, Fig. 2 b and c). These results suggest that the specific membrane topology of ER tubules is required for NE formation. Additionally, comparison of NE formation starting with either intact ER or ER fragments, revealed that ER preformation increased the rate of NE formation in vitro (Fig. 2e). One possible explanation for this

effect is that chromatin recruitment of NE components, such as the nucleoporin POM121, is more rapid from an intact ER network than from ER fragments (Fig. 2f).

NE-transmembrane proteins redistribute into the mitotic ER

One prediction form the in vitro studies is that membrane proteins of the NE are dispersed throughout the ER during mitosis in metazoa, similar to observed mitotic ER localization of the INM protein lamin B receptor [50]. To test this hypothesis we generated stable cell lines epressing GFP tagged versions of Sec61, an ER marker, and the two transmembrane nucleoporins POM121 and gp210. As expected, the two nucleoporins localized specifically to the NE during interphase, while Sec61 localized to the ER. When cells underwent mitosis all three proteins stained the mitotic ER network (Fig. 1e), suggesting that NE formation occurs from the tubular mitotic ER network in vitro and in vivo.

Tubule-end binding to chromatin intitiats nuclear membrane formation

To study the mechanism by which the ER is shaped into the NE we wanted to analyze this process by time-lapse microscopy. High-resolution live imaging attempts on sperm chromatin and live cells failed due to the highly condensed nature of sperm chromatin, the high density of mitotic ER and technical challenges such as focal drift during image acquisition caused by rapid chromatin decondensation (see Supplementary Information, Movie 4). To overcome these limitations we developed a novel NE formation assay which is based on the finding that functional nuclei can be

assembled around heterologous DNA [103]. We spotted 10 kb linear DNA, biotinylated on one end, onto streptavidin-coated glass (Fig. 2a). After addition of cytosol, the immobilized DNA assembled into a two-dimensional (2D) chromatin surface with a diameter of 800 ± 200 μm (Fig. 4a). When fluorescently labeled membranes were added, extensive membrane sheets formed specifically on the chromatin-covered surfaces (Fig. 3a). These membrane sheets were composed of two lipid bilayers into which NPCs had assembled as confirmed by transmission electron microscopy (Fig. 4b). Additionally, NPCs were visualized with fluorescently labeled Importin β, a nuclear transport receptor that stably associates with NPCs [99]. Pores also contained Tpr, a NE-specific nucleoporin [104], suggesting that the formed membranes are not annulate lamellae, NPC-containing ER cisternae [105] (Fig. 4b).

The ability to form NEs on immobilized 2D chromatin allowed us to monitor membrane dynamics on chromatin at high resolution using time-lapse confocal microscopy (Fig. 4c). When we started imaging immediately after addition of cytosol containing an intact ER network, we observed bright membrane dots of uniform size stably associating with chromatin (Fig. 3b). Three-dimensional (3D) reconstruction revealed that the observed dots did not correspond to vesicles but rather to tubule ends bound to chromatin (Fig. 3b). These 'anchored' tubules either bound laterally to chromatin or allowed the recruitment of additional ER tubules to the surface of chromatin, a result of tubules rapidly sliding along each other (Fig. 3b). The addition of nocodazole did not inhibit tubule binding, suggesting that microtubules are not required for NE formation in vitro (data not shown). Tethered tubules, which were at

first highly dynamic between a few stable interaction points, stabilized on the chromatin surface upon further incubation (Fig. 6b).

Since ER tubule end binding on chromatin has not been reported before, we wanted to analyze if similar interactions can occur on sperm chromatin. When cytosol with preformed ER was added to decondensed sperm chromatin [106], we observed the instantaneous tubule end binding from the surrounding ER (Fig. 3c). Consistent with the observations on 2D chromatin, these tubules bound laterally and rapidly immobilized the ER network on the chromatin surface (Fig. 3b). Importantly, a similar membrane conformation was observed in vivo. When ER tubules surrounding mitotic chromatin of NHI3T3 cells were stained with $DiOC_6$ or HeLa cells were transfected with Sec61-GFP and imaged by confocal microscopy, single membrane dots were visible on the surface of chromatin in anaphase, which after 3D reconstitutions of multiple z-sections were identified as tubule ends (Fig. 3d and data not shown). Furthermore, time-lapse microscopy of Sec61-GFP expressing HeLa cells revealed that NE formation was initiated by tubule end binding on telophase chromosomes (Fig. 4d). Taken together these results show that NE formation is initiated by ER tubule end binding and subsequent tethering of the ER network on chromatin in vitro and in vivo.

Once the ER was immobilized on 2D-chromatin, flat sheets formed by lateral growth and expanded steadily over time (Fig. 3e, f). Since individual membrane patches were always connected with each other and the surrounding ER via tubules, the flattening process reorganized patches into large membrane sheets, which

eventually sealed into a continuous NE (Fig. 4e). Importantly, during sheet formation we did not observe the fusion of tubules, which are immobilized at this stage, or additional recruitment of tubules. Therefore we conclude that sheet formation occurs by chromatin mediated membrane flattening. This explains why NE formation occurred efficiently in the presence of GTPγS or ATPγS (Fig. 1b). Taken together, these results suggest that the reorganization of the ER network is sufficient to form the NE. Merging membrane patches are molded around chromatin by continuous expansion but not membrane fusion. However, homotypic fusion events involved in ER maintenance are likely to be required when tubular connections between sheets break.

Nuclear membrane flattening can be mediated by direct DNA intearations

This raised the question of how the flattening of ER tubules into NE sheets is mediated? In a recent report, many NE proteins that are dispersed in the ER during mitosis have been shown to posses DNA-binding activity [63]. These findings prompted us to test if NE formation can occur on protein-free immobilized DNA. When an intact ER network was formed in the absence of cytosol [102] and added to a protein-free DNA area, NE formation occurred specifically on the DNA (Fig. 5a). We noticed that NE formation was more efficient on protein-free DNA in the absence of cytosol compared to reactions with cytosol or NE formation on pre-formed chromatin (Fig. 5b), suggesting that nucleosomes do not contribute to membrane recruitment in vitro. Additional evidence for the mechanistic role of DNA binding in ER

reorganization on chromatin was obtained by studying tubule alignment and sheet formation. When DNA was spotted at lower concentration (see Supplementary Information Fig. S3b), ER tubules failed to immobilize even during prolonged incubations when compared to control reactions with higher DNA concentrations. Furthermore, when excess 1 kbp dsDNA was added after the ER was bound to chromatin, flat sheet formation was inhibited (data not shown). ER interactions with chromatin were protein mediated since proteinase K treatment of membranes abolished DNA binding (Fig. 6a). Taken together, these results suggest the following model for NE formation. DNA-binding proteins residing in tubule ends initially bind to chromatin. Since the ER is a three-dimensional, highly dynamic network with tubules constantly sliding along each other [12], additional DNA-binding events are sufficient to stabilize tubules and to rapidly cover the chromatin surface with a membrane network. Additional tethering of DNA binding proteins results in tubules flattening and thereby merging of sheets resulting in a closed NE (Fig. 5c). Since the chromatin-bound sheets are connected via tubules with each other and the surrounding ER, lipids required for the NE are not limiting and do not necessitate a separate enzymatic fusion process. However, membrane fusion is required when ER is fragmented (e.g. during fractionation) or tubules break and membrane sheets become disconnected from the ER. Therefore, NE formation requires chromatin-mediated membrane flattening and the active maintenance of the ER by homotypic membrane fusion.

Nuclear expansion requires connection with the peripheral ER

Once nuclei are formed they grow in size and the NE expands [99]. It has been suggested that vesicle fusion is involved in this process [3, 107]. To test if the ER network is required for NE expansion or if vesicle fusion can account for the size increase, we mechanically fragmented the ER network by constant shaking (Fig. 7a). Vesicle fusion was not inhibited under these conditions since large vesicles were generated, which did not form when GTPγS was added (Fig. 7b). Nuclei were assembled for 60 min and then incubated for an additional 60 min in the absence or presence of mechanical stress (Fig. 7c). While the nuclei expanded dramatically in the control, physical disruption of the ER blocked NE growth. When mechanical stress was stopped the ER network recovered (Fig. 7c, d) and NE expanded, showing that the shearing forces did not inactivate the extracts. The nuclei incubated in constant mechanical stress imported fluorescently labeled BSA-NLS, excluded 70 kD dextran and inserted NPCs (Fig. 8a,b), further strengthening the idea that the observed block in expansion was due to disruption of the NE-ER connections and not due to compromised nuclear function or transport [99]. Consistent with these results, we have previously shown that NE expansion is blocked when the function of the AAA-ATPase p97, which is required for ER network maintenance in vitro, was impaired [58]. Taken together these results suggest that NE expansion requires an intact ER, which provides the lipids necessary to accommodate the increase in NE surface area.

Conclusion

In summary, we propose that the intrinsic capacity of the ER to form sheets [102] is utilized and coordinated by chromatin (i.e. accessible DNA in chromatin) to mediate the rapid conversion of the ER network into NE sheets. DNA-binding proteins, which are dispersed in the ER, target the membranes to chromatin and mediate NE sheet formation. Since DNA binding is a feature of many NE proteins and depletion of individual polypeptides failed to block NE formation this is likely a redundant process [63] (data not shown). Interestingly, the recruitment of the nucleoporins POM121 and Ndc1 correlates with the strength of their basic DNA binding domains [63] (data not shown). It remains to be determined if tubule end binding, alignment and sheet formation is mediated by multiple ER proteins with different DNA-binding affinities or whether structural elements in the ER lumen are needed to stabilize the NE sheets.

Our data also suggest that homotypic membrane fusion is not the prevalent mechanism of NE formation from an intact ER network, but required for ER reconstitution and maintenance. We cannot exclude the possibility that other membrane structures, such as mitotically generated COPI vesicles [43], fuse with the ER during NE formation. However, since the forming NE is continuous with the ER at all stages of nuclear assembly, we propose that the formation of membrane patches on chromatin, which are continuous with each other, and their chromatin-dependent expansion inevitably results in NE sheets. Therefore, an enzymatic machinery might not be required to reorganize the ER into the NE. In contrast, fusion of separated membrane units (e.g. fragmented ER or vesicles) requires a fusion machinery,

explaining the GTPγS sensitivity of ER reconstitution and other fusion processes. Interestingly, in the absence of RanGTP, a small GTPase required for NE formation[100], NE formation from intact ER occurred efficiently whereas ER fragments immobilized on chromatin did not fuse [100] (data not shown). Similarly, nuclear assembly was blocked when chromatin decondensation occurred in the presence of GTPγS, followed by the addition of intact ER (data not shown). This suggests that Ran, which is also involved in nuclear pore assembly [105], and potentially other GTPases might be involved in chromatin organization prior to NE formation.

Methods

Recombinant Proteins and Antibodies

Importin-β was purified as previously described [105]. Antibodies against Rtn2 and Rtn4 were used at 10μM for inhibition and at 0.5μM for immunofluorescence [102].

In Vitro Nuclear and ER Assembly

Xenopus egg extracts and sperm chromatin were prepared as previously described [100]. Membranes were stained with either $DiIC_{18}$ or $DiOC_6$ as previously described [58]. Nuclei were formed by either the classical method of combining fragmented ER membranes, cytosol, and sperm chromatin on ice; or by first reconstituting the ER network by mixing membranes with cytosol and incubating at

room temperature for 10-20 min, then carefully adding sperm chromatin to the intact ER network. Nuclear growth was monitored by measuring cross-sectional areas using Adobe® Photoshop® 7.0 and Microsoft® Excel® 2004. Nuclear exclusion experiments were carried-out by first de-condensing sperm chromatin with the addition of heat-inactivated cytosol, along with biotinylated histones. Sperm chromatin containing incorporated biotinylated histones was then combined with membranes and cytosol, Alexa Fluor® 568 conjugated streptavadin (Molecular Probes) was added at various points during nuclear assembly and rapidly fixed and quenched with 4% paraformaldehyde along with biotinylated WGA. ER was assembled with Xenopus egg extracts as previously described [70]. Intact ER network was pipetted with cutoff tips to reduce fragmentation. The ER network and nuclear assembly reactions were deliberately sheared by shaking in an orbital shaker at 900 rpm or pipetting 5 times. Import of BSA-NLS and exclusion of dextran were carried-out as previously described[100].

Real Time Imaging of Nuclear Assembly

Sperm chromatin was first de-condensed with heat-inactivated cytosol. 35mm culture dishes with a cover-slip insert (MatTek) were pre-coated with poly-L-lysine, de-condensed chromatin was then spotted on dishes and pelleted at 1000 g for 5 min. Pelleted chromatin was then stained with Syto® 62 (Molecular Probes) and time-lapse microscopy was performed at 25˚C with frames acquired every 2 sec. Pre-formed ER network was then added to capture the initial interactions of nuclear assembly. Two-

dimension nuclear assembly was carried-out using biotinylated dsDNA, which was prepared as previously described [108]. DNA was spotted on streptavadin-coated cover slips (Xenoprobe) and washed 3X with TE. Nuclear assembly reactions were performed in slide chambers of 10μl in volume on which the DNA-spotted cover slips were sealed. Time-lapse images were acquired and processed as previously described [99].

In vivo Cellular Imaging

NIH3T3 cells were grown asynchronously in DMED with 10% fetal calf serum at 37˚C in 10% CO_2 in Lab-Tek®II 8-chamber coverglass slides (Nalge Nunc). $DiOC_6$ was added to growth medium at 0.5μg/ml along with Hoechst 3222 at 1μg/ml. Cells were incubated for 10min then mitotic cells were imaged live with SP2 confocal microscope (Leica). Z-stacks were then analyzed in 3D using Imaris (Bitplane), in which representative 3D projections were generated.

ACKNOWLEDGEMENTS.

Antibodies against Rtn4a and Rtn2 were kindly provided by G. Voeltz and Tpr antibodies by V. Cordes. We thank members of our lab for helpful discussions and T. Hunter for critically reading the manuscript.

Chapter 2, in full, consists of the following publication.

Anderson DJ, Hetzer MW. 2007. Nuclear envelope formation by chromatin-mediated reorganization of the endoplasmic reticulum. Nat Cell Biol. 10, 1160-6.

I was the primary researcher of these studies under the supervision and direction of Martin Hetzer. The manuscript was co-written by Martin Hetzer and myself.

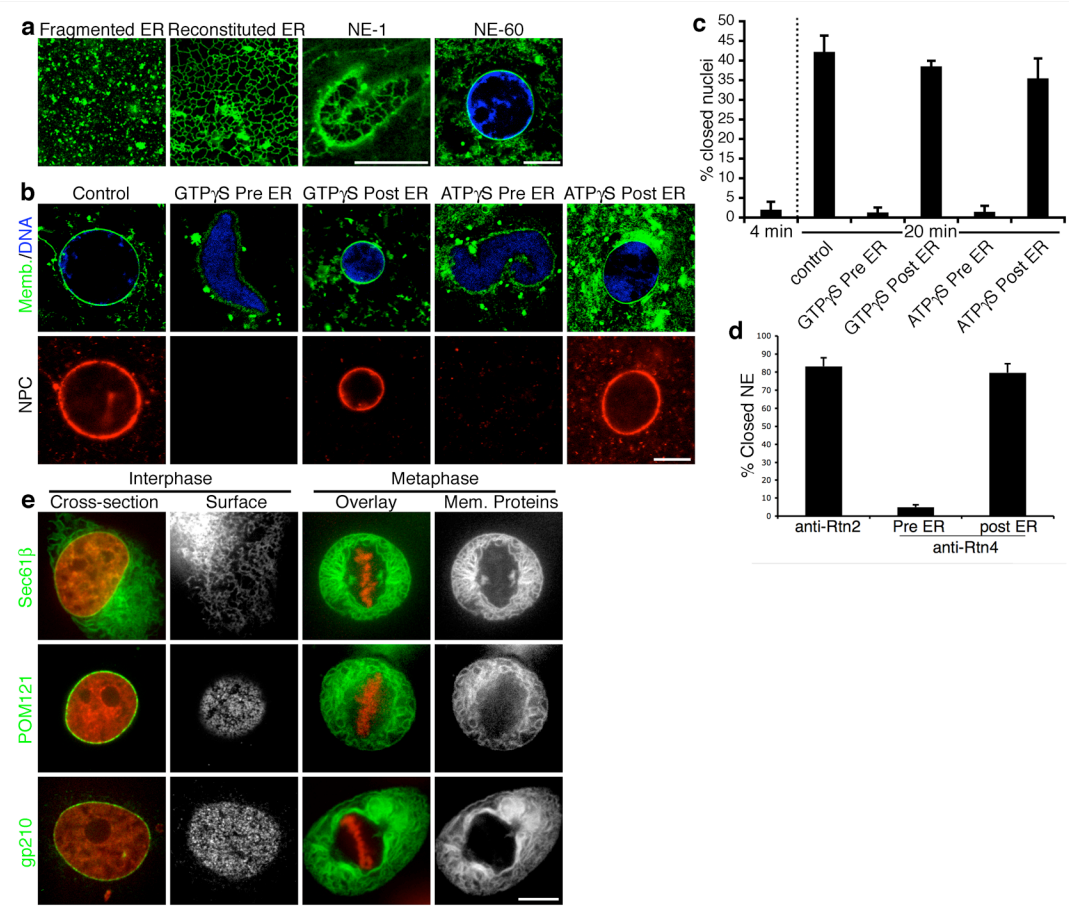

Chapter II Figure 1

The ER network is required for nuclear envelope formation.
(a) Fragmented ER membranes were stained with DiIC¬6 (green) and imaged at 4˚C using confocal microscopy. The ER network was reconstituted by incubating membranes with cytosol for 20 min at 25˚C. NE formation was induced by adding nucleoplasmin-decondensed sperm chromatin22, DNA was stained with Hoechst 3222 (blue) and imaged live after 1 min (NE-1) and 60 min (NE-60) incubations. (b) Nuclei were assembled as in (a) in the absence or presence of 4 mM GTPγS or ATPγS either before (Pre ER) or after ER reconstitution (Post ER) for 90 min. Before GTPγS was added, sperm chromatin was first decondensed in membrane free cytosol. Nuclear pores were stained with Alexafluor©568 conjugated WGA (red). (c) NEs were formed as described in (b) around sperm chromatin containing biotinylated histones14. After 4 min or 20 min, Alexafluor©568 conjugated streptavidin was added, which was excluded only when a closed NE had formed, n=60. (d) 10 µM anti-Rtn2 or anti-Rtn4 were added to nuclear assembly reactions either before or after ER formation and the percentage of closed nuclei was determined as described in (c) , n=100. (e) HeLa cells were co-transfected with histone H2B- tdTomato and GFP fused Sec61β (aa 1-65) and imaged live during interphase and mitosis. Additionally, HeLa cells stably expressing POM121-EGFP3 and gp210-EGFP3 were transfected with tdTomato H2B and imaged during interphase and mitosis. Scale bar, 10µm.

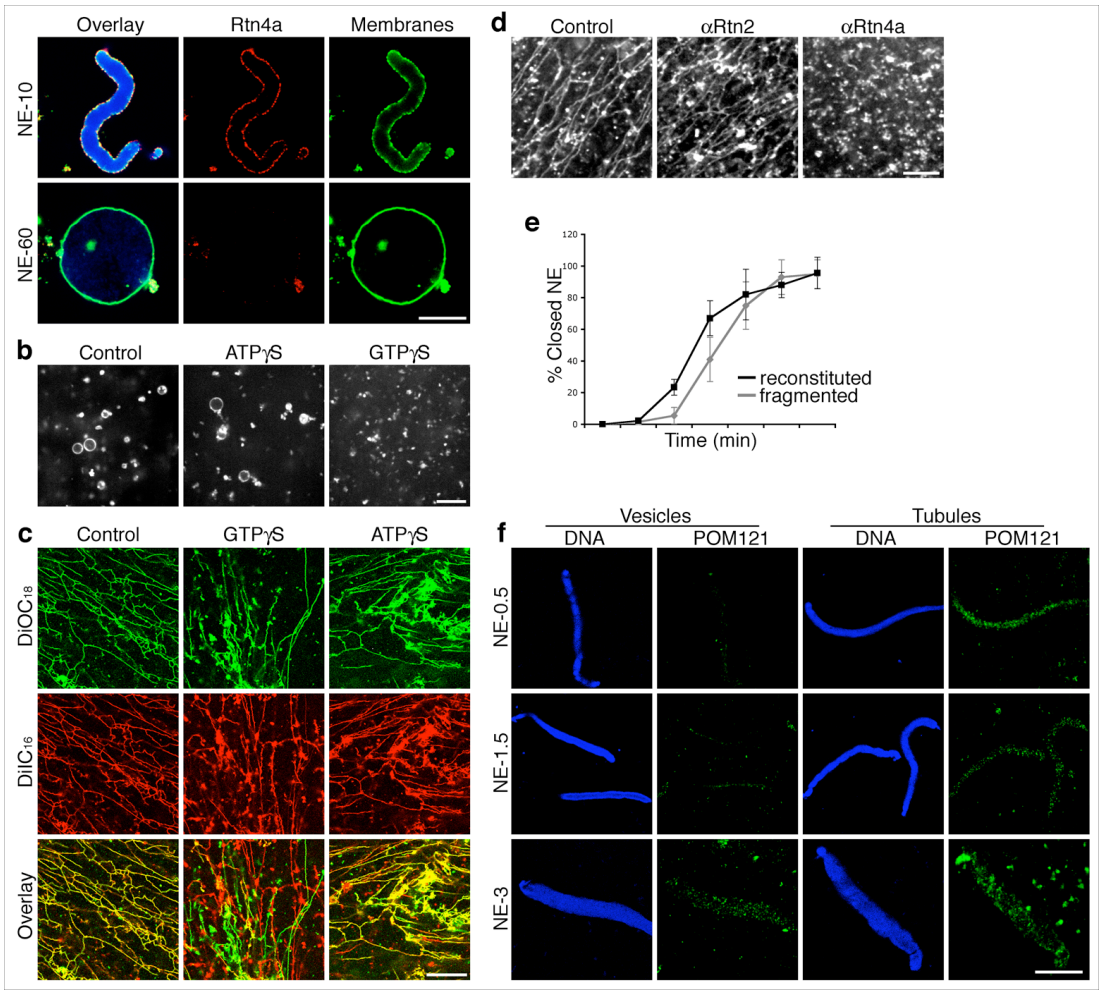

Chapter II Figure 2

NE formation from intact ER. (a) Nuclei were assembled with DiIC16-labeled membranes (green), fixed at 10 min (NE-10) and 60 min (NE-60) and analyzed by immunofluoresence using αRtn4 (red). Scale bar, 10µm. (b) DiOC6-stained Membranes were diluted in buffer and incubated in the presence of buffer (control) 4mM ATPγS or 4mM GTPγS at 25˚C for 60 min, then imaged with confocal microscopy. Scale bars, 10 µm. (c) DiOC18 or DiIC16 stained membranes were incubated with cytosol to generate ER network and then mixed in the presence of buffer (control), 4mM GTPγS, or 4mM ATPγS and imaged after 10 min. Scale bar,10µm. (d) DiIC16-stained membranes were incubated with cytosol in the presence of 10 µM anti-Rtn2 or anti-Rtn4a 18 and analyzed without fixation. Scale bars, 10 µm. (e) The percentages of nuclei formed either from fragmented ER (grey) or reconstituted ER (black) were determined using the streptavidin exclusion assay, n=60. (f) Nucleoplasmin-decondensed sperm 29 chromatin was incubated with fragmented or preformed ER network, fixed after 30 sec (NE-0.5), 90 sec (NE-1.5) or 3 min (NE-3) and analyzed by immunofluorescence using antibodies against POM121 (green). Chromatin was stained with Hoechst 3222 (blue). Scale bar, 5µm.

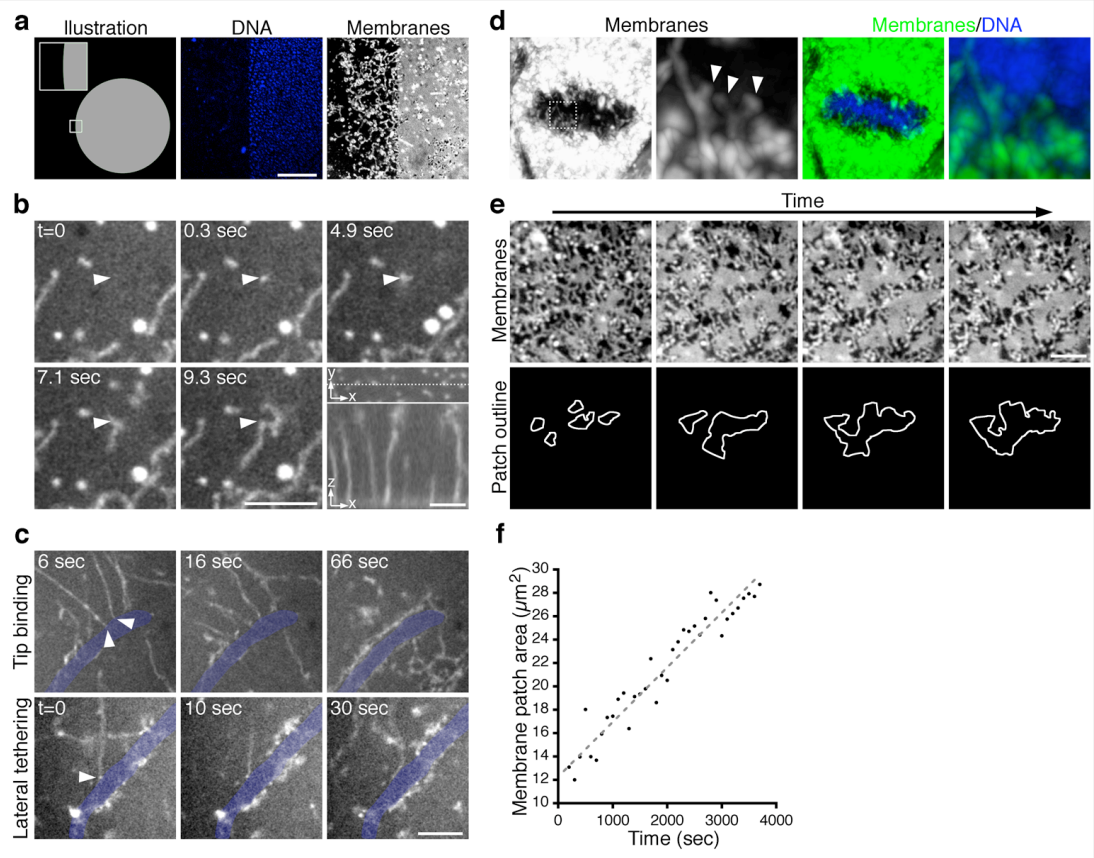

Chpater II Figure 3

Chromatin-mediated reshaping of the ER. (a) Biotinylated 10 kb dsDNA was immobilized on streptavidin-coated cover glass (schematic, left panel) and visualized by Hoechst 3222 (blue, middle panel). After the addition of cytosol and membranes a NE formed specifically on the 2D chromatin spot (right panel). Scale bar, 10 µm. (b) Early chromatin/membrane interactions were imaged with time-lapse microscopy on 2D-chromatin at a rate of ~4 frames/sec. Initial interaction occurred via membrane tubule tips (arrowhead). Tubule ends on the surface of 2D chromatin were imaged in 3D by confocal microscopy (lower right panel). Scale bars, 2µm. (c) De-condensed sperm chromatin was spun onto cover slips and stained with Syto©62 (blue). Preformed ER network was added and membrane/chromatin interactions were instantaneously imaged. Cross-sections of the chromatin are shown and arrowheads indicate initial membrane contact to chromatin. Scale bar, 5 µm. (d) NIH3T3 cells were plated onto chambered slides and stained with DiOC6 and Hoechst 3222 in growth medium. Live mitotic cells were imaged with confocal microscopy and 3D reconstructions were generated. Arrowheads indicate tubule tip binding. NE formation was performed as in (a). Confocal images were taken every 10 sec. Membrane sheets were schematically outlined (lower panels). Scale bar, 5 µm. (e) Expansion of membrane sheets was monitored by measuring the surface area of a single patch every 10 sec. (f) Expansion of membrane sheets was monitored by measuring the surface area of a single patch every 10 sec.

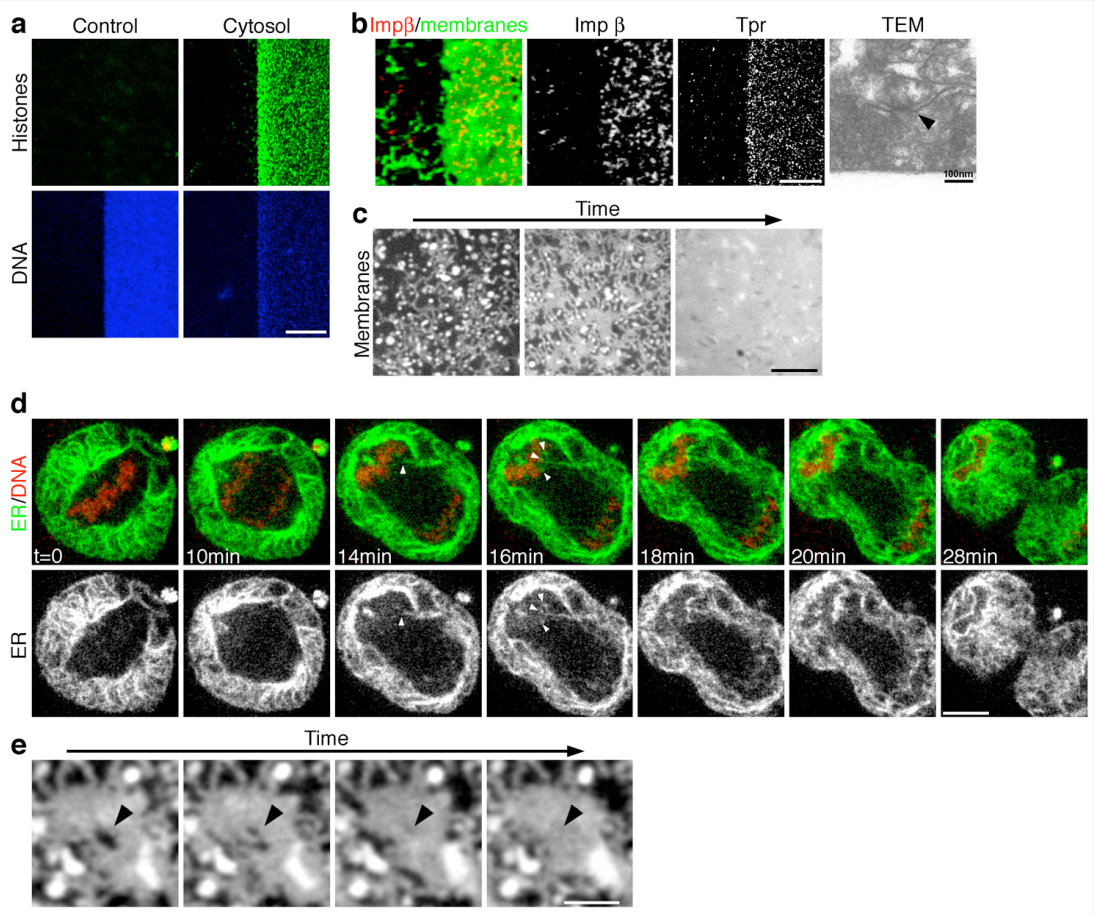

Chpater II Figure 4

Characterization of NE formation assay. (a) Immobilized dsDNA on a glass surface was incubated with buffer (control) or egg extracts (cytosol) and analyzed by immunofluorescence using histone H2B antibodies (green). Scale bar, 10 µm (b) TAP-Impβ coupled to FITC-streptavidin (Impβ) was added to the NE formation assay to label assembled NPCs (left and center panels). Presence and orientation of NPCs was confirmed by TEM of fixed flat NE reactions (right panel). Scale bars, 5 µm and 10 nm, respectively. (c) NE formation reaction was started and imaged with time-lapse confocal microscopy for 2 hrs. Scale bar, 5 µm. (d) HeLa cells were co-transfected with histone H2B-tdTomato and GFP Sec61β (aa 1-65) and imaged live during mitosis, arrowhead indicate initial ER contact to chromatin. Scale bar, 10µm. (e) Sealing of holes within the NE was imaged using the flat-chromatin assay, where time-lapse images were acquired every 10 sec. Scale bar, 2 µm.

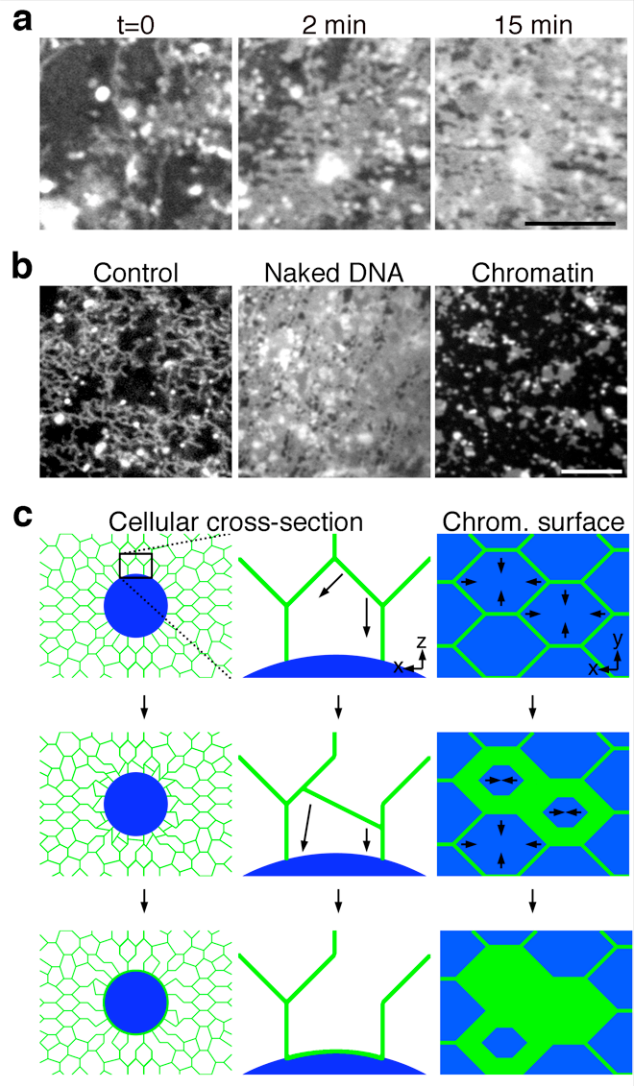

Chpater II Figure 5

NE formation is mediated by protein-DNA interactions. (a) ER network was formed with heat inactivated cytosol and added to immobilized DNA and imaged in real-time every 10 sec. (b) Immobilized DNA was first incubated with buffer (left and middle panels) or cytosol (right panel), ER network was formed with cytosol (left panel) or heat inactivated cytosol (center and right panel) and added to DNA surface. (c) Schematic illustration of NE formation. The ER network is recruited to chromatin via tubule ends, which anchor tubules on chromatin. Tubule sliding along these immobilized tubules results in membrane network coating of chromatin. Cross-section of chromatin, where ER is drawn in green and DNA in blue, illustrates the tubular network formation on the surface of chromatin (left and center columns). Surface image of chromatin illustrates membrane tubule flattening into the NE (right column). Scale bars, 5µm.

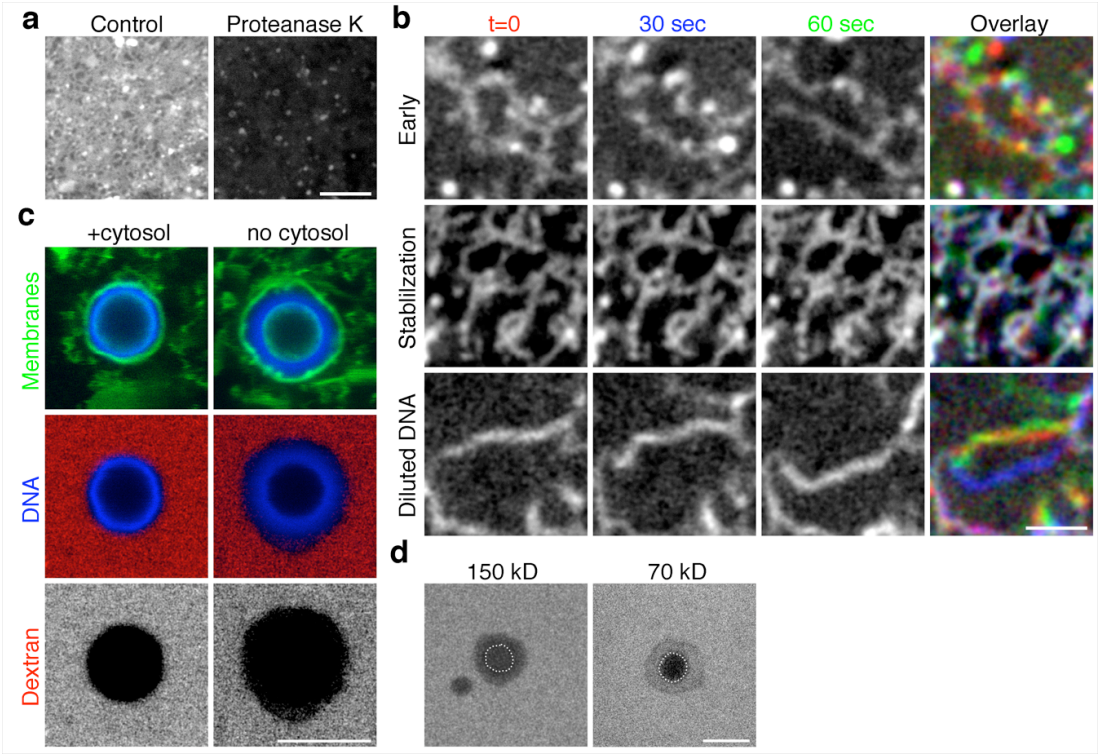

Chapter II Figure 6

Membrane tubule stabilization by DNA-binding proteins in the ER. (a) DiOC6-stained membranes were incubated with buffer (control) or 2µg proteinase K for 10 min at 25˚C, and then diluted in heat-inactivated cytosol at incubated for 30 min at 25˚C. Membranes were subsequently added to DNA coated glass and imaged after 10 min. Scale bar, 5µm. (b) Membrane tubules were imaged on 2D chromatin after for 60 sec. Images of 3 different time points were false color labeled (t=0 red, 30 sec. blue, and 60 sec. green) and merged (overlay). Membrane tubules were dynamic at early time points (5 min) and when DNA was diluted to a concentration of 10 pg/µl (diluted DNA), but stable after 20 min with concentrated DNA. Scale bar, 2 µm. (c) Strepavidin-conjugated magnetic beads were coated with biotinylated DNA and incubated with preformed ER (green) in the presence or absence of cytosol for 60 min. After the addition of fluorescently labeled 150 kD dextran (red) and DAPI (blue), reactions were imaged live by confocal microscopy. Scale bar, 5µm. (d) Reactions were performed as described in (c) except that either 150 kD or 70 kD dextrans were added. Scale bar, 5µm.

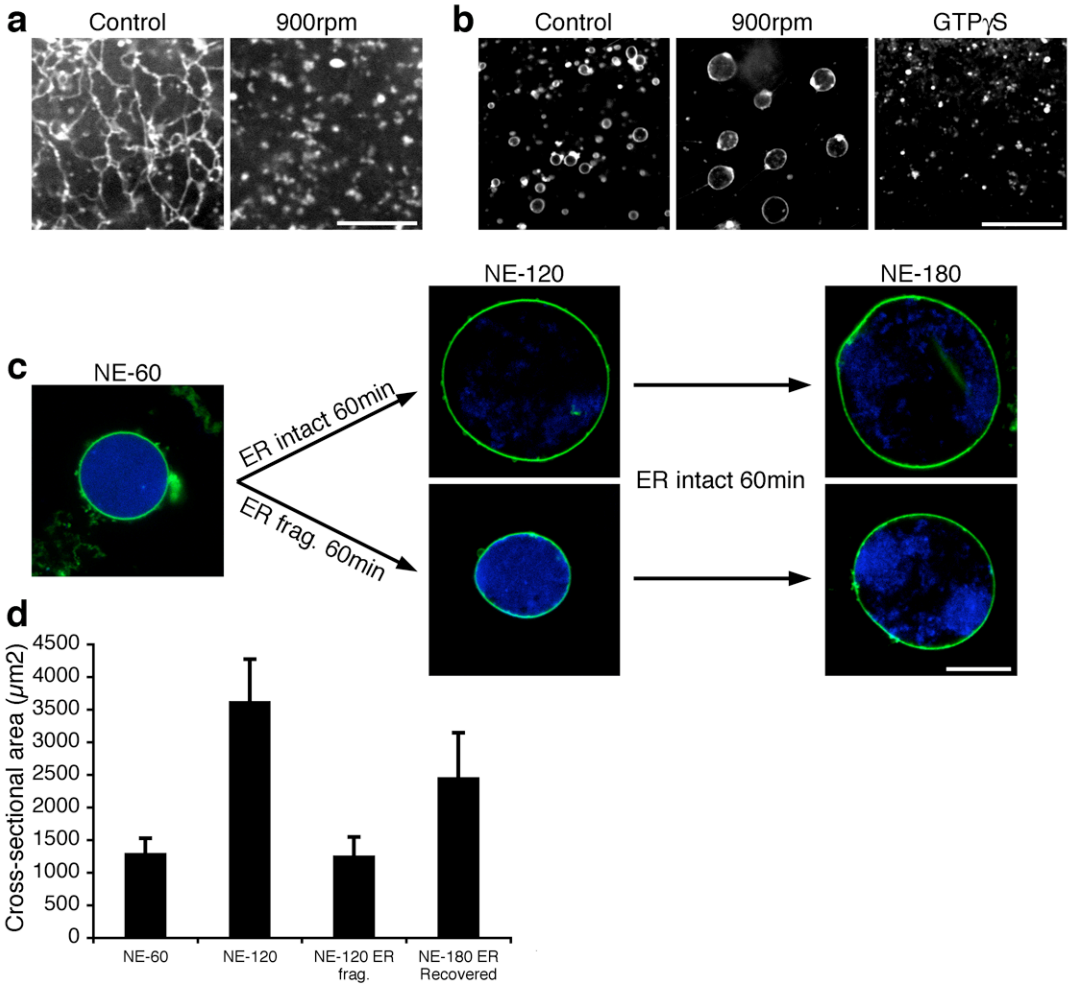

Chapter II Figure 7
NE expansion requires an intact ER network. (a) ER was preformed for 20 min, then 2 mM GTPγS was added and the membrane network was incubated unperturbed (control) or fragmented at 900rpm for 60 min. (b) Membrane fusion was tested by combining washed membrane fragments with 5 mM ATP and 5 mM GTP and incubated unperturbed (control), shaken at 900rpm, or incubated unperturbed with the addition of GTPγS for 60 min. (c) Nuclei were assembled for 60 min (NE-60) and then incubated unperturbed or shaken at 900 rpm for 60 min, both reactions were then incubated an additional 60 min unperturbed. Nuclei were fixed and imaged at each step. (d) Nuclear cross-sectional areas from (c) were measured to determine the extent of nuclear growth, n<50. Scale bar, 10 μm.

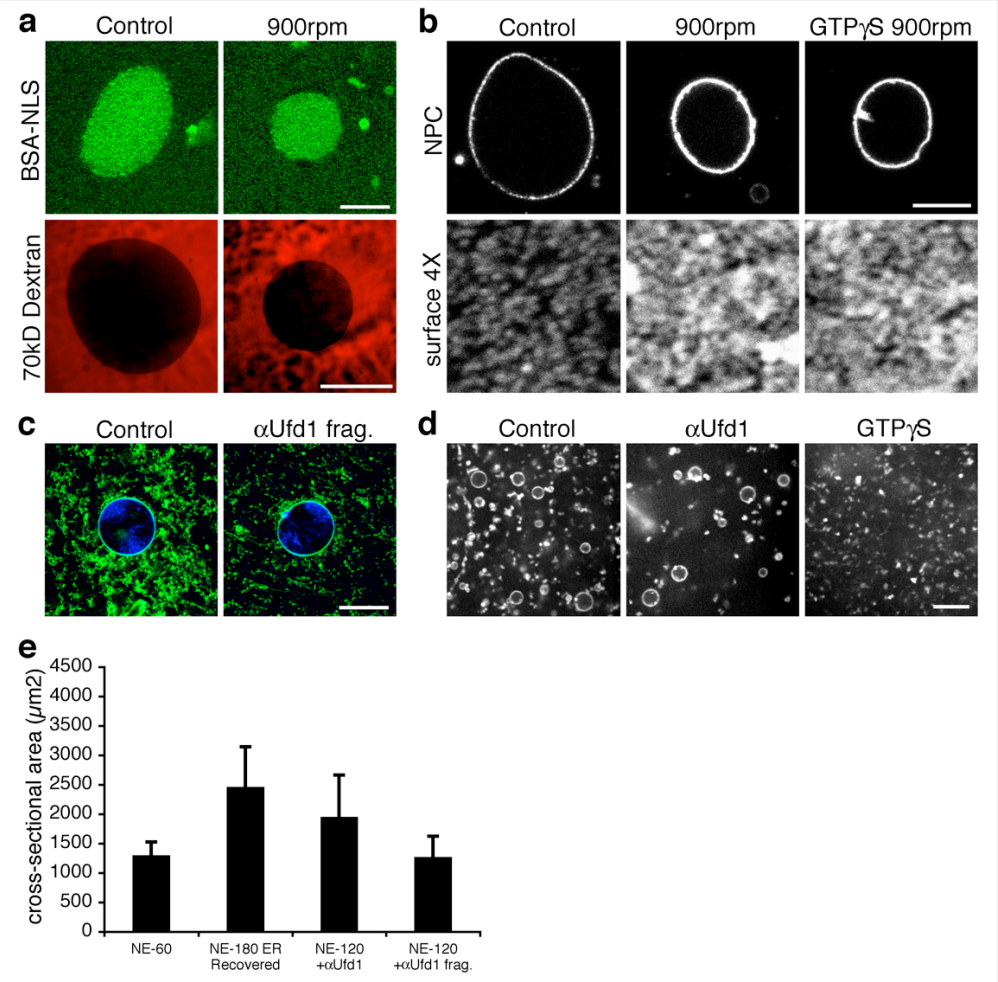

Chapter II Figure 8

Nuclei are functional when subjected to mechanical stress. (a) Nuclei were formed for 60 min (control) and subsequently incubated formed for additional 60 min in the absence (control) or presence of mechanical force (900rpm). BSA-NLS conjugated to FITC (green) and Alexafluor©568-conjugated 70kD dextran (red) was added for 10 min before nuclei were imaged unfixed. (b) Alexafluor©568-conjugated WGA was added to NE-60 nuclei and then incubated for an addition 60 min (control), shaken at 900 rpm for 60 min (900rpm), or 2mM GTPγS was added and nuclei were shaken for 60 min (GTPγS 900rpm). Cross-sectional and surface images of NPCs were then taken. (c) Nuclei were assembled for 60 min and subsequently the ER was sheared by repeated pipetting in the absence or presence of anti-Ufd1 antibody, which inhibits p97 function26. The ER was allowed to recover for 5 min. before nuclei were imaged by confocal microscopy. (d) DiOC6-stained Membranes were diluted in buffer and incubated in the presence of non-specific antibody (control), anti-Ufd1, or 4mM GTPγS at 25˚C for 60 min, then imaged with confocal microscopy. Scale bars, 10 μm. (e) Nuclei were formed for 60 min (NE-60); anti-Ufd1 antibody was then added to block ER reformation. Nuclei were then incubated an additional 60 min (NE-120, un-fragmented) or pipetted 5 times and incubated 60 min (NE-120, fragmented). Nuclear cross-sectional areas were measured to determine the extent of nuclear growth, n=50.

CHAPTER III

Reshaping of the endoplasmic reticulum limits the rate for nuclear envelope formation

Abstract

During mitosis in metazoa segregated chromosomes become enclosed by the nuclear envelope (NE), a double membrane that is continuous with the endoplasmic reticulum (ER). Recent *in vitro* data suggest that NE formation occurs by chromatin-mediated reorganization of the tubular ER, however, the basic principles of such a membrane re-shaping process remains uncharacterized. Here we present a quantitative analysis of nuclear membrane assembly in mammalian cells using time-lapse microscopy. From the initial recruitment of ER tubules to chromatin, the formation of a membrane-enclosed, transport-competent nucleus occurs within ~12 min. Over-expression of ER tubule-forming proteins reticulon 3, reticulon 4 and DP1 inhibits NE formation and nuclear expansion, whereas their knockdown accelerates nuclear assembly. This suggests that the transition from membrane tubules to sheets is rate-limiting for nuclear assembly. Our results provide evidence that ER-shaping proteins are directly involved in the reconstruction of the nuclear compartment and that morphological restructuring of the ER is the principal mechanism of NE formation *in vivo*.

Introduction

A hallmark of eukaryotic cellular organization is the compartmentalization of distinct metabolic functions into membrane-enclosed organelles. The inheritance of these organelles is an essential homeostatic process in dividing cells. One of the most morphologically elaborate organelles is the endoplasmic reticulum (ER), which is

organized into membrane tubules and sheets [101]. The relative distribution of these ER domains changes continuously as cells move through the cell cycle. Dynamic processes involving fission and homotypic fusion of membranes maintain the overall architecture of the ER [109, 110].

Connected to the ER is the nuclear envelope (NE), an extensive spheroid membrane sheet that is composed of two lipid bilayers that enclose the nuclear genome. The outer and inner nuclear membranes are fused at sites where nuclear pore complexes (NPC) are inserted. NPCs are large multi-protein channels that mediate nucleo-cytoplasmic trafficking [4]. Despite the physical connection between NE and ER, the nuclear membrane contains a unique set of proteins that are not present in the ER. One class of proteins is localized in the outer NE and provides contacts to the cytoskeleton [111]. A second class of proteins preferentially associates with the inner NE and has been shown to interact with the nuclear lamina and chromatin [reviewed in [112] and [92]].

Only recently have proteins been identified that exclusively localize to ER tubules and are excluded from flat membrane sheets such as the NE [102]. This class of ER membrane proteins contains the reticulons and the functionally-related protein DP1/YOP1, both of which are expressed across all eukaryotic species [113]. These proteins contain a domain of ~200 amino acids that includes two hydrophobic segments, which are thought to form a hairpin in the membrane. The ability of reticulons to oligomerize appears to allow these proteins to generate and/or stabilize tubules *in vitro* [114]. While the mechanism of reticulon function is still being

characterized, it is known that the levels of these proteins can shift the balance between the tubular network and the flat membrane sheets [102].

In addition to differences in protein composition, the NE and the ER exhibit a striking difference in their dynamic behavior during mitosis. While it is well documented that the NE completely breaks down in prophase of metazoa [reviewed in: [115, 116]], it has become clear that the ER network remains intact during cell division [50]. Electron microcopy data has recently demonstrated that the mitotic ER is a highly interconnected network of tubules during metaphase [117]. Considering the dramatic difference in the fates of NE and ER during mitosis, the questions arise how the disassembled NE components are dispersed, and consequently, how the nuclear membrane is reformed around the segregated chromosomes? Historically, data obtained from biochemical fractionation of ER membranes supported a model where the NE is fragmented into vesicles that remain distinct from the ER [49]. In contrast, live imaging has revealed that GFP-tagged NE components reside in the mitotic ER, suggesting that the lipids and membrane proteins of the NE retract into the tubular ER network [86, 118, 119]. The idea of mitotic NE retraction implies that at the end of mitosis, the nuclear membrane reemerges from the ER and does not form by fusion of a separate pool of vesicles [49]. In support of such a mechanism, *in vitro* analyses suggest that the intact tubular ER is required for NE formation [117, 119]. Using live imaging, we were able to provide the first insights into the membrane dynamics of NE formation. We showed that the ER is targeted to chromosomes via tubule-end binding and subsequently immobilized on the chromatin surface. This chromatin-bound

network then flattens and seals into a closed NE [119]. *In vitro* data also demonstrates that targeting of membranes to chromatin is at least partially regulated by NE-specific transmembrane proteins binding to DNA and/or chromatin [63, 65, 119]. The general mechanism of membrane reshaping from tubules to the double lipid-bilayer sheets of the NE is unclear, and *in vivo* evidence for such a process remains sparse.

Here, we set out to determine if changes in ER morphology play a role in NE formation *in vivo*. A novel assay to study the dynamic relationship between the organization of the ER and forming NE in dividing cells was developed. This assay and other live-cell imaging approaches provide direct evidence that NE formation occurs by the reorganization of the ER on chromatin. Furthermore our studies reveal that reticulons and DP1 act to regulate NE formation. In addition we show that NE expansion is mechanistically coupled to the ER organization.

Results

Displacement of reticulons from the re-forming NE

In order to determine if chromatin-mediated reshaping of ER tubules is the principal mechanism of NE formation *in vivo*, we compared ER membrane dynamics during mitosis in different tissue culture cells. We selected U2OS cells, an osteosarcoma cell line, because they remain relatively flat during mitosis making them suitable for high-resolution time-lapse microscopy. To directly test if ER tubules are recruited to chromatin we co-transfected the ER marker Sec61β fused to GFP (Sec61-GFP) as well as the histone subunit H2B fused to tdTomato (H2B-tdTomato) to

visualize chromatin [120]. In interphase, Sec61-GFP stained the NE and the ER, highlighting the continuity of the two membrane systems (Movie 1). In metaphase, chromatin was essentially free of membranes and as expected from recent observations, the ER remained intact during mitosis. As cells progressed to telophase, the cell cycle phase when NE reformation occurs, ER membranes contacted chromatin via tubule end binding (Fig. 1A). Once a few tubules were immobilized, additional tubules sliding along each other were captured on chromatin and eventually coated the entire chromatin surface (Fig. 1C), confirming that ER recruitment to chromatin is an early event in nuclear assembly.

To confirm that the linear structures seen in the two-dimensional images of membrane-chromatin contact points were tubules, confocal z-stacks of cells expressing Sec61-GFP and H2B-tdTomato were acquired every 30 sec. After three-dimensional reconstruction membrane tubules contacting the surface of chromatin were clearly resolved (Fig. 1B) confirming that the linear structures represent membrane tubules.

We have recently shown that transmembrane components of the NPC such as POM121 are dispersed throughout the ER network during NE breakdown [119]. Therefore we expected that POM121 should be incorporated into the reforming NE via ER tubules connected to chromatin. To test this, we expressed the NE marker POM121-GFP and found that it was indeed present in tubules that initially contacted chromatin (Fig. 1A,D). As NE formation proceeded, POM121-3GFP was cleared from surrounding tubules and accumulated on the chromatin surface, supporting the

idea that NE proteins are recruited to chromatin from the ER network. Taken together, these results suggest that the ER serves as the precursor membrane for the NE.

In combination with previous data, these results imply a two-step process of NE formation in which ER tubules first become immobilized on chromatin and then reorganize into flat membrane sheets. As a consequence of such a step-wise membrane reorganization process, chromatin-bound ER tubules should initially contain tubulating proteins like reticulons. However, as the transition into sheets progresses, these proteins should be displaced since they are ultimately excluded from flat membranes [102]. To directly test for this possibility, we co-expressed POM121-3GFP and the tubular ER protein Rtn3 fused to tdTomato and imaged their dynamic behavior by fluorescence microscopy in real time. As expected, POM121-3GFP accumulated at the forming NE and therefore served as a reporter for membrane-chromatin contact sites (Fig. 2A). Similar to POM121-3GFP, Rtn3-dtTomato was detectable on the surface of chromatin (Fig. 2B) but as cells moved through telophase, POM121-3GFP accumulated in the reforming NE while the fluorescence intensity of Rtn3-tdTomato at the forming NE gradually decreased to background levels once the NE was formed (Fig. 2B). The rate of reticulon decrease at the forming NE was steady for ~10 min from the start of POM121 accumulation until the fluorescence signal reached background levels as measured by threshold selection of regions of bright POM121-3GFP (Fig. 1C). Strikingly, during NE formation the intensity of Rtn3-tdTomato in the surrounding ER increased. This suggests that in order to generate an extensive membrane surface around chromosomes a large number of

tubules were flattened and a considerable amount of reticulons were displaced from chromatin-bound membranes to surrounding ER tubules (Fig. 1C). These results uncovered a reciprocal behavior in protein dynamics in the forming nuclear membrane with reticulons being displaced and proteins that accumulate in NE sheets being recruited. This supports the idea that NE formation occurs by the gradual reorganization of ER tubules into flat membrane sheets on the surface of chromatin. We cannot exclude the possibility that ER patches contribute to NE formation, however such a contribution would likely be minor, since only tubules are detected in the mitotic ER [117].

Kinetics of NE formation

Since the observed ER membrane reorganization events occur on the highly condensed surface of chromatin [121], visualization of individual tubules and their transition into sheets by light microscopy in living cells was not feasible. Therefore, we developed an assay to study the kinetics and molecular mechanism of NE formation in real time in proliferating cells. The basic principles of the assay design are outlined in Fig. 4A. To monitor mitotic progression and provide spatial reference for NE formation we expressed histone H2B-tdTomato. To determine the exact time when an intact NE has formed we co-transfected a triple GFP fused to the SV40 large T-antigen nuclear localization signal (GFP-NLS). The rationale for using this approach was that the nuclear accumulation of GFP-NLS would require an intact NE. This assumption was made because the rate of diffusion of a protein the size of our

GFP-NLS reporter through a small hole the size of an NPC is ~7 times greater than the rate of facilitated nuclear-cytoplasmic transport [122]. Thus, by co-transfecting GFP-NLS and H2B-tdTomato, we were able to determine the time from metaphase-anaphase transition to nuclear accumulation of GFP-NLS, encompassing the onset of NE formation to its completion.

We first used this assay to determine the exact time of NE formation *in vivo* and the metaphase to anaphase transition, which was detectable by the separation of the sister chromatid clusters, was defined as time zero (Fig. 4B). In metaphase GFP-NLS localized diffusely in the cytoplasm (Fig. 4B, first panel). During cytokinesis, ~5 min after the onset of chromosome segregation, GFP-NLS was cytoplasmic, but accumulation of GFP-NLS into the daughter nuclei was observed after 10.2 min, followed by nuclear expansion (Fig. 4B). To accurately determine the onset of nuclear accumulation of GFP-NLS, the fluorescence intensity of GFP was measured over the areas occupied by the daughter chromatin clusters from anaphase into G1 and then GFP-NLS accumulation measurements were synchronized starting from chromosome segregation (Fig. 4C). In summary, our live imaging assay allowed us to determine that NE formation occurs within ~10 min in U2OS cells. Similar results were obtained in HeLa cells (data not shown).

To validate the assumption that accumulation of GFP-NLS is an accurate marker for NE closure, the timing of NE formation was determined by the visual appearance of a smooth rim around chromatin, an unequivocal sign of a closed NE (Fig. 1C). Chromosomes were completely enclosed by a smooth membrane rim

within an average 11.9 ±2.3 min after chromosome segregation (Table 1). Since the accurate assessment of nuclear rim formation requires higher resolution than the measurement of GFP-NLS accumulation, membrane dynamics were imaged at 63x magnification where GFP-NLS accumulation was imaged at 20x. The increased exposure to laser light with higher magnification imaging likely explains the time discrepancy in timing of NE formation of these two methods. However, it is clear that NE formation occurs within 12 min in U2OS cells.

Over expression of reticulons delay NE formation

Having established a kinetic framework for NE assembly, we next wanted to study the molecular mechanisms involved in this pivotal membrane-remodeling event. The release of reticulons from the forming NE [[119], Fig. 2] suggested that these ER tubule-forming proteins might act as antagonists of membrane flattening. To directly test this possibility, human reticulon 3 (Rtn3) or reticulon 4 (Rtn4), each fused to a V5 tag at their N-termini, were transfected into U2OS cells. Both V5-Rtn3 and V5-Rtn4 expressed at the expected size and specifically localized to ER tubules, similar to the immuno-staining pattern of endogenous Rtn4 (Fig. 3A, B). Since the analysis of reticulon over-expression using the NE-kinetic assay required transfection of several genes at once, it was important to determine the co-transfection efficiency. While GFP-NLS and H2B-tdTomato were visualized using their intrinsic fluorescence, V5-tagged reticulon proteins were detected by indirect immunofluorescence using antibodies against the V5 epitope (Fig. 3C). More than 94% of cells expressing

detectable levels of both fluorescent reporter proteins also expressed detectable levels of the V5-tagged proteins (Fig. 3D). These data demonstrate that triple transfection efficiency into U2OS cells was robust, thus allowing us to analyze the effect of protein over-expression on NE formation kinetics.

Using this approach we found that elevated reticulon levels significantly delayed NE formation when compared to control cells expressing only the recombinant GPF-NLS and H2B-tdTomato proteins (Fig. 5A, B). This effect was specific for reticulons since the over-expression of full-length V5-Sec61β, a transmembrane component of the ER protein translocator, did not delay NE formation (Fig. 5A, B). On average, in control cells NEs were closed after 10.2 min., whereas the over-expression of Rtn3 caused a significant delay to 21.9 min. and the over-expression of Rtn4 to 26.3 min. (Table 1). These data suggest that over-tubulation counteracts NE membrane flattening and that ER organization by reticulons and NE formation are tightly linked processes. It is important to note that the observed delay in the onset of nuclear accumulation is not due to a defect in NPC assembly since the rate of nuclear accumulation in the delayed cells was comparable to that of control cells (Fig. 5A).

Similar to elevated levels of reticulons, overexpression of V5-tagged DP1 (Fig. 3 A-C), a reticulon-like protein, delayed NE formation (Fig. 5A, B). Nuclear accumulation of GFP-NLS was significantly delayed when compared to control cells and only occurs after 25.2 min. as measured from chromosome segregation (Table 1). DP1 is composed of the two membrane-inserting, hydrophobic domains but lacks N-

terminal extension found in most reticulons. Importantly, DP1 can be considered a functional homolog to the reticulon in the context of membrane shaping, since it localizes to the tubular ER *in vivo* [102] and it's yeast homolog, yop1, has been demonstrated to directly tubulate membranes *in vitro* [123].

These data suggest that increased levels of DP1 caused a delay in NE formation possibly due to the induction of membrane curvature and tubulation. They also provide strong support for the general idea that NE formation *in vivo* occurs by reshaping of ER tubules.

NE protein recruitment is unaffected by Rtn4 over-expression

Although we did not detect any differences in ER dynamics and protein diffusion through the membrane network as determined by fluorescence recovery after photobleaching studies (data not shown), in principal it was possible that Rtn4 over-expression inhibited the targeting of ER membranes and the NE-specific membrane proteins to chromatin. To examine this possibility, an assay was developed that allowed us to monitor the recruitment of GFP-tagged ER membrane proteins around H2B-tdTomato-labeled chromatin (Fig. 6A). Since the NE forms tightly around the segregated chromatin clusters, a thin border around the edge of the chromatin clusters was selected and the GFP fluorescence intensity was measured from the metaphase-anaphase transition to G1 (Fig. 6A).

Using this assay we found that Rtn4 over-expression had no effect on the recruitment of the transmembrane nucleoporin, POM121-3GFP (Fig. 6B) and Sun1

(Fig. 6C), an inner nuclear membrane protein that has been implicated in the maintenance of nuclear membrane spacing [124]. These data suggest that the inhibition in NE formation caused by the over-expression of reticulons is caused by a defect in membrane flattening and not membrane targeting to chromatin. These results also suggest that NE formation *in vivo*, similar to the situation in cell-free assembly systems, is a two-step process where the rapid first step of membrane targeting to chromatin can be distinguished from the slower second step of enclosing chromatin by a sealed nuclear membrane.

Rtn3 and DP1 removal from the NE is concentration dependent

Since protein diffusion was not detectably affected by the over-expression of V5-Rtn4, we predicted that reticulon/DP1 removal from chromatin-bound membranes in these over-expressing cells might be causing a delay in NE formation. To test this possibility, the removal of fluorescently-tagged Rtn3 and DP1 was imaged. Cells were grouped based on their expression level and NE-removal rates were compared.

Both Rtn3 and DP1 were fused to GFP, Rtn3 at the N-terminus and DP1 at the C-terminus. These constructs localized to the tubule ER (Fig. 6E,F inset) and exhibited limited mobility when tested with fluorescence recover after photobleaching (data not shown), which is consistent with published observations [114] and suggests that GFP-Rtn3 and DP1-GFP are functional. U2OS cells were transfected with H2B-tdTomato along with Sec61-GFP, GFP-Rtn3 or DP1-GFP and imaged through mitosis. GFP intensity at the forming NE was measured as in Figure 5A and cells were divided

into low and high GFP expression. Localization of Sec61-GFP at the forming NE was similar with low or high expression levels (Fig. 6D). However, high expression of GFP-Rtn3 or DP1-GFP caused a delay in the release of these proteins from the forming NE (Fig. 6E,F). These data suggest that the delay in NE formation observed in cells over-expressing reticulon/DP1 is caused by the reduced release of these proteins from the chromatin-bound membrane, which may cause a delay in tubule to sheet transition.

Membrane flattening is blocked by the over-expression of Rtn4

Altogether the above findings suggest a tug-of-war like mechanism of NE formation in which the intrinsic propensity of the ER to move from tubules to flat sheets is shifted towards sheet formation by membrane immobilization on chromatin. To further explore this hypothesis, cells were transfected with Sec61-GFP and H2B-tdTomato and imaged through mitosis with or without the over expression of V5-Rtn4. As described above, a smooth rim, an unequivocal sign of an assembled NE, formed in control cells in 11.9 ±2.3 min (Fig. 7A and B, Table 1). When V5-Rtn4 was over-expressed, membranes rapidly targeted to chromatin (Fig. 6A), however, the formation of a smooth rim was significantly inhibited taking 25.4 ±13.8 min (Fig. 7A and B, Table 1). These data further suggest that over-expression of Rtn4 specifically antagonizes the second step of NE formation where, after ER tubules are targeted to chromatin, they are re-shaped into flat membrane sheets.

Lowering the levels of endogenous reticulons accelerates NE formation

The observation that increased levels of reticulons inhibited NE formation raised the interesting possibility that displacement of reticulons might be a crucial step in NE formation. If this were the case, the rate of NE formation should be inversely proportional to the levels of reticulon proteins in the ER. To test this possibility we measured the time of NE formation in control cells versus cells in which the overall concentrations of reticulons had been reduced by siRNA-mediated knock down. Since studies in yeast have shown that the double knockout of both reticulons, rtn1 and rtn2, was necessary to cause a transformation of the tubular ER into membrane sheets [102], we expected that a similar redundancy would exist in mammalian cells where four reticulon isoforms have been reported. In order to test for a potential redundancy in reticulon function we knocked down Rtn1, Rtn3, and Rtn4 individually or in combination. Reduction in reticulon mRNA levels was confirmed by quantitative PCR. Transfection of siRNA oligos against Rtn1, Rtn3, and Rtn4 simultaneously caused a 94%, 74% and 94% reduction mRNA levels of Rtn1,3, and 4 respectively in comparison to scrambled RNA. As expected, when U2OS cells were transfected with Sec61-GFP and scrambled RNA the ER contained an extensive tubular network (Fig. 8A) in 83% of the cells imaged. In striking contrast, cells in which Rtn1, Rtn3, and Rtn4 levels were reduced, only 34% of the cells contained a visible tubular network, the other 66% of the cells exhibited an altered ER morphology, which was almost entirely composed of membrane sheets (Fig. 8A). The knockdown of each single reticulon had no detectable change in ER morphology (data not shown).

Having established conditions to knock down reticulons to levels that alter the overall morphology of the ER, we performed our kinetic analysis in control and triple-siRNA knock down cells. Strikingly, NE formation was accelerated in cells with reduced levels of reticulons (Fig. 8B). While NEs formed on average after 10.6 min ±0.4 from chromosome segregation in cells transfected with scrambled RNA, reticulon knockdown resulted in an acceleration of nuclear assembly to 7.8 min ±0.2 (Fig. 8C, Table 1), providing first evidence that flattening of the ER might be rate limiting for NE formation.

Consistent with increased rates of membrane flattening, the appearance of a smooth membrane rim around chromatin, an unequivocal sign of a closed NE, was detected earlier in cells treated with siRNAs against reticulons when compared to control cells (Fig. 8D). Rim formation occurred in an average of 12.9 ±2.7 min from chromosome segregation in cells transfected with scrambled RNA and was accelerated to 9.7 ±2.2 min with the knockdown of Rtn1, Rtn3, and Rtn4 (Fig. 8E, Table 1). Taken together these results suggest that the concentration of reticulons is rate-limiting for NE formation. It is possible that the reduction of reticulons partially converts the mitotic ER into membrane sheet, which more efficiently contribute to nuclear membrane formation. Alternatively, the transition from tubules to sheets of membrane bound to chromatin may be accelerated by the decrease in reticulon concentration.

Rtn4 over-expression inhibits nuclear expansion

Our data revealed a tight link between the organization of the ER and NE formation. Since the closed NE is continuous with the surrounding ER network and nuclei grow in size as they move through interphase [125], we wanted to investigate if reticulons might be involved in NE expansion. We have recently shown that nuclear expansion *in vitro* requires connection with the peripheral ER [119], suggesting that membranes feed into the expanding NE through connections with ER tubules. To determine if hyper-tubulation inhibits nuclear expansion, the effect of Rtn4 over-expression during G1 was analyzed. Because GFP-NLS targets diffusely in the nucleus it provides a close approximation of NE surface area. Using three-dimensional reconstructions of confocal z-stacks from nuclei stained with GFP-NLS, nuclear surface area can be accurately measured [99]. We found that asynchronously growing cells have an average nuclear surface area of 1063.3 μm^2 ±270.1 μm^2. Nuclear growth was then monitored starting when the NE was fully formed, as judged by the nuclear accumulation of GFP-NLS. NE expansion was significantly slower in cells over-expressing V5-Rtn4 compared to control cells (Fig. 9 A and B). Interestingly nuclear growth was not accelerated by the triple knockdown of reticulons, suggesting that there is an additional rate-limiting step in nuclear expansion (data not shown). These data suggest that the membrane-shaping proteins control nuclear growth and that the propagation of the NE-ER membrane continuum during cell division is mechanistically linked.

Discussion

At the end of mitosis, nuclear assembly is an essential process in establishing eukaryotic cell compartmentalization. Our data provide the first detailed kinetic analysis of NE formation in dividing cells, and uncovers novel molecular regulators of this membrane-shaping process. A major conclusion from these studies is that the NE is the result of massive reorganization of the tubular ER network on chromatin. Surprisingly, the displacement of reticulons is rate-limiting for nuclear assembly, suggesting a bottle-neck at the tubule-to-sheet transition. Furthermore, the levels of reticulons, which directly affect the balance between tubules and sheets in the ER, are linked to NE expansion. Therefore, our data suggest that the intrinsic ability of the ER to move between membrane sheets and tubules is utilized to form the NE.

The state of the mitotic NE

Historically, NE formation has been discussed as an example of a cell cycle specific membrane fusion event similar to the reassembly of the Golgi apparatus. This hypothesis was based on nuclear reconstitution experiments using *Xenopus* eggs. These experiments have revealed distinct vesicle populations that contribute to NE formation, suggesting that these vesicles were not part of a continuous membrane network prior to extract preparation [53]. When membrane vesicles were mixed with chromatin and cytosol, nuclear assembly was found to depend on the presence of ATP ad GTP, suggesting that there is membrane fusion machinery involved in the creation of the NE [57, 58]. These data further suggest that the NE is formed by the fusion of NE-specific mitotic vesicles.

However, a growing line of evidence supports an alternative model where the NE resides in the ER during open mitosis. Proteins of the NE have been visualized in the continuous mitotic ER in a growing number of studies implying that these NE components do not reside in distinct vesicles [86, 118, 119]. In addition, a recent study utilized EM to detect regions of the mitotic ER with high concentration of NE-components and areas where these components are undetected [117]. Combined, these data are evidence that the NE resides in certain regions of the mitotic ER, and when these membranes are purified heterogeneous vesicles are formed [126].

In addition, Puhka et al. (2007) utilized 3D reconstruction methods to demonstrate that membrane tubules coated chromatin during anaphase, and these tubules were connected to the mitotic ER. In our previous study, a modified *in vitro* nuclear formation method, where membranes are first allowed to reform an intact ER network and then used in nuclear assembly, we uncovered the NE formation from an intact ER can occur in the presence of fusion inhibitors [119]. These data suggest that the fusion machinery previously thought to be required for NE formation is likely only required for ER homotypic fusion.

In our current study we provide direct *in vivo* evidence to support the model that the NE reemerges from the mitotic ER. Reticulons, proteins found exclusively on ER tubules, are found on membranes of the forming NE, demonstrating that the ER contributes directly to NE formation. In addition, our data show that elevated levels of ER shaping proteins, reticulons and DP1, inhibit NE formation. In contrast, the reduction of reticulons by siRNA accelerates NE formation. Taken together, these

data provide compelling *in vivo* evidence in favor of the model where the ER contributes directly to NE formation.

It is tempting to speculate that reticulons might also play a role in NE breakdown by re-tubulating the NE into the ER. Consistent with this idea, the knock-down of reticulon 1 and YOP1/DP1 in *C. elegans* causes a defect in NE break-down [127]. Retraction into the ER provides a simple and direct mechanism for the disappearance and appearance of the NE during mitosis that only requires the regulation of chromatin targeting of NE proteins and subsequent coordinated ER reorganization.

Membrane reshaping

The nascent NE is a massive membrane sheet with a surface area of ~450μm^2 (Fig. 9B). Given the diameter of an ER tubule is ~60nm, the formation of the NE would require the conversion of ER tubules measuring over 4.5 mm in length. This quantity of membrane likely represents a substantial fraction of the entire ER network. How these ER membranes are targeted to chromatin specifically during anaphase remain to be determined, but likely involves the coordinated effort of numerous proteins [128]. The simplest explanation is that inner nuclear membrane proteins, which have the capacity to bind DNA directly or via chromatin, mediate the targeting of membranes to the chromatin surface. How is this massive amount of tubules transformed into sheets? The simplest interpretation of our results is that some type of "tug-of-war" between sheet and tubule formation occurs on the surface of chromatin.

Overexpression of the reticulon isoform Rtn4a leads to the proliferation of bundled ER tubules and therefore NE sheet formation is reduced. In a reciprocal fashion, when the reticulons or DP1 were deleted the tubulating activity diminished and NE sheet formation predominated. We speculate that displacement of reticulons results in a local loss of tubule-stabilizing activity and thereby increases tubule diameter, promoting the flattening of tubules into sheets.

How reticulons are displaced from the forming NE is unclear since very little is known about the biochemical properties of these proteins. One possibility is that reticulons are pushed aside by incoming NE proteins as they become concentrated in the chromatin-bound tubules. The reciprocal behavior of Rtn3 and POM121 is consistent with this idea. Alternatively, although not mutually exclusive, reticulons are phosphorylated [129], which may regulate their ability to oligomerize and therefore modulate their membrane-bending capacities.

Considering the regularity of the spacing between the outer and inner nuclear membranes, it is likely that structural elements are needed to stabilize the NE. It remains to be determined whether luminal-domains of membrane proteins might contribute to membrane flattening by bridging the gap between the two membranes and thereby forming a stable connection to maintain a constant separation. A kinetic analysis using our NE formation assay in cells with modulated concentrations of these inner NE proteins should be useful in answering these questions.

Nuclear Expansion

Nuclear expansion is an important mechanism of growth in dividing cells, however, the regulation of this growth is currently unknown. Our data provide a novel link between the levels of membrane deforming proteins of the ER and nuclear size. Since the NE can be viewed as a single continuous ER sheet, levels of lipid synthesis and expression of reticulons might be one determinant of the overall size of nuclei. It will be interesting to test if the total size of the ER plays a role in nuclear expansion. Since reduction of reticulons does not accelerate NE growth, additional regulators are likely to exist. For example, nuclear import or lipid synthesis might limit the rate of nuclear expansion during G1. The uncovering of this interesting interaction between the ER and NE formation and expansion provides a starting point for further investigation of the interaction between these two organelles.

Materials and Methods

DNA constructs

Sec61β aa1-65 with GFP fused to the c-terminus (Sec61frag) was described previously [119]. POM121 fused to a triple repeat of GFP at the c-terminus was a kind gift from the lab of Jan Ellenberg [130]. H2B with tdTomato fused to the c-terminus was a kind gift from Gray Pearson (Salk). The NLS from SV-40 large T-antigen (PPKKKRKV) was added to tandem EGFP by PCR and then inserted the N-terminal containing cycle-3 GFP vector pcDNA6.2 DEST53 using Gateway cloning (Invitrogen™). Human reticulon 3 was isolated from IMAGE clone #3873400 (BC011394) by PCR and inserted in pDEST R4,R3 along with a CMV promoter and a

c-terminal tdTomato using multi-site Gateway cloning (Invitrogen™). Human reticulon 4 was isolated from IMAGE clone #3505850 (BC016165) and human DP1 was isolated from IMAGE clone #3350749 (BC000232), both along with reticulon 3 were inserted into pcDNA6.2-nLumio, an n-terminus V5 epitope containing vector, using Gateway cloning. Human Sun1 was isolated from IMAGE clone #3864251 (BC013613) and cloned into pcDNA6.2 DEST47 using Gateway cloning.

Cell transfection and live-cell imaging

U2OS cells were grown and imaged in DMEM with 10% fetal bovine serum with 1X antibiotic-antimycotic (Gibco™). Cells were plated on 8-well μ-slides (ibidi) and transfected with 0.6 μl Lipfectamine2000 (Invitrogen™) and 0.3-0.6 μg of each DNA construct two days prior to live-cell imaging as recommended by Invitrogen™. For siRNA knock-down, cells were transfected 25-50 nmol of RNA two and four days prior to imaging. siRNA oligo sequences used to knock-down reticulons were as follows: Rtn1: UAGAUGCGGAAACUGAUGGTT, Rtn3: CCUUCUAAUUCUUGCUGAATT, Rtn4: GAAUCUGAAGUUGCUAUATT (Invitrogen™). Live cells were imaged at 37˚C maintained by air stream incubator and enriched with CO_2 (Solent Scientific). Time-lapse images were taken on a spinning disk confocal microscope (McBain Instruments) built around a DMRIE2 inverted stage microscope (Leica). Images were captured on an EM-CCD digital camera (Hamamatsu) and acquired using SimplePCI (Compix). Cells were imaged using a 63x oil objective with a 1.4 numerical aperture (Leica).

Antibody production and Immunohistochemistry

Amino acids 1-117 of human reticulon 4 were inserted into pDEST15 using Gateway cloning (Invitrogen™). This GST-tagged protein fragment was then expressed in BL21 *E.coli* cells and purified using Glutathione-Agarose beads (Sigma™). Guinea pigs were injected with two rounds ~100μg of protein and then bled 10 days after the second injection. Serum was used at a 1:1000 dilution for indirect immuno-fluorescence and 1:5000 for Western blotting. Monoclonal antibodies against the V5 epitope were used at a dilution of 1:1000 for indirect immuno-fluorescence and 1:5000 for Western blotting.

Image analysis and statistics

Regional and intensity threshold selections as well as subsequent average pixel intensities were measured using Photoshop® Extended CS3 (Adobe®). Nuclear surface area was measured as previously described [99]. Numerical data was then analyzed and summarized graphically using Excel® (Microsoft®). Data for each experiment was collected from three independent experiments and combined for statistical analysis. P-values were determined using student's t-test, error bars represent standard errors, and ± values represent the standard deviations. 3-D reconstructions were generated using the iso-surface function of Imaris (Bitplane).

Acknowledgments

Joshua Hsiao aided in the cloning of several constructs used in this manuscript. We thank Maximiliano D'Angelo, Maya Capelson, Christine Doucet, Sebastian Gomez, Robbie Schulte, Jessica Talamas, and Jesse Vergas for critically reading the manuscript and helpful discussion. This work was supported by a grant from NIH (R01 GM073994).

Chapter 3, in full, consists of the following publication.

Anderson DJ, Hetzer MW. 2008. Morphological reshaping of the endoplasmic reticulum limits the rate for nuclear envelope formation in vivo. J Cell Biol. in press.

I was the primary researcher and author of these studies under the supervision and direction of Martin Hetzer.

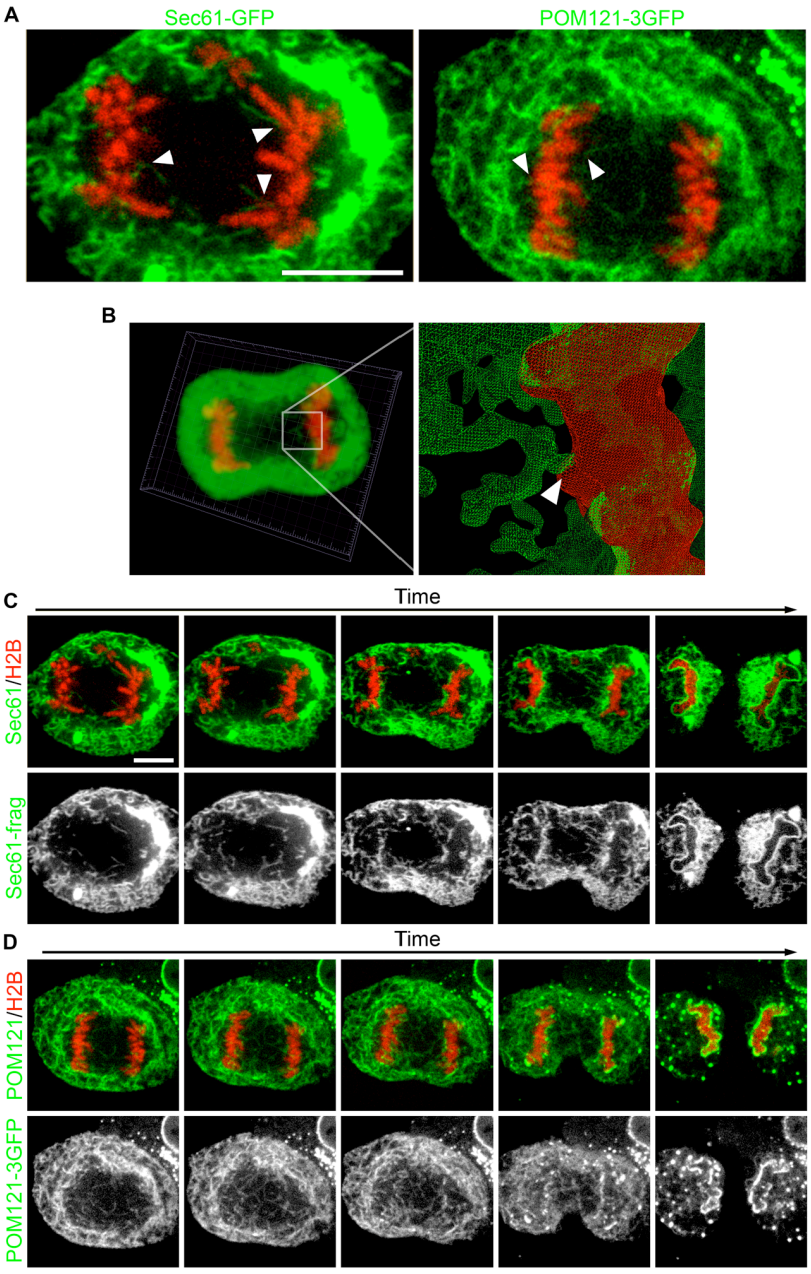

Chapter III Figure 1

ER tubules bind and collapse on chromatin in vivo. U2OS cells were transfected with GFP fusion proteins and H2B-tdTomato and imaged through mitosis with real-time spinning-disk confocal microscopy. (A) Large images of the initial interactions of Sec61-GFP and POM121-3GFP are shown. Arrowheads indicate initial membrane-chromatin contact. (B) Z-stacks were acquired every 30 sec., initial membrane-chromatin contact points were characterized by 3D reconstruction. (C) Sec61-GFP was imaged every 5 sec. to monitor ER dynamics. (D) POM121-3GFP was imaged every 10 sec. to monitor the redistribution from the ER to the forming NE. Scale bars are 10µm.

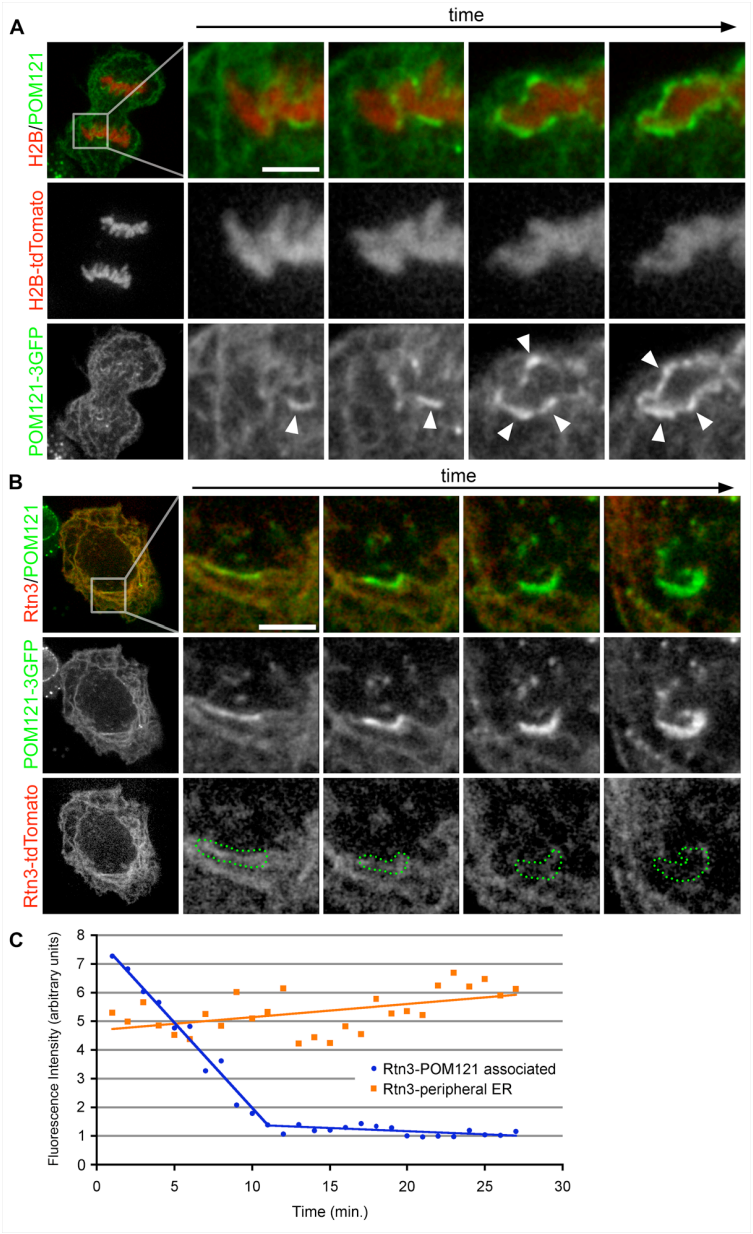

Chapter III Figure 2

Reticulon 3 is removed from NE-forming tubules. (A) U2OS cells were transfected with POM121-3GFP and H2B-tdTomato to monitor the accumulation of POM121 at the forming NE. Scale bar is 5µm. (B) U2OS cells were transfected with POM121-3GFP and Rtn3-tdTomato to monitor the dynamic localization of these proteins at the forming NE. Arrowheads indicate forming NE. Scale bar is 5µm. (C) Intensity threshold selections of accumulating POM121 were used to define the regions of NE formation (dotted green regions in B). Fluorescence intensity of Rtn3-tdTomato was measured in these regions through NE formation (blue circles), intensity was also measured in the peripheral ER (orange squares). Cells were imaged every 30 sec.

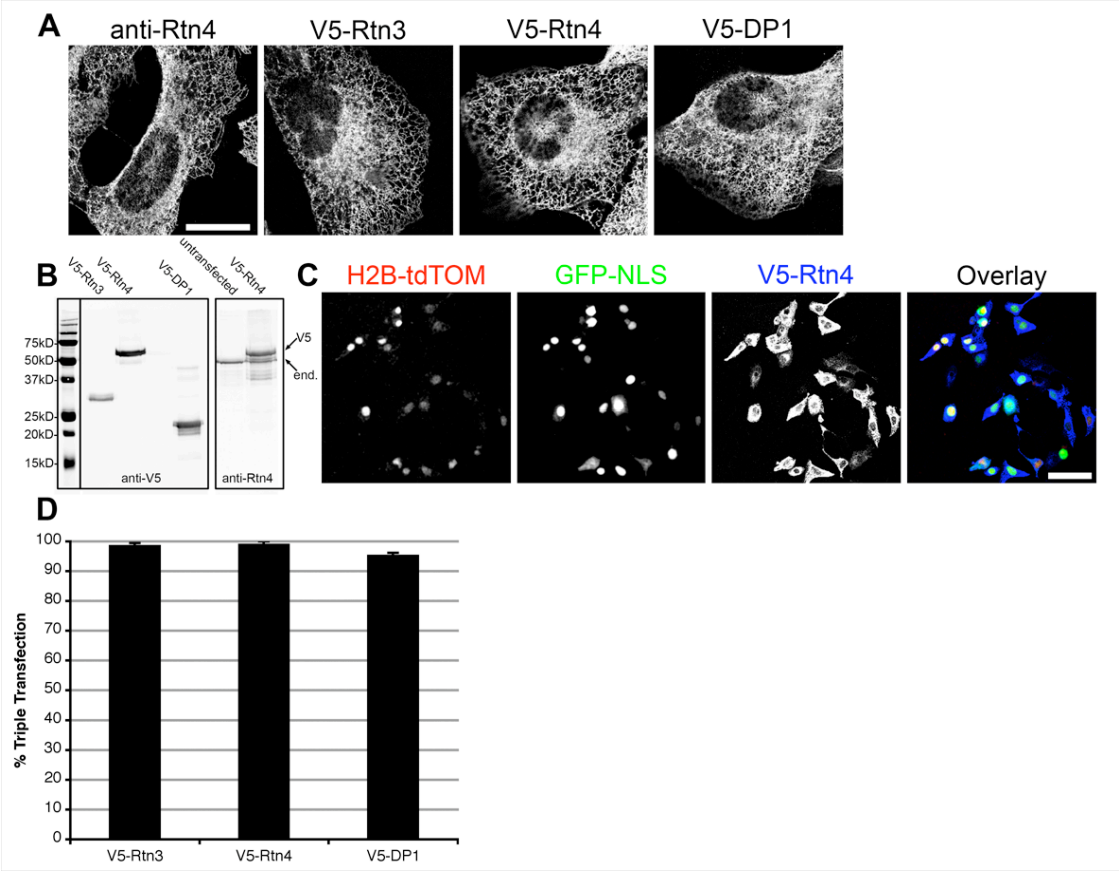

Chpater III Figure 3

U2OS are efficiently transfected simultaneously with three different constructs. (A) U2OS cells were immuno-stained with antibodies against Rtn4 and imaged with confocal microscopy to show endogenous localization (anti-Rtn4). U2OS cells were transfected with V5-Rtn3, V5-Rtn4, V5-DP1 and imaged using V5 antibodies (images 2-4, respectively). Scale bar is 20µm and applies to all panels. (B) U2OS cells were transfected with V5-Rtn3, V5-Rtn4, and V5-DP1 and analyzed by Western blotting using anti-V5 and anti-Rtn4 antibodies. (C) U2OS cells were transfected with H2B-tdTomato, GFP-NLS and V5-Rtn4 and then immuno-stained with anti-V5 antibodies and imaged in three colors. Scale bar is 100µm. (D) The percentage of GFP-NLS, H2B-tdTomato positive cells that were also positive for the indicated V5-tagged proteins.

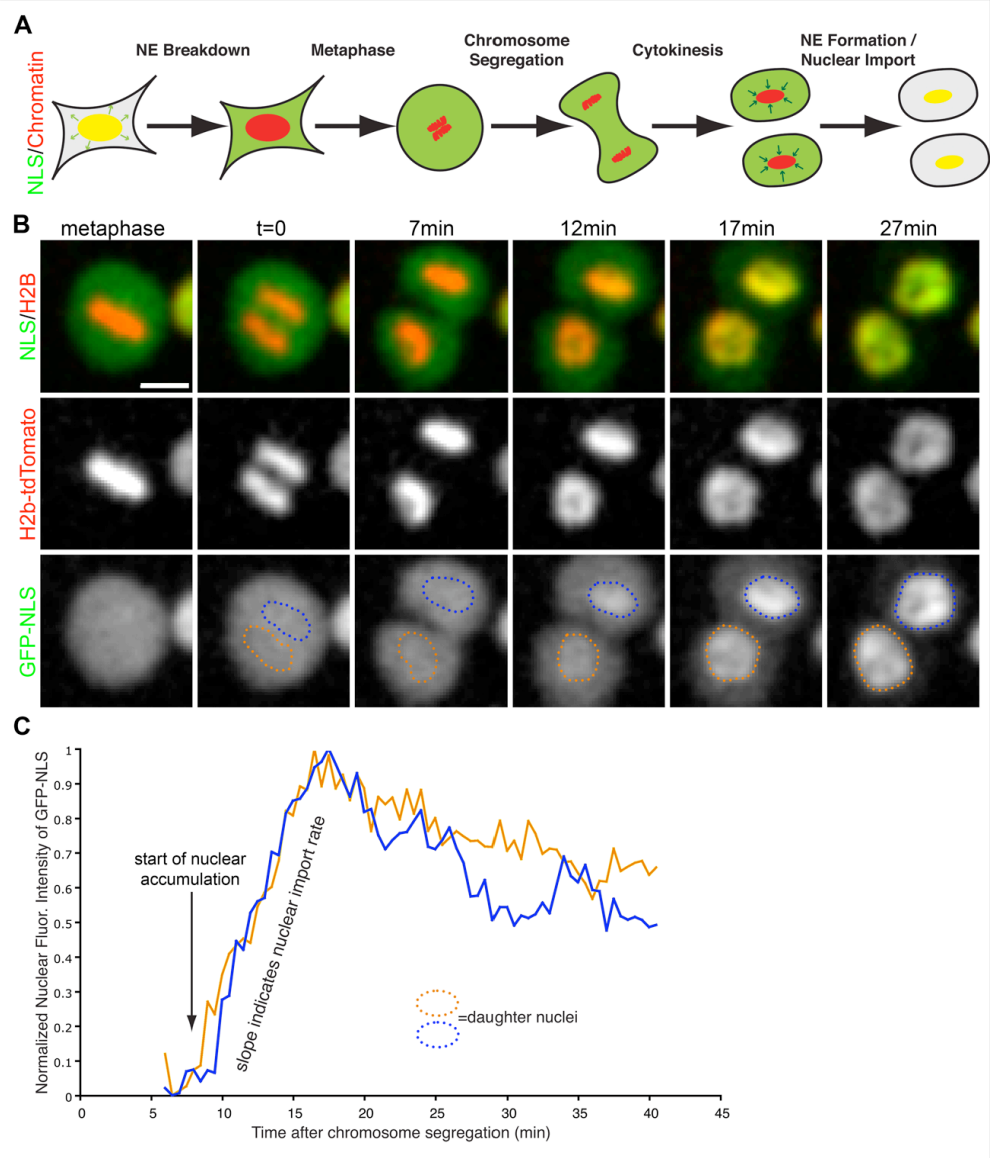

Chapter III Figure 4

Assay developed to measure NE-formation kinetics. (A) Schematic of the dynamic localization of the reporter genes for nuclear localization (NLS) and chromatin during mitosis. Yellow represents the colocalization of NLS (green) and chromatin (red) in the intact nucleus. (B) U2OS were transfected with NLS fused to 3 GFPs (GFP-NLS) and H2B-tdTomato and imaged every 30 sec. through mitosis with live-cell confocal microscopy. Scale bar is 20µm and applies to all panels. (C) After chromosome segregation, regions over chromatin were selected and GFL-NLS intensity was measured over time. t=0 corresponds to when the chromatid clusters have completely separated, blue and orange traces correspond to the nuclear influx of GFP-NLS in each daughter nucleus.

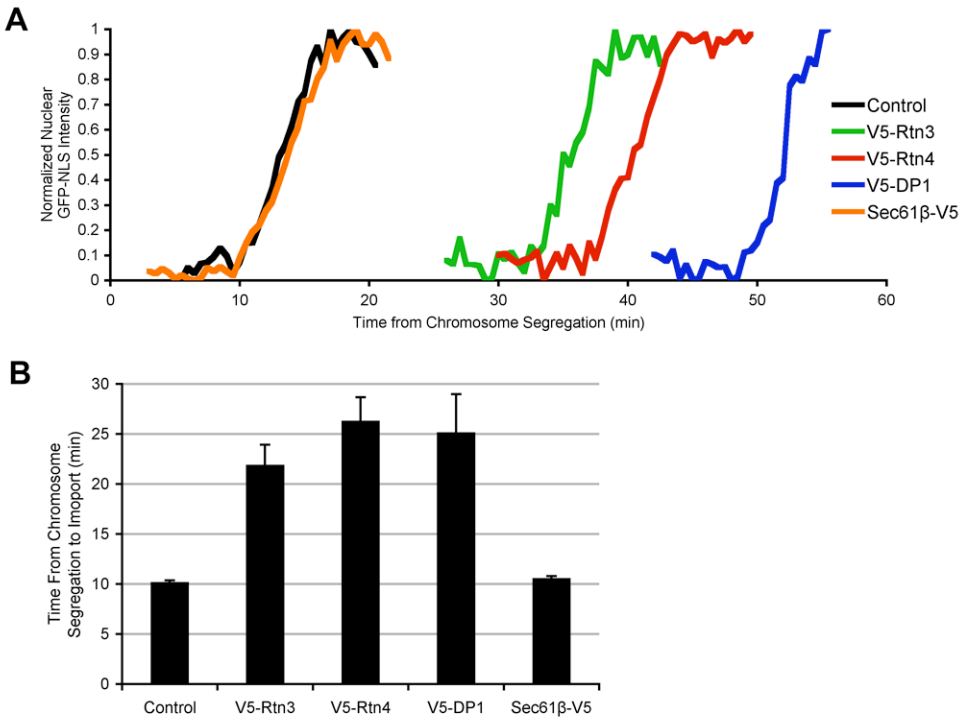

Chapter III Figure 5
ER tubule-shaping proteins delay NE formation. U2OS cells were transfected with GFP-NLS and H2B-tdTomato (control), with V5-tagged ER-shaping protein (Rtn3, Rtn4 or DP1), or with the V5-tagged ER protein Sec61β and NE formation was analyzed. (A) Representative traces of nuclear GFP-NLS intensity during NE formation are shown. (B) Average times from chromosome segregation to the onset of nuclear accumulation are plotted with standard error bars.

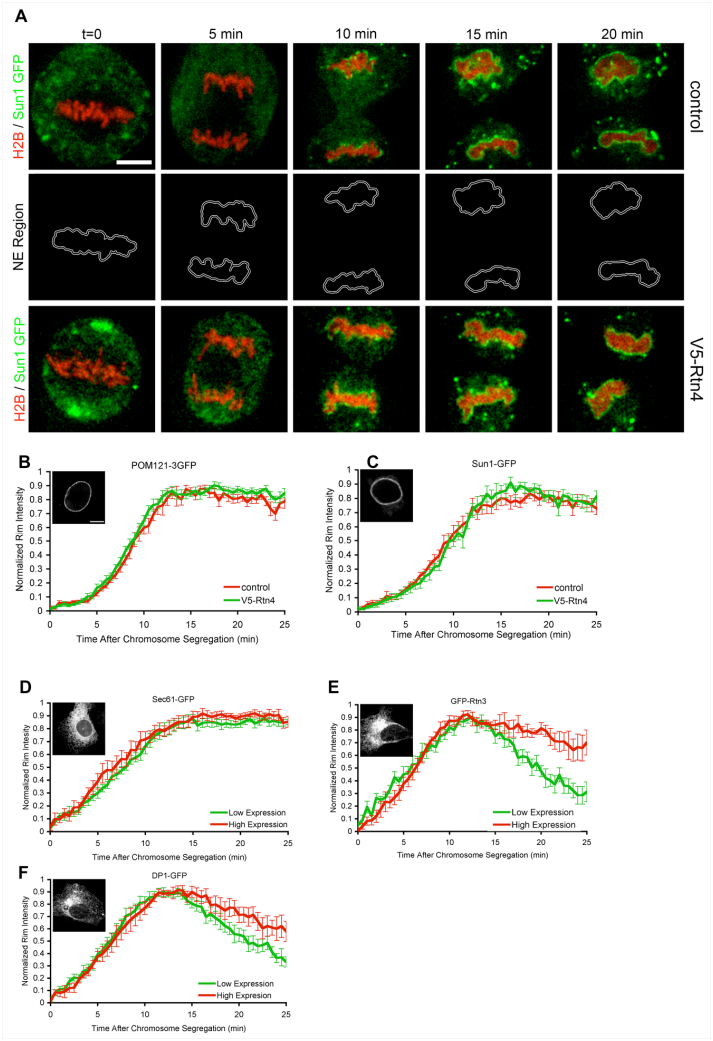

Chapter III Figure 6

NE protein recruitment is not delayed by Rtn4 over-expression. A real-time microscopic assay was established to measure the recruitment of GFP-fusion proteins to the forming NE. (A) U2OS cells were transfected with H2B-tdTomato and Sun1-GFP with or without the over-expression of V5-Rtn4 and imaged every 30 sec. through mitosis. A thin region surrounding the chromatin (NE Region) was selected to measure the intensity of Sun1-GFP at the forming NE. Bar is 10µm and applies to all panels. (B) Fluorescence intensity of POM121-3GFP was measured at the NE Region in control cells (red) or cells expressing V5-Rtn4 (green) starting and the onset of chromosome segregation, then normalized, averaged, and plotted with standard error bars. (C) Cells expressing Sun1-GFP were analyzed as in (B). (D) U2OS cells were grouped for high (red) and low (green) expression of GFP-Sec61 and fluorescence intensity was measured at the forming NE as in A. (E) Cells expressing GFP-Rtn3 were analyzed as in D. (F) Cells expressing DP1-GFP were analyzed as in D. Interphase localization of each GFP-fusion protein is provided as insects in B-F, bar is 5µm and applies to all insets in B-F.

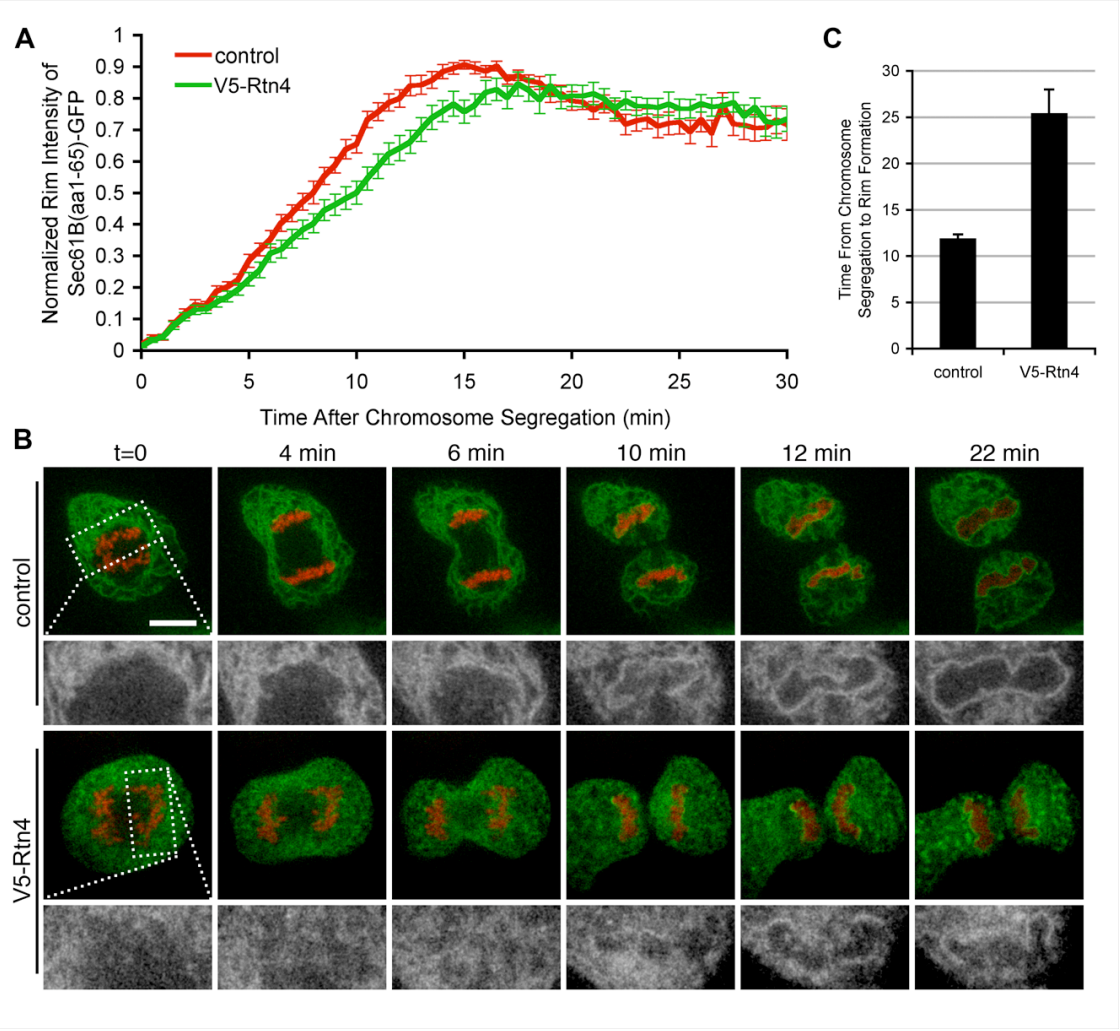

Chapter III Figure 7

NE rim formation is delayed by the over-expression of Rtn4. U2OS cells were transfected with Sec61-GFP and H2B-tdTomato and imaged every 30 sec. in real-time with confocal microscopy to quantify the time required for membrane rim formation. (A) Control cells and cells expressing V5-Rtn4 were imaged to focus on the membrane dynamics at the forming NE (high zoom in lower rows). (B) Time from chromosome segregation to nuclear rim formation was measure and averaged, error bars represent standard error. (C) Recruitment assay described in Figure 6 was used to measure the recruitment of Sec61-GFP in control cells (red) and cells over-expressing Rtn4 (green).

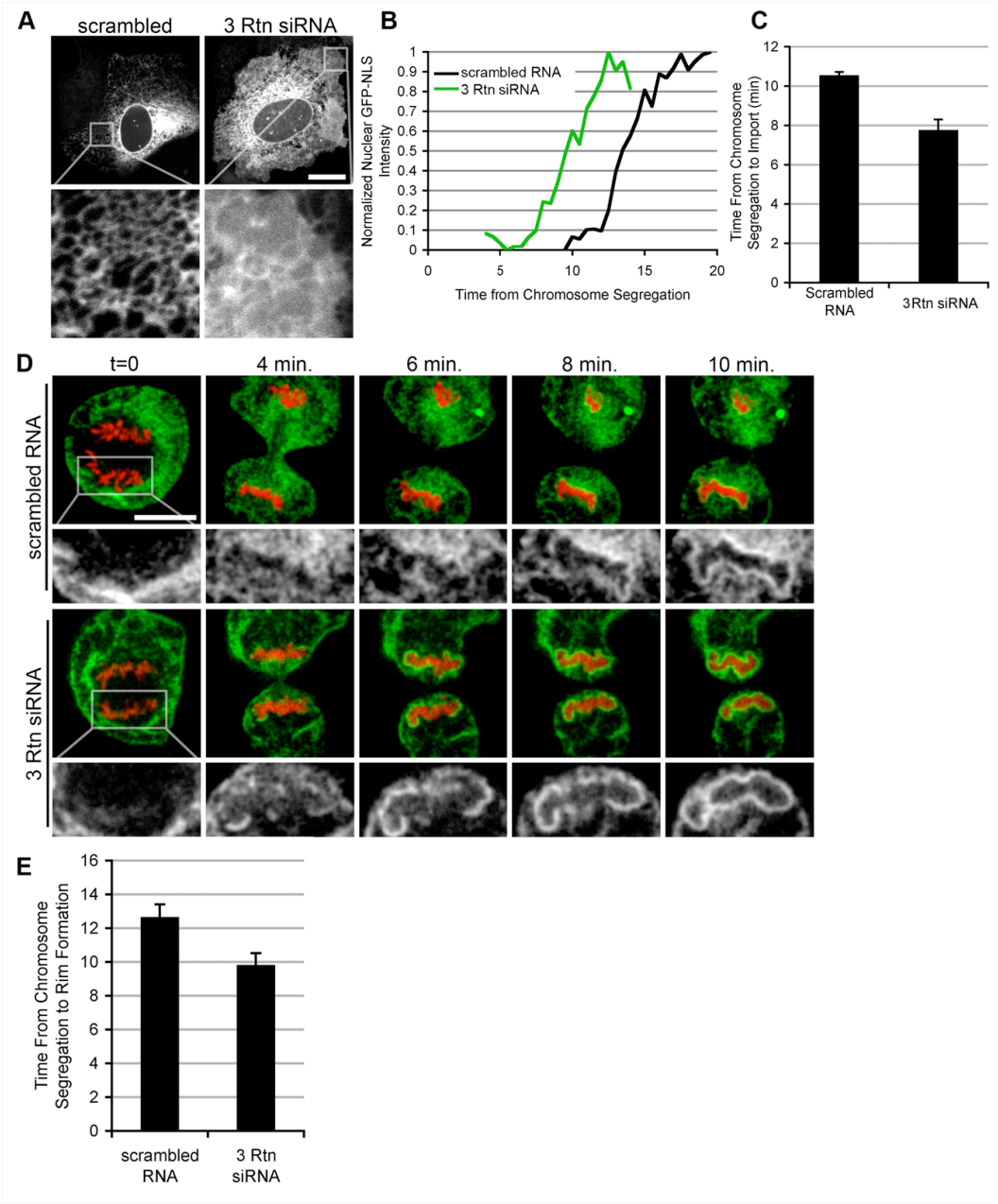

Chapter III Figure 8

Reticulon knock-down accelerates NE formation.

(A) U2OS cells were transfected with Sec61-GFP and scrambled RNA oligos or siRNA oligos directed against Rtn1, Rtn3, and Rtn4 (3 Rtn siRNA). ER morphology was then analyzed with confocal microscopy. Scale bar is 20µm. (B) Cells transfected with scrambled RNA (black) or 3 Rtn siRNA (green) were analyzed using the NE-formation kinetics assay as in Figure 5. (C) Time of NE formation was averaged for cells transfected with scrambled RNA and 3 Rtn siRNA, error bars represent standard error. (D) Nuclear rim was analyzed as in Figure 7 with cells transfected with either scrambled RNA or 3 Rtn siRNA. (E) Time from chromosome segregation to rim formation was averaged. Error bars represent standard error.

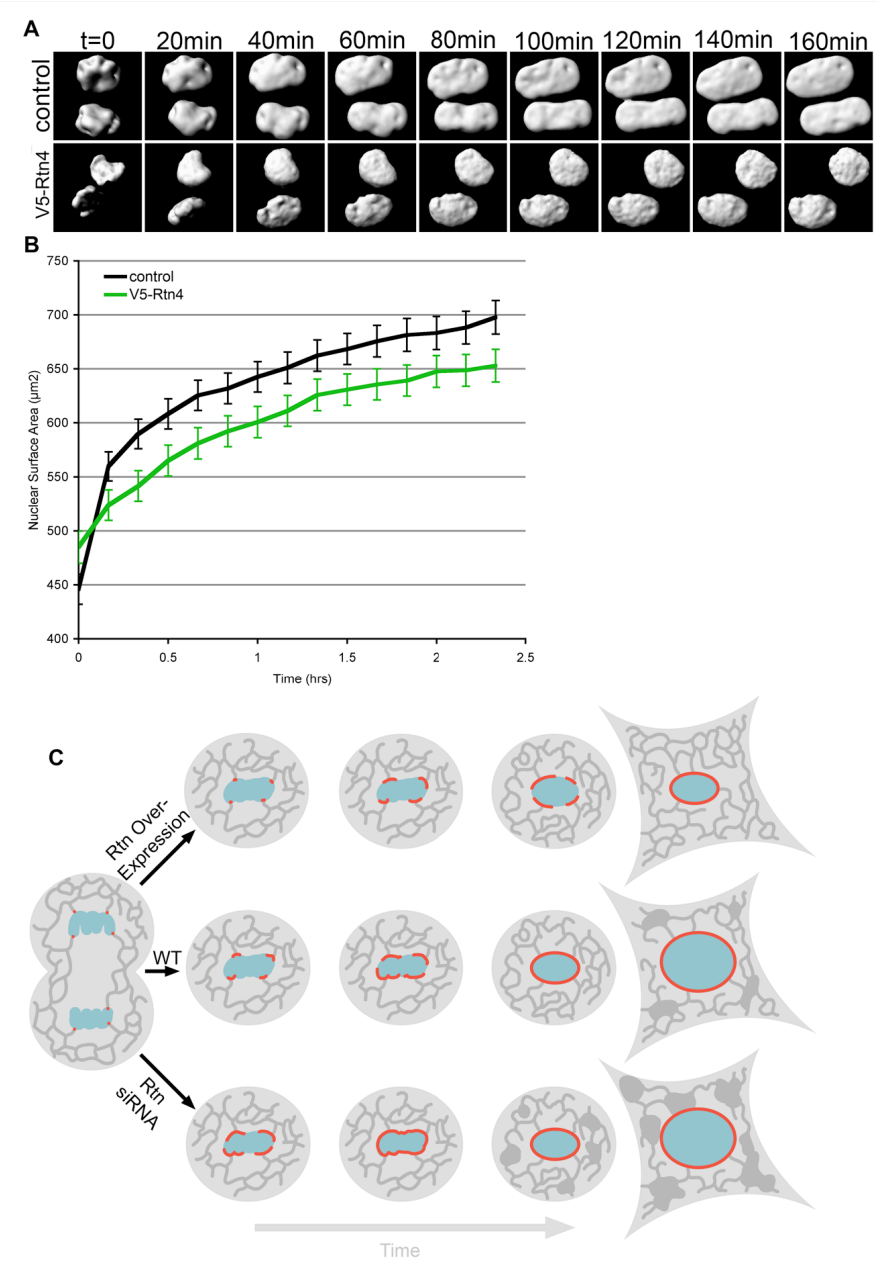

Chapter III Figure 9

Nuclear expansion is inhibited by Rtn4. U2OS cells were transfected with GFP-NLS and imaged every 10 min. in 3D from mitosis through G1 by acquiring z-stacks using confocal microscopy. (A) Nuclear surfaces were re-constructed from z-stacks for control cells and cells over-expressing V5-Rtn4. (B) The surface areas of expanding nuclei were synchronized starting after nuclear accumulation of GFP-NLS and then averaged. Error bars indicate standard error. (C) Schematic shows the affects of ER-shaping protein concentration on NE formation and expansion, where the ER is represented in dark gray, chromatin is represented in blue, and red represents the forming NE.

	Nuclear Accumulation				Rim Formation			
	from chrom. seg.	std. dev.	n	p-value	from chrom. seg.	std. dev.	n	p-value
wild type	10.2 min.	1.5 min.	85	n/a	11.9 min.	2.3 min.	28	n/a
V5-Rtn3	21.9 min.	14.1 min.	49	<0.001	n.d.			
V5-Rtn4	26.3 min.	16.8 min.	51	<0.001	25.4 min.	13.8 min	29	<0.001
V5-DP1	25.2 min.	22.3 min.	34	<0.001	n.d.			
Sec61β-V5	10.6 min.	1.6 min.	54	0.36	n.d.			
scramble RNA	10.6 min.	0.4 min.	19	0.38	12.9 min.	2.7 min.	20	0.2
reticulon siRNA	7.8 min	0.2 min.	57	<0.001	9.7 min.	2.2 min.	17	0.003

Chapter III Table 1
Kinetic events of NE formation. Time from chromosome segregation (from chrom. seg.) to nuclear accumulation and NE rim formation a represented as mean values in minutes. Standard deviation (std. dev.) is provided alone with number of cells measured (n) and t-test calculated p-values.

Chapter IV

Bulk recruitment of functionally distinct membrane proteins to chromatin mediates nuclear envelope formation

Abstract

The formation of the nuclear envelope (NE) around segregated chromosomes occurs by the reshaping of the endoplasmic reticulum (ER), which in mitosis serves as a reservoir for disassembled nuclear membrane components. Utilizing quantitative *in vivo* assays we show that the nucleoporin Ndc1, and inner nuclear membrane proteins such as LBR and Lap2B, bind in a redundant and non-competitive manner to chromatin and thereby mediate the flattening of ER tubules into sheets. Decreasing the levels of any of these trans-membrane proteins by RNAi-mediated knockdown reduced the rate of NE formation, whereas their overexpression had the opposite effect, suggesting that the recruitment of each of these proteins to chromatin is rate-limiting for nuclear assembly. Strikingly, acceleration of NE formation resulted in severe chromosome segregation defects indicating that the time-frame over which chromatin becomes membrane enclosed is tightly regulated. Thus, functionally distinct classes of chromatin-binding membrane proteins collaborate to rapidly re-establish the nuclear compartment at the end of mitosis.

Results

The interphase NE is composed of two concentric lipid bilayers, the inner (INM) and outer nuclear membranes (ONM), which are connected at sites of nuclear pore complex (NPC) insertion [3]. Although the NE is continuous with the endoplasmic reticulum (ER) [12], the INM contains a unique set of membrane proteins that provide functional interactions with chromatin and the nuclear lamina [92]. During cell division, the nuclear compartment disintegrates in order to allow the

mitotic spindle to access chromosomes [93]. During NE breakdown, trans-membrane proteins of the NE are redistributed into the ER network, which remains intact during mitosis [92] and consequently, the sheet-like NE must reemerge from ER tubules. This massive membrane-restructuring event at the end of mitosis was recently shown to be initiated by the recruitment of tubule ends to the chromatin surface. This initial step is followed by the coating of the chromosome mass by a membrane network and the subsequent flattening of these tubules into the sheet-like NE [131]. While these results suggest that chromatin acts as a structural mediator of NE formation, the mechanisms that generate the flat sheets of the nuclear membrane remain unclear.

The flattening of highly curved ER tubules into membrane sheets requires the reduction of the overall membrane curvature. We have recently shown that the removal of reticulons and DP1, membrane-bending proteins that mediate tubule formation [102], from the reforming NE is rate limiting for nuclear assembly. Since in mitosis the ER is entirely tubular and lacks detectable sheets [117], a mechanism must exist that counteracts tubulation by the reticulons and drives the local membrane flattening around chromatin. One class of proteins that, in principle, could fulfill such a function are the trans-membrane proteins of the INM that can bind to chromatin [63, 132] and have previously been implicated in the targeting of membranes to chromosomes [64, 66, 67, 133]. To test the potential involvement of INM proteins in promoting the transition from tubules to sheets on chromatin, we used a kinetic assay that allows us to accurately measure the kinetics of NE formation (Fig. 1A) [134-136]. Briefly, we monitor the time between chromosome separation (t=0), visualized by a

histone H2B-tdTomato reporter, and the onset of nuclear accumulation of GFP-NLS, which marks the completion of NE formation. In all tissue culture cells that we analyzed this process occurs within ~ 10 min. We first reduced the levels of the ubiquitously expressed INM proteins LBR, Lap2B and MAN1 [137-139], as well as BAF, the chromatin binding linker of Lap2B and MAN1, in U2OS cells using RNAi-mediated gene silencing. We were able to lower the levels of each of these proteins by 90% (Fig. 2A), and found that the reduction of each significantly delayed NE formation compared to control cells transfected with scrambled RNA oligos. Knockdown of INM proteins that are not known to bind to chromatin, such as Sun1, or the ER protein Reticulon 4 gave no significant effect in this assay (Fig. 1 B,C and data not shown), suggesting that only a subset of NE proteins are involved in NE formation.

The finding that reducing the levels of either LBR, Lap2b or MAN1 resulted in a significant delay, but not a complete block of NE formation, raised the question whether these proteins act redundantly. It has been shown that INM proteins can bind to DNA through different chromatin associated proteins, for example LBR interacts with HP1[140], whereas LEM domain proteins such as Lap2B and MAN1 bind to BAF[141]. Therefore, it was possible that these INM proteins interact with chromatin at non-overlapping sites during nuclear assembly. Supporting this idea, the knockdown of BAF delayed, but did not block nuclear assembly (Fig. 1 B and C). To further test this idea, we examined the kinetics of NE formation under conditions where levels of both Lap2B and LBR were reduced in combination. Consistent with

the idea that both proteins have non-overlapping functions, nuclear membrane formation was further delayed in cells where both LBR and Lap2B were knocked down when compared to cells in which the levels of only one of the two proteins had been reduced (Fig. 2B), suggesting that these two proteins are rate-limiting for NE formation alone, but act cooperatively in the process. However, the double knockdown of LBR and Lap2B was not able to completely block nuclear assembly, suggesting that additional proteins are involved, and that possibly a large number of proteins may act in a highly redundant fashion to promote NE formation. The latter idea is supported by a recent study that showed many NE proteins, including the integral-membrane nuclear pore protein Ndc1, can bind to DNA [63]. To test the possibility that functionally distinct classes of NE proteins, such as INM proteins and nucleoporins, mediate NE formation, we tested the knock down of Ndc1 in our assay [142]. Strikingly, Ndc1 reduction slowed the rate of nuclear membrane formation, suggesting that mediators of this process are not confined to the INM, and that functionally distinct classes of proteins are involved in NE formation (Fig. 1 B and C). Importantly, reduction of Ndc1 did not reduce the rate of transport as judged by the slope of nuclear GFP-NLS accumulation (Fig. 1B), suggesting that the observed delay in NE formation was not due to a defect in NPC assembly or transport. Taken together, these findings suggest that different classes of integral membrane proteins of the NE that bind to chromatin collaborate in a highly redundant manner to promote NE formation, and also establish a novel mitotic function for the nucleoporin Ndc1.

Since NE formation proceeds through two distinct steps, i.e. the targeting of membranes to chromatin and flattening into sheets, we wanted to determine if the observed delay in the NE timing reflected a block in membrane targeting or sheet formation. To discriminate between these two steps we used a recently developed experimental strategy and measured the fluorescence intensity of Sec61-GFP, an ER marker [119], at the forming NE (Fig. 2C). Since Sec61-GFP does not bind to chromatin and does not accumulate at the NE, but provides a fluorescent readout of the amount of NE that surrounds chromatin at any given time point, it is a useful tool for examining membrane dynamics at the chromatin surface. Reduction of Lap2B or BAF did not significantly delay the increase in Sec61-GFP intensity during early stages of NE formation, however, knock down of either protein was able to significantly reduce Sec61-GFP intensity during the last few minutes of NE formation, suggesting that the final expansion and closure, but not initial targeting of membranes, are affected by the reduction of each of these proteins (Fig. 2D). Furthermore, reduction of either Lap2B, BAF or Ndc1 protein levels delayed the appearance of a nuclear rim (green arrows), which is an indicator of the formation of a flat NE (Fig. 1D and E). Together, these data suggest that Lap2B, BAF and Ndc1 function directly in membrane spreading around chromatin.

Our findings that multiple NE proteins collaborate in nuclear membrane formation in a redundant manner, yet knockdowns of a single components result in a significant delay in nuclear assembly, suggested that this process involves multiple rate limiting steps. If this were the case, it is possible that the concentrations of

chromatin-binding NE proteins are non-saturating at endogenous levels, and that an excess of binding sites may exist on chromatin. Due to this possibility, and the large number of NE proteins that are thought to interact with chromatin [63], we next wanted to determine if these proteins are saturated in the process of nuclear assembly at endogenous concentrations. To test this we increased the levels of NE formation mediators by over-expression. Epitope-tagged versions of Lap2B, LBR, and Ndc1 were found to properly localize to the nuclear rim, and BAF colocalized with chromatin when transfected in U2OS cells (Fig. 4A). Western blot analysis showed that these proteins expressed between ~2.5-8.8 times endogenous levels (data not shown). Surprisingly, over-expression of Lap2B, LBR, BAF or Ndc1 accelerated nuclear formation, suggesting that these NE-chromatin interacting proteins act as promoters of membrane recruitment to chromatin (Fig. 3 A and B). Confirming that the observed acceleration was specific to the over-expression of chromatin interacting proteins, Nesprin 3a, an integral membrane protein of the ONM [143], had no significant effect on the timing of nuclear assembly (Fig. 3 A and B). Furthermore, NE formation could not be further accelerated by the increased expression of multiple nuclear promoting proteins suggesting that rate-limiting steps defined by other aspects of nuclear assembly may be reached (data not shown, see below).

Acceleration of NE formation with the increased expression of these NE-membrane proteins further supports the idea that their targeting to the NE is not saturated at endogenous levels. To test this directly, a GFP-fusion of Lap2B was transfected into U2OS cells and the efficiency of NE targeting was measured at 20

min. after chromosome separation (Fig. 3C). Consistent with idea that endogenous levels of Lap2B are not saturated at the forming NE, expression levels of GFP-Lap2B did not effect its NE targeting. Taken together, these finding suggest that proteins involved in the flattening of membranes on chromatin promote NE assembly, and that at endogenous concentrations, these proteins limit the rate of nuclear assembly.

The idea that NE formation promoting proteins are endogenously present at sub-saturating levels suggests that an excess of binding sites are present on chromatin. To test this hypothesis, we expressed the DNA and BAF interacting domains of Lap2B (Fig. 5A and Fig. 6A) to see if chromatin binding sites of endogenous Lap2B would be blocked [133, 141]. When the DNA binding domain, the LEM domain or a protein fragment containing both of these domains were over-expressed in U2OS cells, nuclear formation was significantly delayed suggesting that these soluble fragments act as competitive inhibitors for the targeting of endogenous Lap2B, or other LEM-domain INM proteins to chromatin (Fig. 5B). To directly test if chromatin-binding fragments of Lap2B were competing with endogenous protein, V5-Lap2B aa1-187 was transfected into U2OS cells and endogenous Lap2B was labeled with immunohisto-chemistry (Fig. 5C). In cells expressing the chromatin-binding fragment, endogenous Lap2B staining with antibody unable to recognize the fragment was found to be greatly reduced at the NE in early G1 cells, and was mainly found in peri-nuclear aggregates, suggesting a competitive inhibition by this fragment. Interestingly, in cells where endogenous Lap2B was displaced, LBR targeting was unaffected, suggesting that these proteins bind to different sites on chromatin

consistent with their proposed non-competitive redundancy (Fig. 6B). Together these data suggest that Lap2B acts to promote NE assembly by tethering of the trans-membrane domain to distinct chromatin regions.

Over-expression of trans-membrane proteins can induce the formation of membrane sheets independently of a scaffold structure [144]. Therefore it was important to test if the observed increase in NE formation was in fact due to the ability of INM proteins to bind to chromatin. When a fragment containing the lamin binding and transmembrane domains of Lap2B was expressed in U2OS cells no change in the rate of NE formation was detected (Fig. 5B), suggesting that tethering of the transmembrane domain to the chromatin interacting domains is required for promoting nuclear membrane formation. Furthermore, these data precludes structural changes that may be induced by the over-expression of the trans-membrane domain as the cause for acceleration of NE formation. Additionally, the lack of rate change with lamin binding domain expression suggested that lamins were disconnected from NE formation. To test this we used siRNA-mediated reduction of lamin A and C, B1, B2, or all four in combination to analyze their contribution to NE formation. Strikingly, the reduction of all lamins did not block nuclear assembly (Fig. 8 A and B). However, lamin B2 knockdown significantly slowed the rate of NE formation (Fig. 8 A and B). Interestingly, lamin B2 has been shown to reside in the mitotic ER, possibly as a result of its anchoring by tight interaction with LBR [145, 146]. In summary, *in vivo* analysis of Lap2B protein fragments provides evidence that bridges between

membranes and chromatin are formed by INM proteins, which act to drive NE formation.

Our data suggest that endogenous concentrations of NE-promoting trans-membrane proteins limit the rate of nuclear assembly, as when they are over-expressed the process is accelerated (Fig. 3 A and B). Similarly, NE formation is also limited by endogenous levels of the ER-shaping Reticulon proteins [135]. However, Reticulons negatively regulate in NE formation, and when these proteins are reduced nuclear assembly is accelerated to a greater extent than that observed with increased expression of NE-promoting proteins. These findings suggest a tug-of-war mechanism between reticulons and their activity to form tubules and NE proteins involved in membrane flattening (Fig. 5D). The unexpected finding that NE formation can be accelerated raised the interesting question: is NE formation timing crucial for cell cycle progression? To analyze the mitotic consequence of changing the rate of NE formation, nuclear assembly was accelerated in U2OS cells by siRNA-mediated reduction of Reticulons 1, 3 and 4. In cells with reduced Reticulons a striking impairment in the segregation of chromosomes was observed (Fig. 7A and B). This block in chromosome segregation appeared to be caused by rapid spreading of membranes around the chromosome clusters before adequate separation occurred. Impairment in chromosome segregation occasionally led to joining of the nuclear membrane between daughter nuclei (Fig 7A). This suggests that regulating the rate of NE formation is important in coordination with other mitotic events. Interestingly, alteration of protein concentration of promoting or repressive regulators of NE

formation never caused acceleration greater than ~2.5 min., suggesting that an additional level of regulation is present. One possibility is that dephosphorylation of NE-promoting proteins is initiated during anaphase and required for targeting of these proteins to chromatin.

In summary, we propose that during NE formation chromatin serves as platform to utilize the intrinsic propensity of the ER to efficiently transition between tubule and sheets. In order to shift the equilibrium of the reaction towards sheet formation, NE proteins collaborate to cover the entire chromosome mass with a membrane sheet in less than 12 minutes. Independent of their function in interphase, such as chromatin organization or gene regulation, the common trait of all the proteins shown to mediate NE formation is their ability to bind to chromatin. In principle the number of NE-forming trans-membrane proteins might be substantial, as ~ 40 NE proteins exhibit potential DNA binding domains. We also suggest that the redundancy in using a large number of NE proteins provides a fail-safe mechanism, increasing the reliability of NE formation by the multiplication of critical components. In such a system, if a single NE promoting protein fails to target, NE formation can still be accomplished. Despite the observed redundancy, it is striking that each of these proteins contributes to the overall rate of NE formation. In light of the finding that acceleration of NE formation causes a mitotic defect, the regulatory role of NE-membrane proteins may be physiologically relevant. Consistent with this idea, the expression of Lap2B was recently shown to be up regulated in certain cancers [147]. Combined with the excess of binding sites on chromatin, this unique mechanism,

which temporarily uses functionally distinct classes of membrane proteins for chromatin targeting and tethering explains both the rapid depletion of these proteins from the ER [134], and the rapid transformation of membranes around the chromatin mass.

Methods

Molecular constructs and antibodies

Human Lap2B, LBR, BAF, Ndc1 and Nesprin 3a were amplified by PCR from IMAGE clones and inserted into the V5 containing pcDNA6.2/Lumio (V5 of either amino or carboxyl-terminus) vectors using Gateway cloning (Invitrogen™). Fragments of human Lap2B were amplified by PCR and inserted into pcDNA6.2/Lumio by Gateway cloning. Full-length Lap2B was also inserted into the n-terminal GFP containing vector pCDNA6.2/Dest53 vector using Gateway cloning. Sec61-GFP and H2B-tdTomato were previously described [135]. Antibodies against V5 (mouse Invitrogen, rabbit Novus Biological®), BAF (Novus) and LBR (Abcam, ab32535) are commercially available. Antibodies against Lap2B were a kind gift from the lab of Roland Foisner. Antibodies against Ndc1 were a kind gift from the lab of Ulrike Kutay [142]. Monoclonal antibodies against the V5 epitope were used at a dilution of 1:1000 for indirect immuno-fluorescence and 1:5000 for Western blotting. Monoclonal antibodies against Lap2B were used 1:1 for both indirect immunofluorescence and Western blotting. Antibodies against BAF were used at a dilution 1:500 for Western blotting. Antibodies against LBR were used at a dilution

of 1:1000 for western blotting. Antibodies against Ndc1 were used at a dilution of 1:500 for Western blotting.

Cell transfection and live-cell imaging

U2OS cells were grown and imaged in DMEM with 10% fetal bovine serum with 1X antibiotic-antimycotic (Gibco™). Cells were plated on 8-well µ-slides (ibidi) and transfected with 0.6 µl Lipfectamine2000 (Invitrogen™) and 0.3µg of each DNA construct two days prior to live-cell imaging as recommended by Invitrogen™. For siRNA knockdown, cells were transfected 25nmol of RNA two and four days prior to imaging. siRNA oligo sequences used were as follows: Lap2B: AGGCAUUAACUAGGGAAUdTdT, LBR: LBR Stealth™ Select RNAi HSS105976, BAF: GGCCUAUGUUGUCCUUGGCdTdT, Ndc1: CUGCACCACAGUAUUUAUA, Rtn1: UAGAUGCGGAAACUGAUGGTT, Rtn3: CCUUCUAAUUCUUGCUGAATT, Rtn4: GAAUCUGAAGUUGCUAUATT, scrambled: UAGAUACCAUGCACAAUCCTT (Invitrogen™). Live cells were imaged at 37˚C maintained by air stream incubator and enriched with CO_2 (Solent Scientific). Time-lapse images were taken on a spinning disk confocal microscope (McBain Instruments) built around a DMRIE2 inverted stage microscope (Leica). Images were captured on an EM-CCD digital camera (Hamamatsu) and acquired using SimplePCI (Compix). Cells were imaged using a 63x oil objective with a 1.4 numerical aperture (Leica).

Image analysis and statistics

Images were analyzed and statistics used were as previously published [135].

Acknowledgments

We thank Maximiliano D'Angelo, Maya Capelson, Christine Doucet, Sebastian Gomez, Robbie Schulte and Jessica Talamas for critically reading the manuscript and helpful discussion. This work was supported by a grant from NIH (R01 GM073994).

Chapter 4, in full, consists of the following manuscript submitted for publication in *Science*

Jesse Vargas and I were the primary researchers and authors for these studies under the supervision and direction of Martin Hetzer. Joshua Hsia contributed the cloning of constructs used in this study.

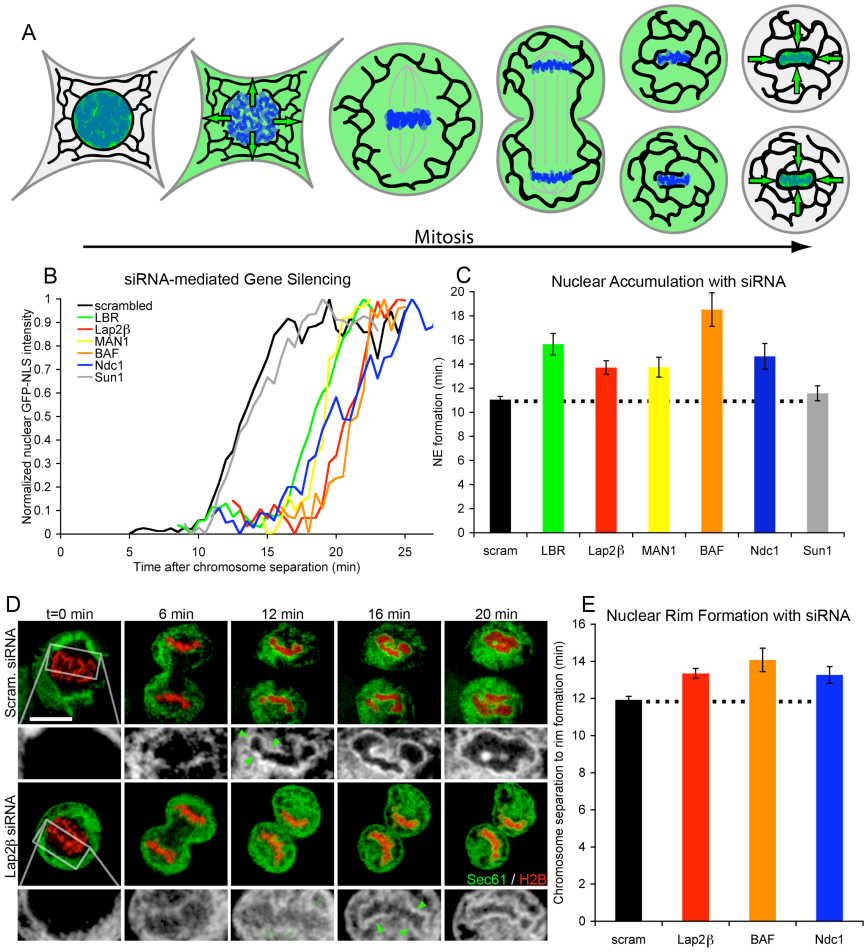

Chapter IV Figure 1

Chromatin-binding NE proteins act redundantly during nuclear membrane assembly. (A) A schematic diagram shows the dynamic localization of nuclear-targeted GFP (green) throughout open mitosis. Re-accumulation of GFP-NLS into the daughter nuclei serves as an indicator for completed NE formation. (B) Cells were transfected with H2B-tdTomato and GFP-NLS and imaged through mitosis. Representative traces of chromatin-localized GFP-NLS where t=0 is set at the onset of chromosome separation show the time required for NE formation in U2OS cells with reduction of protein levels by siRNA-mediated gene knockdown. (C) Average time from chromosome separation to GFP-NLS nuclear accumulation was plotted with standard error bars. >20 cells where analyzed for each condition with $p<0.01$ when LBR, Lap2B, MAN1, BAF or Ndc1 siRNA was compared to scrambled RNA control and $p=0.4$ for Sun1 (t-test). (D) U2OS cells were transfected with H2B-tdTomato (red) and Sec61-GFP (green, black and white insets) and imaged from mitosis. Nuclear rim formation was compared in cells transfected with scrambled RNA or siRNA against Lap2B (green arrows). After 12 min. no nuclear rim was detected with the knockdown of Lap2B (open arrows) compared to clear rim signal present in scrambled siRNA controls. Scale bar is 20µm. (E) Average time from chromosome separation to complete nuclear rim formation potted with standard error bars. $p<0.01$ when Lap2B, BAF or Ndc1 knockdown was compared to scrambled RNA.

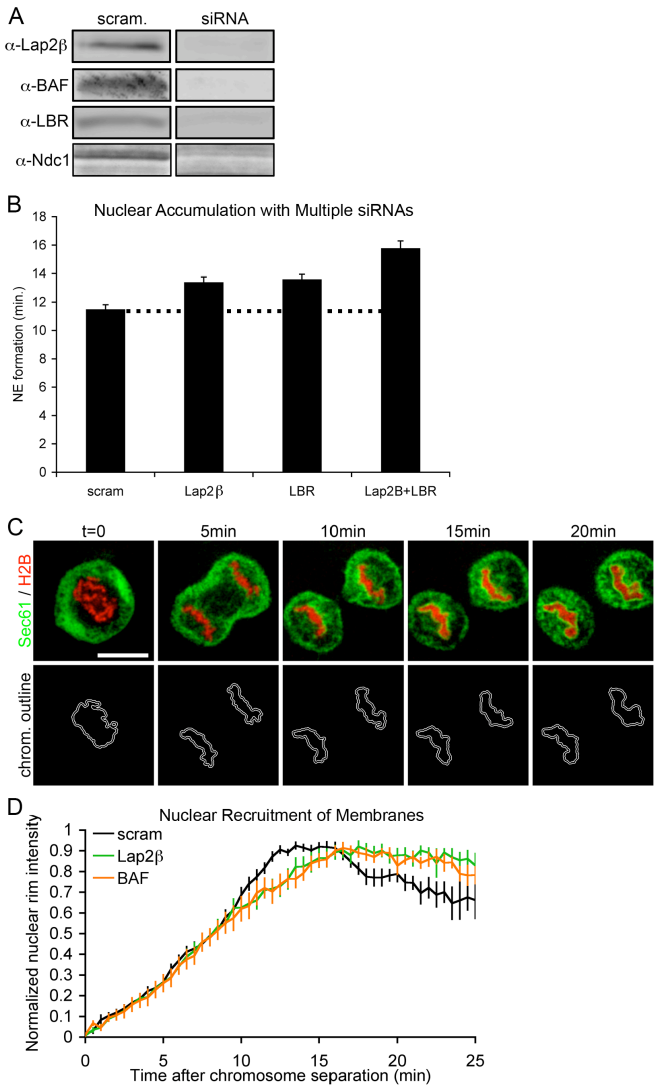

Chapter IV Figure 2

Reduction of chromatin binding proteins delays accumulation of membranes at the chromatin surface during NE formation. (A) Reduction of protein levels by siRNA-mediated gene silencing was measured by Western blot analysis using antibodies that detect endogenous Lap2B, BAF, LBR or Ndc1. (B) NE formation time was measured after partial knockdown of Lap2B, LBR, or both with a single round of siRNA transfection. >30 cells were analyzed for each condition, $p<0.001$ when Lap2B or LBR were compared to scrambled, or when Lap2B+LBR was compared to Lap2B or LBR alone. (C) Intensity of the Sec61-GFP at the forming NE was quantified by measuring fluorescence signal in a boarder directly around chromatin over time with t=0 set at the metaphase to anaphase transition. Scale bar is 20µm. (D) Sec61-GFP intensity at the forming NE was measured in cells where Lap2B (green) or BAF (orange) protein levels were reduced by siRNA and compared to cells transfected with scrambled siRNA (black). Error bars represent standard error.

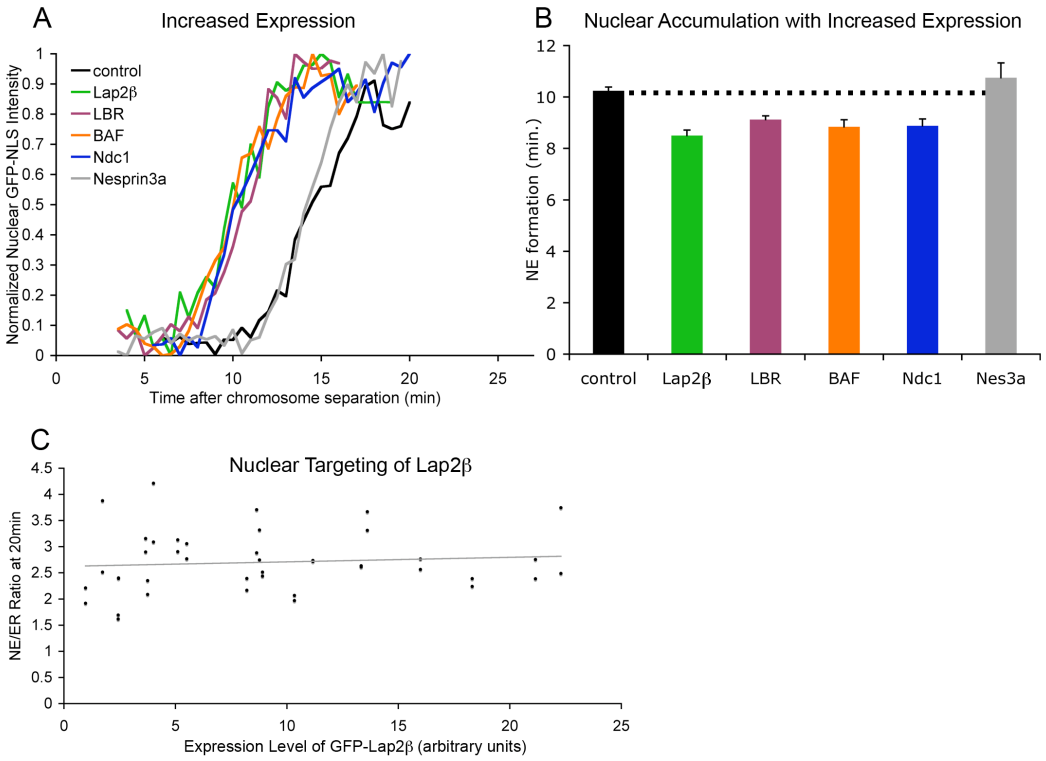

Chapter IV Figure 3

Chromatin-interacting NE proteins promote nuclear assembly. (A) Cells were transfected with H2B-tdTomato and GFP-NLS and imaged through mitosis. Representative traces of chromatin-localized GFP-NLS where t=0 is set at the onset of chromosome separation show the time required for NE formation in U2OS cells where protein levels were increased by transfection with epitope-tagged constructs. (B) Average time from chromosome separation to GFP-NLS nuclear accumulation was plotted with standard error bars. >20 cells where analyzed for each condition. $p<0.001$ when Lap2B, LBR, BAF or Ndc1 increased expression was compared to control cells and $p=0.2$ for nesprin 3a (Nes3a). (C) U2OS cells were transfected with GFP-Lap2B and H2B-tdTomato and imaged through mitosis. Average GFP fluorescence intensity was measured over entire cell to determine expression level and plotted against the ratio of GFP-Lap2 at the NE to peripheral GFP-Lap2 (NE/ER ratio).

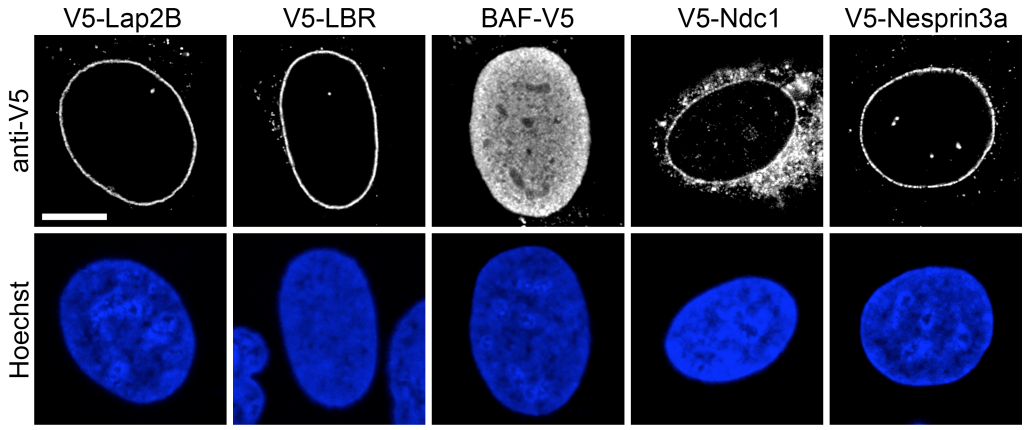

Chapter IV Figure 4
Localization of V5-tagged constructs. Localization of V5-tagged Lap2B, LBR, BAF, Ndc1 and Nesprin 3a was characterized by immunofluorescence. Scale bar is 20µm.

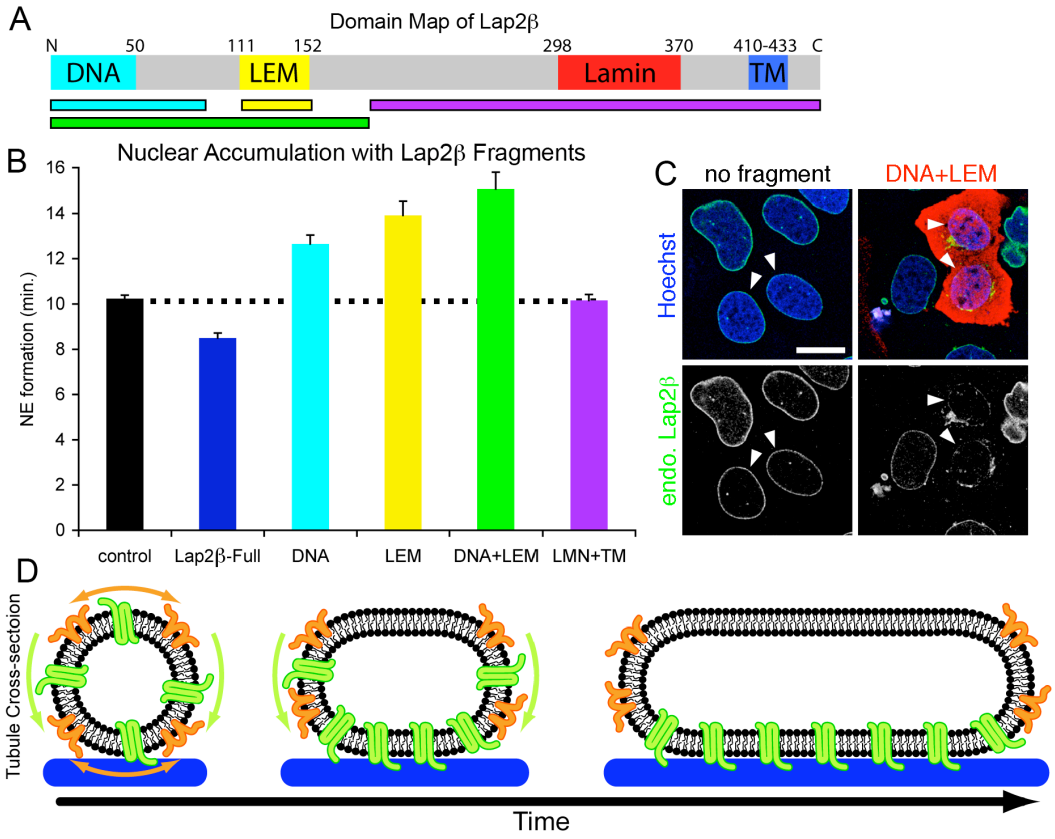

Chapter IV Figure 5

Domain analysis of Lap2B reveals a membrane-chromatin tethering function in NE formation. (A) Schematic map of Lap2B highlights distinct functional domains that interact with DNA, BAF (LEM), Lamins and lipid bilayer (TM). (B) NE formation time was measured with the expression of Lap2B fragments. >40 cells where analyzed for each fragment, $p<0.001$ for the expression of DNA, LEM and DNA+LEM fragments when compared to control cells, $p=0.4$ for LMN+TM. (C) U2OS cells were transfected with the V5-DNA+LEM fragment of Lap2B and stained with antibodies against V5 (red) and endogenous Lap2B (green). Arrowheads indicate early G1 cells as indicated by nuclear size and paired orientation, scale bar is 20µm. (D) Cross-sectional schematic of a membrane tubule expanding onto chromatin (blue). Reticulons (orange) are displaced from the flat membrane where INM proteins (green) are targeted to chromatin and drive membrane expansion around chromatin.

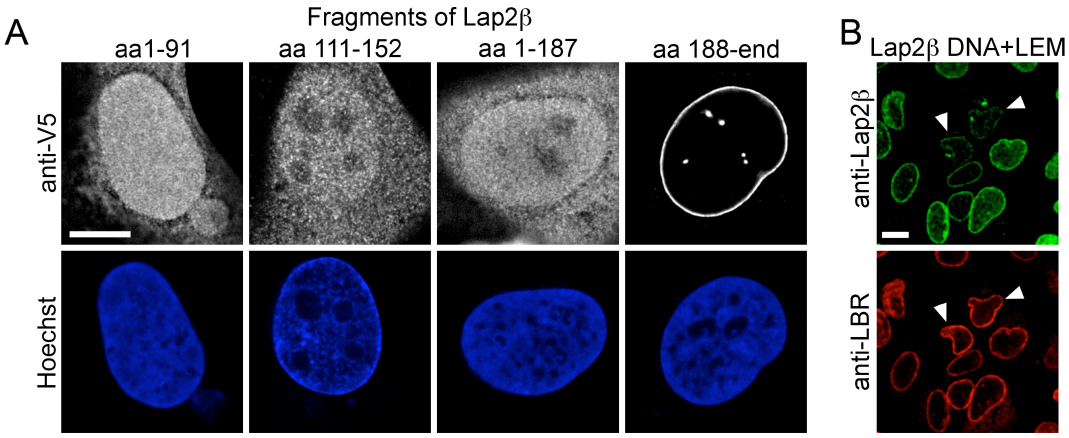

Chapter IV Figure 6
Chromatin Binding domain of Lap2B does not displace LBR. (A) Localization of V5-tagged fragments of Lap2B was characterized by immunofluorescence. Scale bar is 20µm. (B) U2OS cells were transfected with the DNA+LEM fragment of Lap2B and stained with antibodies against endogenous Lap2B and LBR. Arrowheads indicate cells where endogenous Lap2B, but not LBR, is displaced by the chromatin-binding domain of Lap2B. Scale bar is 20µm.

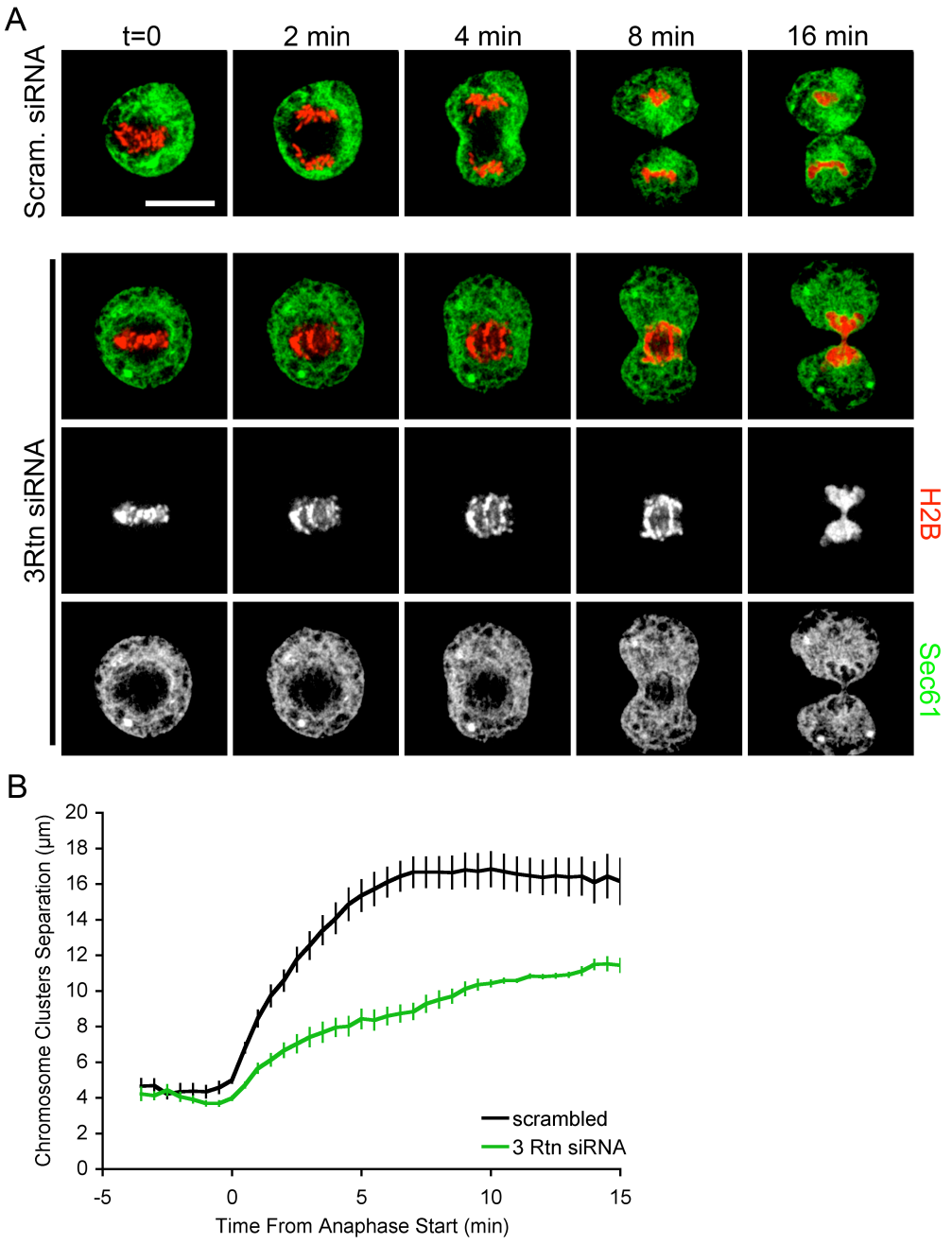

Chapter IV Figure 7
Acceleration of nuclear membrane formation causes a defect in chromosome segregation and cellular division. (A) Mitosis was analyzed by transfecting U2OS cells with Sec61-GFP (green) and H2B-tdTomato (red) and comparing control cells to cells where NE formation was accelerated by the siRNA-mediated knockdown of Reticulon 1, 3 and 4. Arrowheads indicate fusion between daughter nuclei, scale bar is 20µm. (B) Distance between chromosome clusters was measured, t=0 represents initiation of chromosome separation.

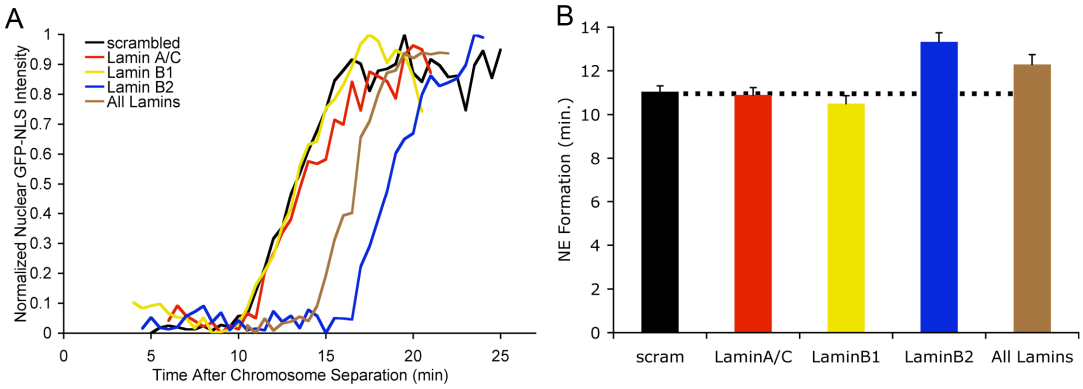

Chapter IV Figure 8

Lamin B2 contributes to nuclear assembly. (A) Cells were transfected with H2B-tdTomato and GFP-NLS and imaged through mitosis. Representative traces of chromatin-localized GFP-NLS where t=0 is set at the onset of chromosome separation show the time required for NE formation in U2OS cells with reduction of protein levels by siRNA-mediated gene knockdown. (B) Average time from chromosome separation to GFP-NLS nuclear accumulation was plotted with standard error bars. >30 cells where analyzed for each condition with $p<0.01$ when Lamin B2 or all Lamins were knocked down and $p>0.1$ when Lamin A and or Lamin B1 were knocked down (t-test).

Chapter V

Nuclear Pores Form De Novo From the Nucleoplasmic and Cytoplasmic Sides of the Nuclear Envelope

Abstract

Nuclear pore complexes are multiprotein channels that span the double lipid bilayer of the nuclear envelope. How new pores are inserted into the intact nuclear envelope of proliferating and differentiating eukaryotic cells is unknown. Here we found that the Nup107-160 complex was incorporated into assembly sites in the nuclear envelope from both the nucleoplasmic and the cytoplasmic sides. Nuclear pore insertion required the generation of RanGTP in the nuclear and cytoplasmic compartments. Newly formed nuclear pore complexes did not contain structural components of preexisting pores, suggesting that they can form de novo.

Results

Nuclear pore complexes (NPCs) are the exclusive sites of trafficking between the nucleus and the cytoplasm [6, 148] and their biogenesis is crucial for the differentiation and metabolic activity of eukaryotic cells [149]. In proliferating cells, the number of pores doubles during interphase prior to mitosis [88, 150]. It is unclear whether NPC assembly occurs from the nucleoplasmic and/or cytoplamsic side(s) of the nuclear envelope (NE) [93]. It is also unknown whether existing NPCs serve as templates for new pores or whether NPCs assemble de novo [3, 151, 152].

To distinguish between these possibilities we analyzed NPC assembly into intact NEs in vitro and in vivo. First, we established a cell-free NPC insertion assay using Xenopus egg extracts [51]. We preassembled nuclei (NE-0) by incubating sperm chromatin and cytosol together with fluorescently labeled membranes [100]. NE-0

nuclei were incubated for an additional period of 80 min (NE-80), during which growth and NE expansion occurred (Fig. 1A). Both NE-0 and NE-80 nuclei were intact and excluded 70 kDa dextran (Fig. 1A). NPCs were monitored with mAb414, an antibody that recognizes four nucleoporins [153] (Fig. 1A). During nuclear growth the density of NPCs remained constant at 4.9 ± 0.6 NPCs/μm^2, indicating that new NPCs had been inserted into the expanding NE.

Using 3D reconstructions of entire nuclei and visualization of individual NPCs by immunofluorescence (Fig. 2 A-C) we found that the NE expanded from 920 ± 104 μm^2 in NE-0 to 3100 ± 229 μm^2 in NE-80 and the number of NPCs increased from 4400 ± 651 to 15800 ± 1054 NPCs (Fig. 1A, B). NPC insertion occurred steadily at a rate of 142 ± 11 NPCs/min.

The insertion of new pores into intact nuclei occurs in the presence of nucleo-cytoplasmic transport, which is driven by the small GTPase Ran [148, 154]. To test whether Ran-mediated transport was required for pore formation we incubated NE-0 nuclei with cytosol in presence of RanT24N, a Ran mutant which blocks the generation of RanGTP [155]. NPC insertion, NE expansion (Fig. 1A, B) and Ran-mediated nuclear transport (Fig. 2D) were all strongly inhibited. The addition of two transport inhibitors, a non-hydrolyzable GTP analog (GTPγS) and wheat germ agglutinin (WGA), which blocks pores by binding to nucleoporins that contain *N*-acetylglucosamine residues [153, 156] both inhibited nuclear import of BSA-NLS (Fig. 2D) and NE expansion (Fig. 1B). However, new NPCs were still efficiently inserted (Fig. 1A, B) and the NPC density increased from 4.9 ± 0.6 to 10.3 ± 1.4

NPC/μm^2 in the presence of GTPγS and to 8.3 ± 0.5 NPC/μm^2 in the presence of WGA (Fig. 1A, B). Thus NPC insertion in vitro requires RanGTP but can occur in the absence of the nuclear transport activity of existing pores and NE expansion.

NPC assembly into the reforming NE at the end of mitosis is negatively regulated by the nuclear transport receptor Importin β [105, 157] and we wanted to test its effect on new NPCs insertion. In the presence of 2 μM Importin β neither NE expansion (Fig. 1A, B) nor nuclear import of BSA-NLS (Fig. 2D) were affected. However, NPC insertion was strongly inhibited when compared to control reactions containing transportin, an import receptor not involved in NPC assembly [105] (Fig. 1A, B). The pore density dropped from 4.9 ± 0.6 NPCs/μm^2 in control reactions to 2.2 ± 0.4 NPCs/μm^2 in the presence of Importin β, an effect that was restored by 10 μM RanGTP (Fig. 1A-B). Thus Importin β negatively regulates NPC insertion into intact nuclei in a transport independent manner.

To analyze from which sides of the NE nucleoporins are inserted we wanted to block RanGTP production only in the cytoplasm or only in the nucleoplasm. First, NE-0 nuclei were assembled and the existing pores were sealed with 20 μg/ml WGA before adding either cytosol or cytosol containing 5 μM RanT24N. RanT24N inhibited NPC insertion (Fig. 3B), even though it was excluded from the nucleus (Fig. 3A). NPC assembly was restored by the addition of 5 μM RanQ69L, a GTPase-deficient mutant of Ran [158, 159] or by 5 μM RCC1 (Fig. 3B), demonstrating that RanT24N specifically inhibited endogenous cytoplasmic RCC1.

Second, we added recombinant RanGAP-RanBP1 complex, Ran's GTPase activating protein (GAP) and its co-factor RanBP1 [155], which are excluded from the nucleus [160] to deplete cytoplasmic RanGTP. NPC insertion was blocked, but unlike RanT24N nuclear transport (Fig. 2D) or NE expansion were not affected (Fig. 3C) and consequently the pore density decreased (Fig. 3D). Thus RanGTP plays a cytoplasmic role in NPC insertion in vitro.

To inhibit nuclear RCC1 we incubated NE-0 nuclei with RanT24N, which accumulated in the nucleoplasm (Fig. 3A) and inhibited NPC insertion (Fig. 3B). After 10 min, either buffer or WGA was added to the reactions to seal the pores. When the WGA-treated nuclei were incubated with 200 volumes fresh cytosol, RanT24N in the cytosol was diluted to non-inhibitory levels. The concentration of RanT24N trapped inside the nucleus was unaffected (Fig. 3A) and NPC insertion was not restored (Fig. 3B). In contrast, nuclei that were diluted in the absence of WGA efficiently inserted new NPCs (Fig. 3B). Thus the generation of RanGTP inside the nucleus is required for NPC insertion. Taken together, these results suggest that NPC assembly involves Ran-dependent steps on both sides of the NE.

Our results imply a model in which RanGTP-mediated release of nucleoporins from Importin β [105] occurs in both the nucleoplasmic and cytoplasmic compartment. To test if soluble Importin β-binding nucleoporins are indeed present in both compartments, we stained NE-80 nuclei with antibodies against several nucleoporins (Fig. 4, Fig. 5). We detected a strong NE rim staining for all of them and an additional nucleoplasmic signal specifically with antibodies to Nup133 and

Nup160, two components of the Nup107-160 complex that has been shown to be essential for NPC formation [161, 162] (Fig. 5A). When the assembly of new pores into NE-0 nuclei was blocked by adding Importin β, an increase in nucleoplasmic Nup107-160 signal was observed, while the rim signal was reduced (Fig. 4A, Fig. 5A). Diluting the nuclei with 200 volumes fresh cytosol or the addition of RanGTP (27) reversed this effect even when nuclear transport was blocked by WGA (Fig. 4B, Fig. 5B). Similarly, the nucleoplasmic Nup107-160 signal increased when NPC insertion was blocked with RanT24N or RanGAP-RanBP1 (Fig. 3B), suggesting that the nucleoplasmic pool of Nup107-160, which is essential for pore formation [162], was not incorporated into the NE when RanGTP production was blocked.

Next we analyzed if Nup107-160 complexes were incorporated from the cytoplasmic side of the NE. We assembled NE-0 nuclei and subsequently added WGA to seal the existing pores. A nucleoplasmic signal was detectable when these nuclei were stained with αNup133 and αNup160 (28). In contrast to mock-depleted cytosol, Nup107-160-depleted cytosol did not induce assembly of new pores (Fig. 5C). This lack of activity was due to the absence of Nup107-160 because the addition of purified Nup107-160 complex (Fig. 4C) restored NPC insertion (Fig. 5C).

Second, nuclei were formed in the presence of BAPTA, a calcium chelator that inhibits NPC formation [163] and a strong nucleoplasmic Nup133 signal was detected (Fig. 5D). When the BAPTA nuclei were diluted in mock-depleted cytosol, NPC insertion was restored, while Nup107-160-depleted cytosol failed to do so (Fig. 5D). Consistent with the cytoplasmic RanGTP-mediated release of Importin b from the

Nup107-160 complex, we found that addition of 5 mM RanT24N resulted in a 60% increase of Importin b associated with immuno-precipitated Nup107-160 complex (29). Thus the incorporation of the Nup107-160 complex into new assembly sites occurs from both sides of the NE. Because nuclear transport is not required for NPC insertion in vitro, the nucleoplasmic pool of Nup107-160 complexes might be generated via chromatin association during nuclear assembly [105].

Next we wanted to analyze if pores assemble de novo or by splitting of existing pores [3, 151, 152]. We assembled NE-0 nuclei and subsequently fluorescently labeled individual pores with WGA-488 (green) (Fig. 7A). Upon dilution, WGA-488 remained stably bound to NPCs while new, unlabeled pores were inserted (Fig. 6a), which could be labeled with WGA-568 (red). Newly formed pores were only labeled with WGA-568 and appeared as red dots while old pores were labeled with both dyes resulting in a yellow overlay. The new pores did not exhibit green signal from existing pores suggesting that NPCs form de novo (Fig. 7A). When the formation of new pores was blocked by the addition of 5 mM RanT24N, all pores appeared yellow in the overlay (Fig. 7A) indicating that red dots represented indeed newly formed pores. Furthermore, the average fluorescence intensity of WGA-488 labeled NPCs remained constant after dilution of the dye and was indistinguishable between nuclei that inserted new pores and nuclei where the formation of new NPCs was blocked by 5 mM RanT24N (Fig. 6B). These results suggest that newly formed pores do not incorporate nucleoporins from existing NPCs and support a de novo mechanism, because in a splitting process the intensity of the old pores would be

expected to decrease. Additionally, we were able to detect pores that stained with aPOM121, a trans-membrane nucleoporin, and aNup133 but not with mAb414 (Fig. 6C). POM121 and Nup133 colocalized with mAb414 when formation of new NPCs was blocked by RanT24N. This indicates that FG-repeat nucleoporins are recruited to new assembly sites after POM121 and Nup107-160 complexes have been incorporated and further supports de novo formation.

To determine whether NPC formation in vivo also occurs by a de novo mechanism we generated a stable HeLa cell line expressing low, non-toxic levels of POM121 containing multiple copies of GFP to visualize individual NPCs in living cells [86]. Four-dimensional confocal time-lapse microscopy was used to follow NPC assembly during S-phase and new pores became visible as single dots in areas where initially no GFP signal was detectable (Fig. 7b) and in areas where pre-existing pores have been photo bleached (Fig. 8C). New NPCs co-localized with neighboring, pre-existing pores along the z-axis (Fig. 8A, B) showing that they were inserted into the NE. Consistent with de novo formation, existing pores did not change fluorescence intensity over time (Fig. 7C). These findings further support a de novo mechanism for NPC biogenesis.

Methods

Recombinant Proteins and antibodies

Ran, RanQ69L, RanT24N and the transport receptors Importin b and transportin, were prepared as previously described(*17*). aNup133, aNup160 were used as previously described (*22*).

Nuclear Assembly and related methods

Extract and sperm chromatin preparation, fluorescently labelling of membranes and proteins and immunofluorescence was performed as previously described (*11, 22*). NE surface was determined form 3D reconstructions of nuclei that had imported fluorescently labeled BSA-NLS. The nuclei were directly analyzed by confocal fluorescence microscopy without fixation and subsequent purification. 3D reconstructions were calculated from ~ 150 confocal sections per nucleus using Imaris software by Bitplane.

We used two approaches to determine the total number of NPCs per nucleus. First, a minimum of five 25 mm^2 NE areas were randomly chosen and imaged from at least 50 nuclei per experiment. The measured NE surface area was then used to calculate the total number of pores per nucleus. Second, we spun fixed mAb414-stained nuclei onto cover-slips which resulted in flattening of large NE areas on the glass surface and used maximum intensity projections of optical sections of these large areas and 3D reconstruction software to automatically count the number of pores. Immunoprecipitation of Nup107-160 complex was performed as previously described (*22*).

Live Cell Confocal Microscopy and Image Analysis

Live cells were imaged at 37˚C maintained by air stream incubator and enriched with CO_2 (Solent Scientific). Time-lapse images of z-stacks were taken on a custom built spinning disk confocal microscope (McBain Instruments). Images were captured on an EM-CCD digital camera (Hamamatsu) and acquired using SimplePCI (Compix). Individual pores were imaged using an HCX Plan Apochromat 100x oil objective and 1.5x mag. changer (both Leica). 3-D surface images were constructed using Imaris (Bitplane), time-lapse images were normalized for photobleaching using Adobe Photoshop® 7.0 and movies were assembled using QuickTime™ Player Version 7.0.3. Single pore analysis was completed using NIH ImageJ.

Pom121-(GFP_3) HeLa cells plated at approx. 50% confluency in 8 Chambered Lab-Tek II Chamber #1.5 German Coverglass System. Cells grown in DMEM +10%FBS +1X P/S +40ug Geneticin (for both experiments). After 16hrs of growth 6 cells were photo-bleached with the scanning confocal microscope. Z-stacks of approximately 12-18 sections were scanned, 2 passes per section at 25% laser intensity, at 32x zoom, with 63x objective. Dish was then transferred to spinning disk scope, Z-stacks 6um thick (30 sections) were acquired every 10 min with 100x objective + 1.5x mag changer. Exposure time was 0.5 sec, maximum gain, laser intensity at 60%. Z stacks were assembled into 3D surfaced in Imaris, and avi files were exported. Avi files were then separated into tiffs and processed in Photoshop to generate the figures.

Acknowledgements

Antibodies against Importin β was kindly provided by L. Gerace. We thank the members of the lab and T. Hunter for helpful discussions and W. Eckhart, J. Karlseder, V. Lundblad, J. Young, B. Sefton and M. Weitzman for critically reading the manuscript. M.A.D and M.H. were supported by The Pew Charitable Trust.

Chapter 5 is modified from the following publication.

D'Angelo MA*, Anderson DJ*, Richard E, Hetzer MW. 2006. Nuclear pores form de novo from both sides of the nuclear envelope. Science 312, 440-3 (*co-first authors)

Maxi D'Angelo, Martin Hetzer and I were the primary researchers of these studies. Martin Hetzer was the primary author of this manuscript. Erin Richard was involved in cloning and protein purification for these studies.

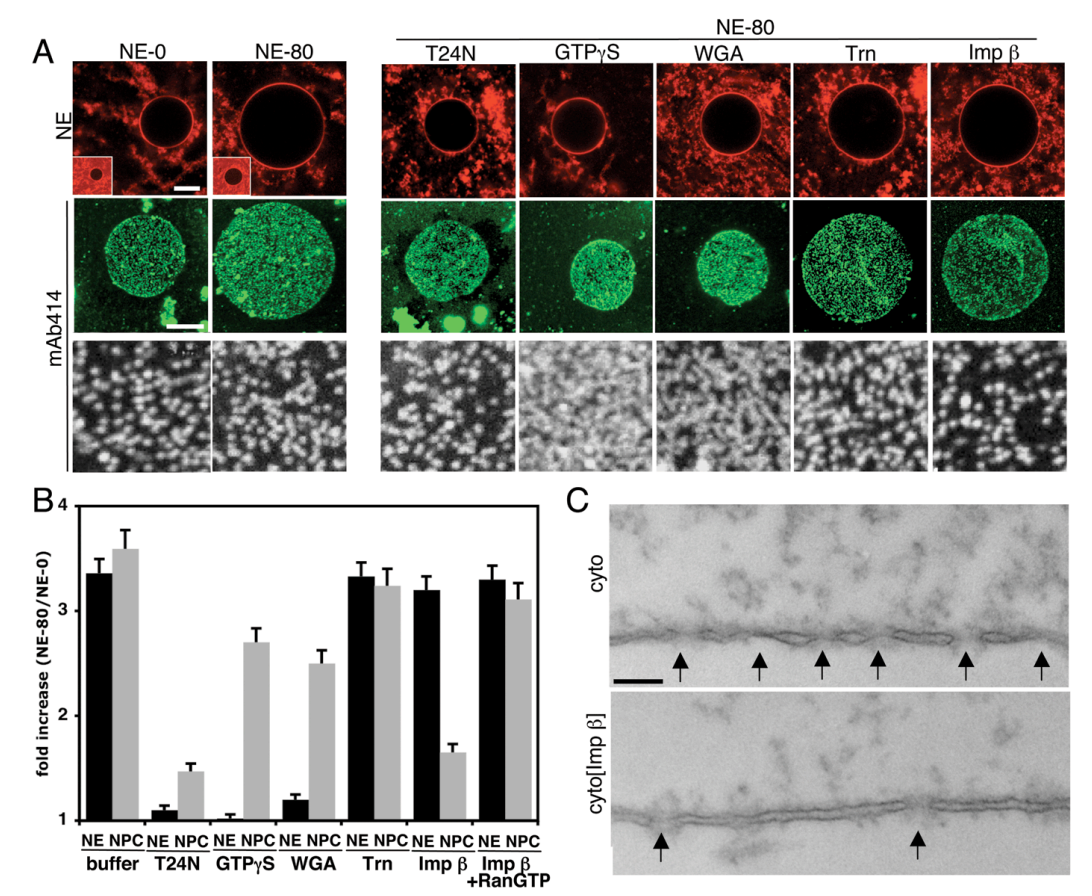

Chapter V Figure 1

Transport-independent role of Importin b in NPC insertion. (**A**) Nuclei (NE-0) were pre-assembled in 5 ml reactions including egg extracts, membranes and sperm chromatin for 40 min [105], and diluted with 50 ml fresh cytosol in the absence or presence of 5 mM RanT24N, 2 mM GTPgS, 20 mg/ml WGA, 2 mM transportin or Importin b (+/- 10 mM RanGTP), for an additional 80 min (NE-80) and analyzed by confocal microscopy. The formation of a closed NE was analyzed in unfixed nuclei using the membrane stain $DiIC_{16}$ [58] and 70 kDa dextran (small insert). Individual NPCs were visualized by immunofluorescence with mAb414 on the surface of the nuclei at low magnification and with 8x zoom. Scale bar, 10 mm. (**B**) NE surface area and total number of pores were calculated using five independent experiments as described in the methods. The relative increase of surface area (black) and pore numbers (grey) during 80 min were plotted. (**C**) Nuclei were assembled in the absence (buffer) and presence of 2 mM Importin b, sectioned and analyzed by transmission EM [105]. Scale bar, 200 nm**.**

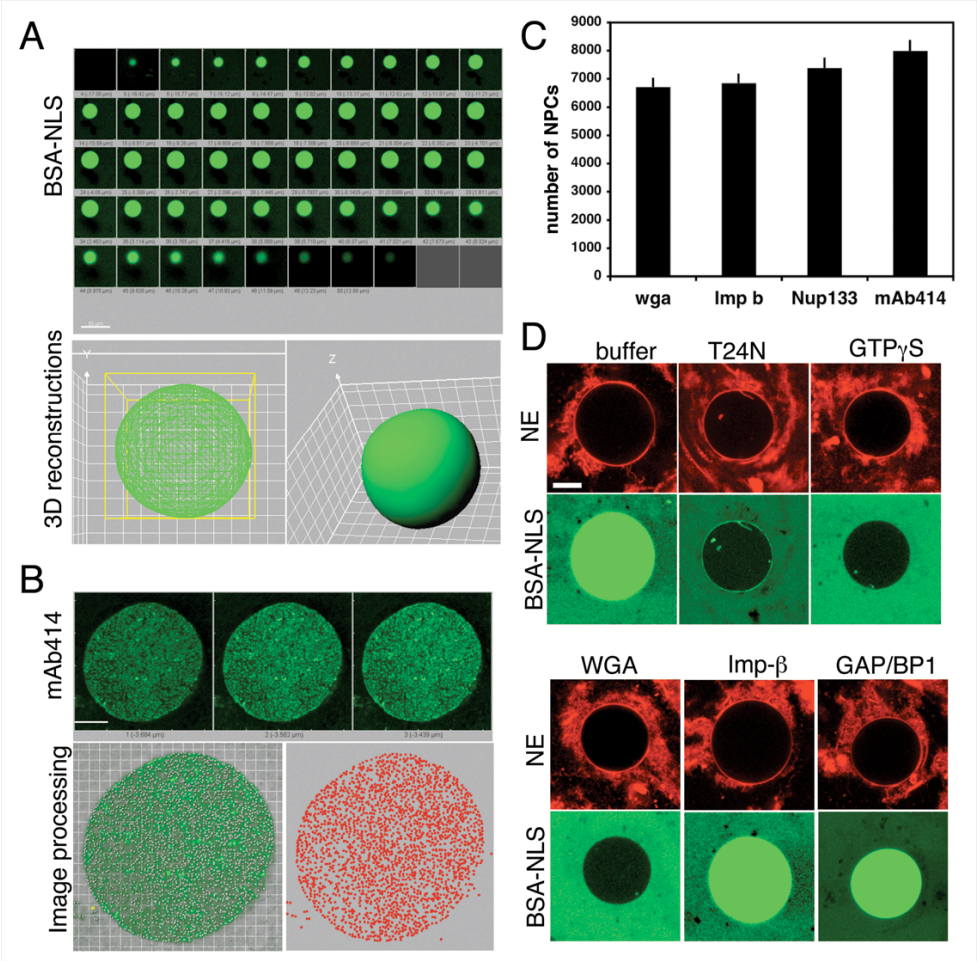

Chapter V Figure 2

Determination of NE surface area and total pore number and characterization of nuclear accumulation of BSA-NLS and RanT24N. (**A**) Assembled nuclei were incubated with fluorescently labeled import substrate BSA-NLS and 3D reconstructions of entire nuclei were calculated from ~ 150 confocal sections per nucleus (upper panels). Scale bar, 10 mm. (**B**) Maximum intensity projections of optical sections (upper panels) of large NE areas and 3D reconstruction software were used to automatically count the number of pores. Scale bar, 10 mm. (**C**) Nuclei were assembled for 60 min and individual NPCs were visualized by WGA-488 and a TAP-tagged version of Importin b which formed a stable complex with fluorescently labeled streptavidin. Alternatively, pores were monitored by immunofluorescence using aNup133 and mAb414 and quantified as described in **Fig.1**. (**D**) Nuclei were assembled with DiIC16-labeled membranes (red) as described in **Fig. 1** and incubated with BSA-NLS (green) in the absence or presence of 5 mM RanT24N, 2 mM Importin b, 2 mM GTPgS, 20 mg/ml WGA and 10 mM RanGAP/RanBP1. Nuclear accumulation of BSA-NLS was directly analyzed without fixation by confocal microscopy. Scale bar, 10 mm.

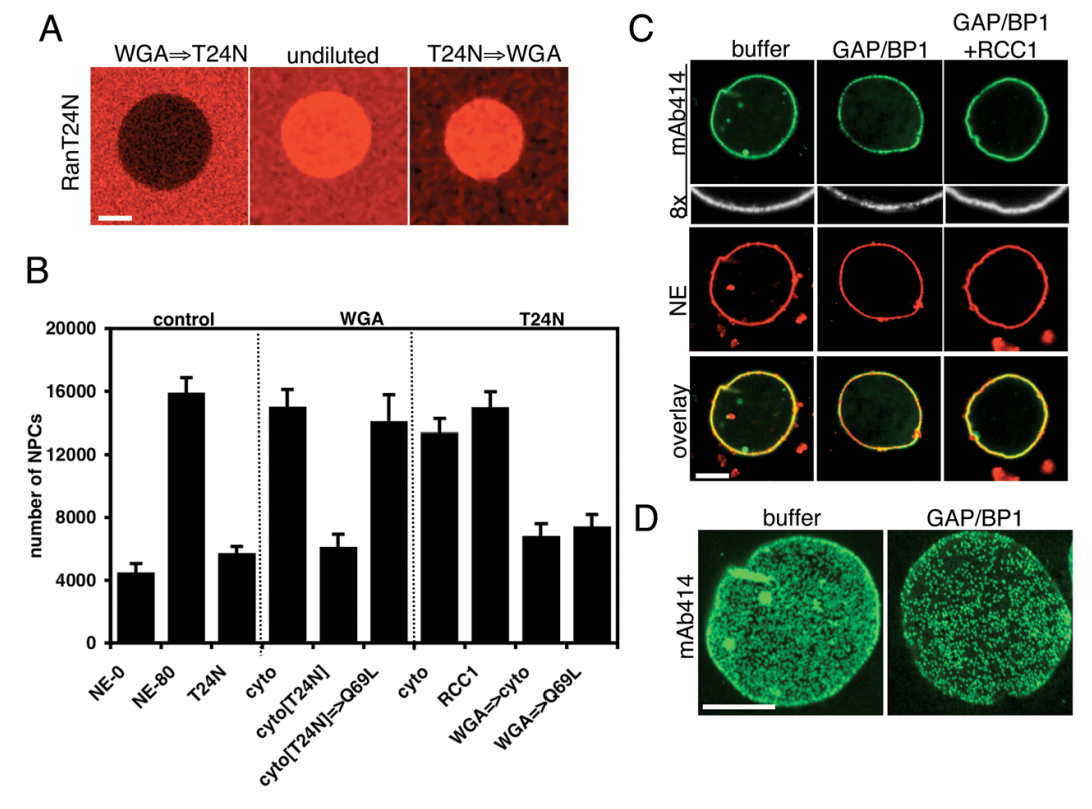

Chapter V Figure 3

RanGTP-mediated incorporation of Nup107-160 complex occurs from the nucleoplasmic and cytoplasmic side of the NE. (**A**) Fluorescently labeled RanT24N accumulated in assembled nuclei and was trapped in the nucleoplasm of WGA sealed nuclei after dilution (T24N⇒WGA). RanT24N was excluded from the nucleoplasm when added after the NPCs were blocked with WGA (WGA⇒T24N). Scale bar, 10 mm. (**B**) control; quantification of total pore numbers of NE-0 and NE-80 nuclei. T24N; NE-0 nuclei were incubated with 5 mM RanT24N for 10 min. NPC insertion was induced with 200 volumes of cytosol (cyto) or 5 mM RCC1. To trap RanT24N inside the nucleus NPCs were sealed with 20 mg/ml WGA for 10 min and NPC insertion was then induced by adding cytosol (WGA⇒cyto) or 5 mM RanGTP (WGA⇒RanGTP). WGA, NE-0 nuclei were incubated with 20 mg/ml WGA for 10 min before the addition of cytosol (cyto), cytosol that contained 5 mM RanT24N (cyto[T24N]) or RanT24N and RanQ69L (cyto[T24N] ⇒Q69L). The number of NPCs was quantified as describe in **Fig. 1**. (**C**) NE-0 nuclei were incubated in the absence or presence of 5 mM RanGAP/RanBP1 or RanGAP/RanBP1 plus 5 mM RCC1 as indicated. Nuclei were stained with mAb414 (green) and $DiIC_{18}$ (red) and analyzed in cross sections or (**D**) on the NE surface to visualize individual NPCs. Scale bar 10 mm.

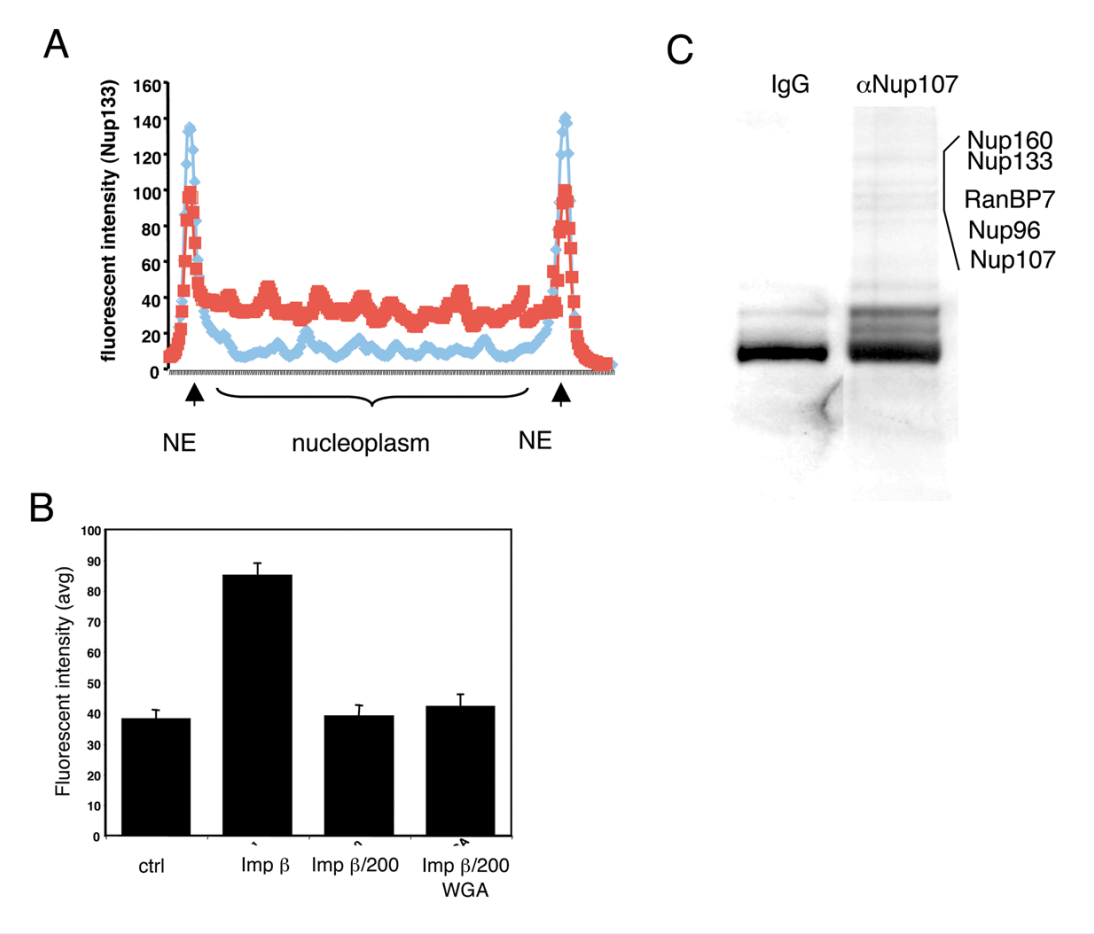

Chapter V Figure 4

Quantification of intranuclear Nup133 levels and reconstitution of Nup160-depleted cytosol with purified Nup160 complex. (**A**) Nuclei were assembled in the absence (blue) or presence of Importin b (red) and stained with aNup133. The relative fluorescence intensity across a 2 x 20 mm^2 region was measured. (**B**) The relative fluorescent intensity of randomly chosen 25 mm^2 nucleoplasmic areas taken from confocal images as shown in **fig. S1**. At least 50 nuclei were analyzed in each experiment. (**C**) Cytosol was incubated with IgG or non-inhibitory, biotinylated aNup107 antibody, washed and eluted with excess biotin. Eluted proteins were separated on SDS-PAGE and proteins visualized by Coomassie.

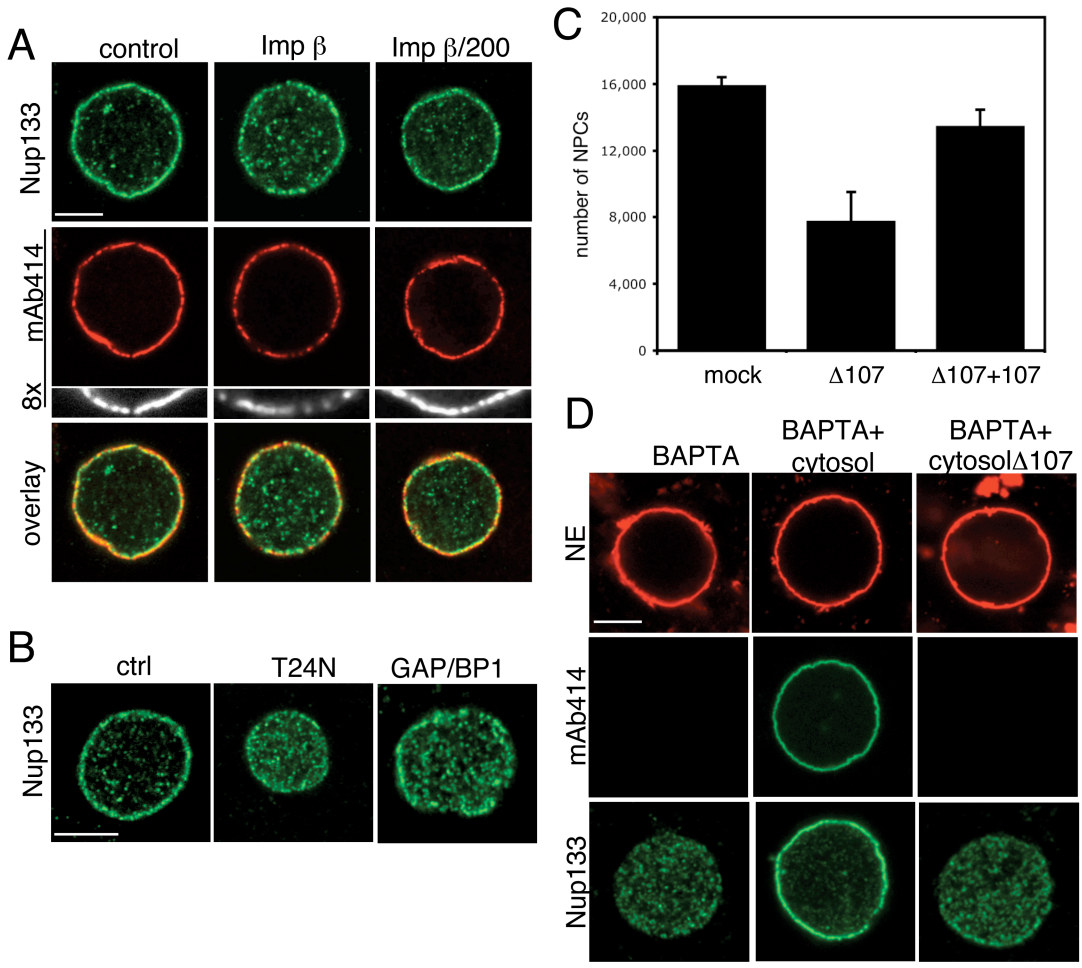

Chapter V Figure 5

Nucleoplasmic and cytoplasmic Nup107-160 complexes are required for NPC insertion. (**A**) NE-0 nuclei were incubated in 5 ml fresh cytosol to which buffer or 2 mM Importin b had been added, and nuclei were analyzed after 80 min by immunofluorescence using aNup133 and mAb414. To reverse the inhibitory effect of Importin b NE-80 nuclei were diluted in 200 volumes cytosol. Scale bar, 10 mm. (**B**) Nuclei were assembled in the presence of Importin b, and subsequently diluted in 200 volumes of cytosol (buffer) or cytosol containing 5 mM RanT24N or 10 mM RanGAP/RanBP1 for 30 min. Nuclei were analyzed by immunofluorescence using aNup133. Scale bar, 10 mm. (**C**) NE-0 nuclei were incubated at room temperature with mock-depleted or Nup107-160-depleted cytosol (in the absence or presence of purified Nup107-160 complex) and the total number of NPCs was quantified as in **Fig. 1**. (**D**) Nuclear assembly was performed using $DiIC_{16}$-labeled NE membranes, sperm chromatin and cytosol in the presence of 5 mM BAPTA for 60 min and the nuclei were diluted with mock-depleted cytosol or Nup107-160-depleted cytosol. NPCs were visualized with mAb414 and aNup133. Scale bar, 10 mm.

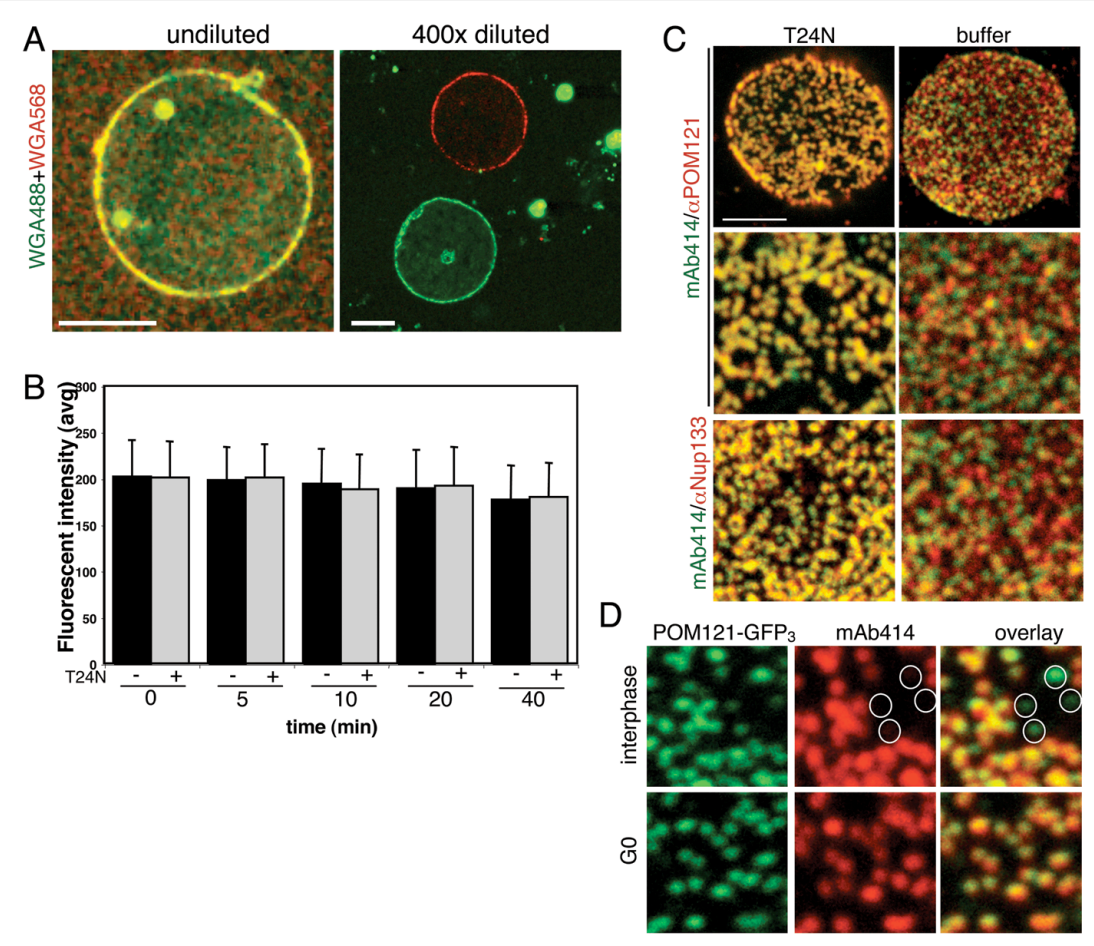

Chapter V Figure 6

WGA stably binds to NPCs. (**A**) Nuclei were assembled and separately stained with 20 mg/ml WGA-488 (green) and WGA-568 (red), respectively. When the nuclei were mixed undiluted red and green dyes mixed, but upon 400-fold dilution the two dyes remained stably bound for 60 min. Scale bar, 10 mm. (**B**) The total fluorescence of 3-5 x 10^5 NPCs, labeled with WGA-488, was analyzed for each time point in the absence or presence of RanT24N and plotted as average pixel values. (**C**) NE-0 nuclei were diluted with cytosol or cytosol containing 5 mM RanT24N for 20 min. Nuclei were analyzed by immunofluorescence using mAb414 (green) and aPOM121 or aNup133 (red) and the two channels were merged. Scale bar, 10 mm.

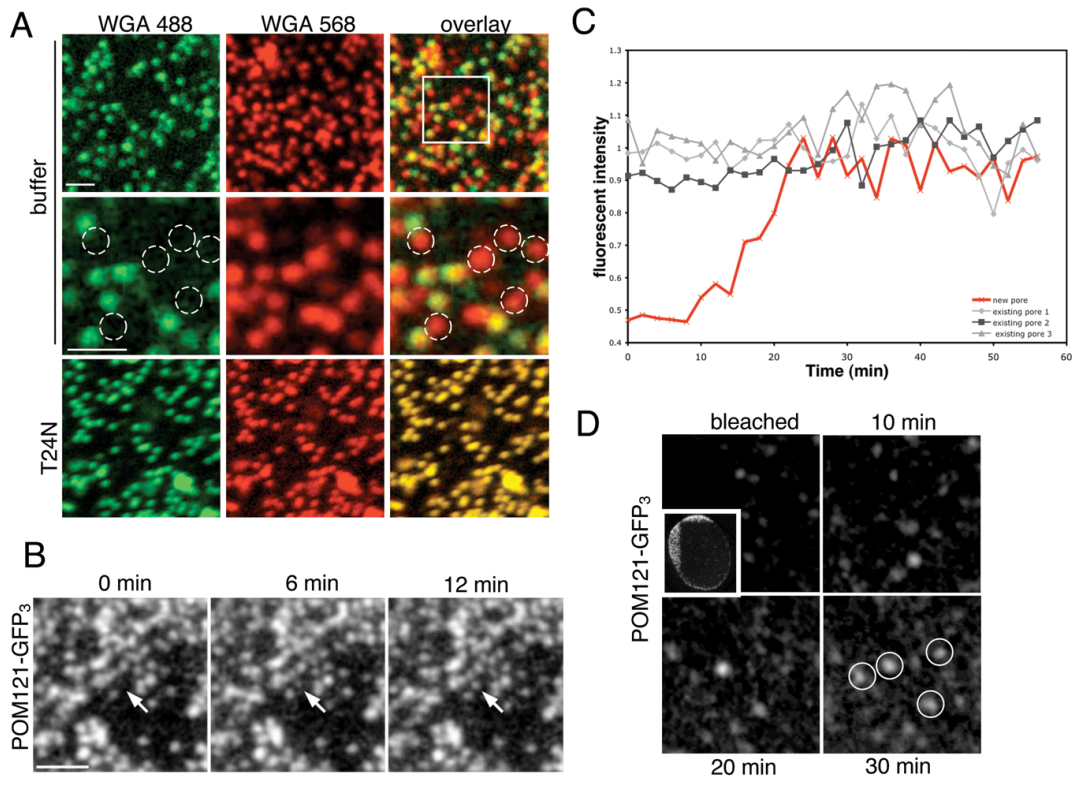

Chapter V Figure 7

NPC insertion occurs by a *de novo* mechanism. (**A**) NE-0 nuclei were labeled with 10 mg/ml fluorescently labeled WGA-488 for 10 min and subsequently incubated with 400 volumes of cytosol in the absence or presence of 5 mM RanT24N for 30 min. Fluorescently labeled WGA-568 was added for 10 min and nuclei were analyzed by confocal microscopy. Newly formed pores are visible as red dots; note that they do not contain a detectable green signal. Scale bar, 1 mm. (**B**) Hela cells expressing POM121-(GFP_3) were analyzed in real time by confocal microscopy on the NE surface every 2 min. Arrows indicate new NPC assembly site. (**C**) Relative fluorescence intensity of pre-existing pores (gray) and new pore (red) was plotted against time. (**D**) Large areas of NEs were photo bleached (insert) and the formation of few pores was monitored by 4D confocal microscopy. Bleached POM121-(GFP_3) did not recover for more than 4 hrs similar to previously published report [130].

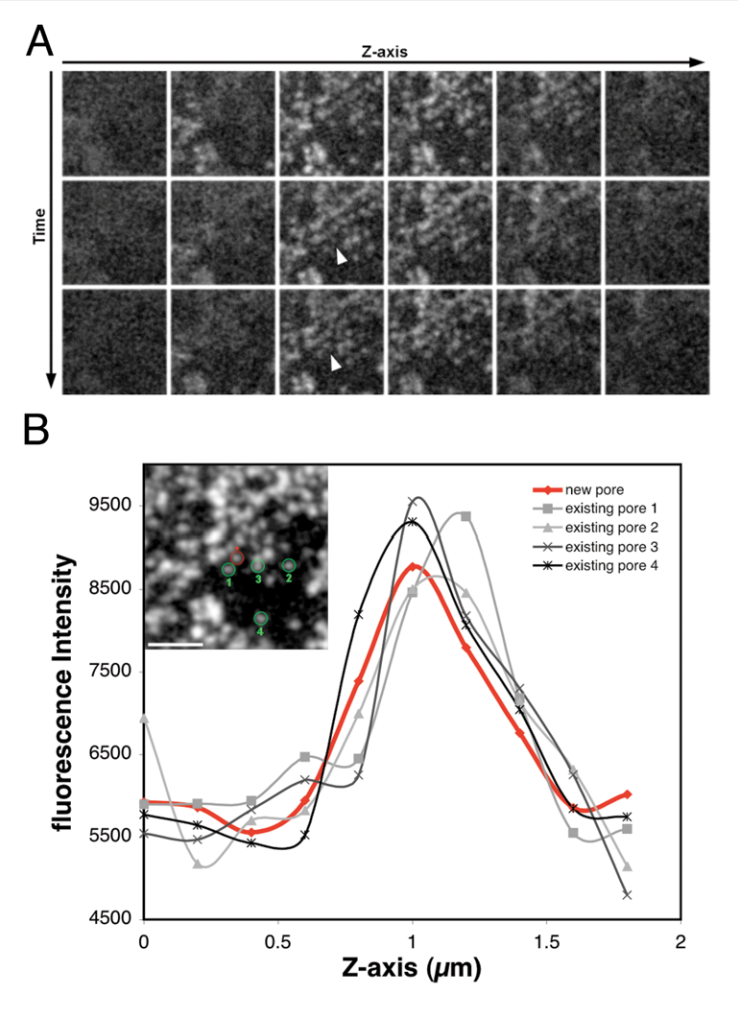

Chapter V Figure 8

New NPCs are inserted into HeLa nuclei by a de novo mechanism. (**A**) HeLa nuclei were analyzed by confocal microscopy obtaining 10 optical sections each 200 nm thick. Arrow indicates new pore. (**B**) Fluorescent intensity of pre-existing (gray) and new pore (red) was plotted along the z-axis, Insert shows the chosen NPCs. Scale bar, 2 mm.

Chapter VI

Conclusion

In this thesis several areas related to the dynamic organization of the nucleus through the cell cycle were investigated. The aim of this chapter is to summarize key finding of my thesis and discuss these results in the context of models that these studies generated.

Nuclear membrane formation

The initial aim of chapter 2 was to determine if the NE vesiculates or is absorbed into the ER during open mitosis. This question was investigated using the *Xenopus in vitro* nuclear reconstitution system [103]. Key findings that support a model where the NE resides in the mitotic ER are as follows: (1) *In vitro* nuclear assembly can occur in the presence of the vesicle fusion inhibitors GTPγS and ATPγS, suggesting that vesicle fusion is not required for NE formation, a process that would be necessary if the NE was present in vesicles during mitosis (Fig. 1). (2) NE formation requires an intact ER membrane network when membrane fusion is blocked, suggesting that the structural conformation of this membrane network is significant for nuclear assembly (Fig1). (3) When NE formation was directly visualized, a tubular membrane network was an intermediate conformation before nuclear membrane assembly, regardless of the structure of the starting membranes. These finding do not preclude the participation of vesicle fusion in NE formation, however they strongly support the idea that nuclear assembly can occur independently of membrane fusion.

Through the studies for chapter 1 several findings initiated novel models related to NE formation. Through our direct imaging of nuclear membrane formation we discovered that the ER contacts chromatin via tubules ends to initiate NE assembly. The membrane topology of the tubule end exhibits unique spherical curvature, rather than the cylindrical curvature found elsewhere in the tubule network. Such unique membrane curvature may allow for the clustering of integral membrane proteins that are involved in the targeting of membranes to chromatin. Alternatively, ER tubule ends may contact chromatin initially, because steric hindrance could preclude lateral elements of tubules to target directly to chromatin.

When membrane sheets merge during NE formation, small holes, the last connections between the INM and ONM, remain (Fig. 2a). How these final holes in the formatting NE close is not known. It is possible that annular fusion [93], is required to close these remaining remnants of the tubular network. Nuclei can seal in the presence of GTPγS and ATPγS, which suggests that energy is not required for the final annular fusion step. In the absence of biophysical characterization of membrane-chromatin interactions at this step, we can only speculate on how hole closure occurs. It could be mediated by a luminal fission machinery [107] that does not require the hydrolysis of ATP or GTP, or close spontaneously as a consequence of the pulling force on the INM due to accumulating DNA or chromatin-binding proteins (Fig. 2b). An alternative scenario is that these holes are targeted to sites of NPC assembly. In this scenario, membrane-bound nucleoporins are simply recruited to the points of fusion between the INM and ONM, targeting these holes to assembling sub-complexes

on the chromatin surface. Membrane-associated nucleoporin targeting could be due to the unique membrane curvature at these small holes, where there is a convex surface across the INM and ONM and concave surface between the two membranes [164]. The fate of the remaining holes in the forming NE will be an interesting future area of study.

Reticulons in NE assembly

In chapter 3 we identify a novel role for the ER membrane curving Reticulons in NE assembly. Key findings in this chapter are as follows: (1) Reticulons are transiently present on the membranes at the forming NE. Since Reticulons are known to be present exclusively in the tubular ER [102], these data provided convincing evidence supporting the idea that ER directly contributes to nuclear membrane formation. (2) The concentration of Reticulons present in the ER membranes regulates the rate of NE formation suggesting that Reticulons act as negative regulators for nuclear assembly. Furthermore, the reduction of Reticulons accelerated nuclear assembly, identifying NE formation as rate limiting in nuclear assembly. Again, the direct role of these ER resident proteins further supports the model where the NE resides in the mitotic ER. (3) The concentration of Reticulons was found to directly affect the flattening of membrane on chromatin via a release from the forming NE (Fig. 3). These data suggest that Reticulon release is directly involved in the change in shape of the membranes during nuclear assembly.

One question raised by chapter three was: how are Reticulons removed from the forming NE? It is possible that Reticulons are simply displaced by from the forming NE by the binding of INM proteins to chromatin (see chapter 4 Fig. 5D). However such a model does not explain how these proteins would be removed from the ONM, where there is not a rapid accumulation of transmembrane proteins. Reticulons are known to oligomerize to mediate tubule curvature [114], such oligomerization limits the mobility of diffusion for these proteins through the ER. It is possible that the oligomerization is Reticulons present on the forming NE is regulated in a manner that mediates removal into the cytoplasmic located ER. An example of such specially targeted regulation can be found in the RanGTP gradient that is formed around chromatin to mediate NPC assembly at the end of mitosis. Further investigation into the mechanism of Reticulon removal from the assembling nuclear membrane will provide mechanistic insight into how membrane shape change is regulated through the cell cycle.

NE-associated membrane proteins role in nuclear assembly

The aim of chapter 4 was to identify and characterize proteins that mediate membrane targeting and spreading around chromatin. We hypothesized that transmembrane proteins found in the interphase NE may play a key role in this process because they are known to disperse into the mitosis ER and many have known interactions with chromatin. We speculated that tethering membranes to chromatin associations could mediate NE targeting and reformation. Key finding of chapter 4

are as follows: (1) Several functionally distinct transmembrane proteins of the NE play redundant roles in nuclear membrane assembly. When the concentration of one of these proteins is reduced, the rate of NE formation is slowed but the process is not blocked. Over 40 transmembrane proteins of the NE have the potential to interact with chromatin [63]. Assuming that each of the proteins participate in nuclear assembly, a robust system exists, where the loss of one, or even several of these proteins does not inhibit faithful enclosure of chromatin. (2) The increased expression of a one NE-membrane protein accelerates nuclear membrane formation, suggesting that binding sites on chromatin are not saturated in this process. (3) De-regulating the rate of NE formation causes a defect in chromosome segregation, suggesting that the pace of nuclear assembly is important for robust cell division. Since INM proteins are known to express higher in cancer cells [147], it will be interesting to investigae if accelerating nuclear assembly by such de-regulation might lead to genomic instability due to nuclear fusions.

The universal action of transmembrane proteins of the NE in targeting and reshaping is fascinating given their diverse functions in interphase (eg. Ndc1 in nuclear-cytoplasmic transport [9] and Lap2B in DNA replication [165]). The functional modularity of these proteins is to our knowledge unique in cellular function. The mechanism that triggers these proteins to target to chromatin starting in anaphase is not characterized. It is known that many proteins of the NE are heavily phosphorylated during NE breakdown [24]. It is believed that these modifications break interactions with chromatins. Therefore, it seems likely that the

dephosphorylation of these proteins might trigger their targeting to chromatin at the end of cell division. It remains to be tested if the interaction of NE-membrane proteins with chromatin is sufficient for membrane enclosure. However, we have shown that flat membrane sheets can assemble on protein-free DNA in the absence of cytosol (Chapter 2, Figure 5), suggesting that this process does not require cytosolic factors. It will be interesting to further investigate the sufficiency of these proteins in NE assembly.

de novo NPC assembly

In chapter 5 we focused on characterizing the mechanism of NPC insertion into the intact interphase NE. The question that initiated this investigation was whether NPC form by budding from existing pores (a mechanism that is possible due to their radial symmetry) or if pores *de novo* without components of existing pores. Many finding of this study were driven by the development of an *in vitro* assay to recapitulate interphase nuclear growth and NPC assembly. With this assay, interphase NPC assembly could be biochemically characterized. Importantly, many of the key regulators of this process have other essential cellular function, making *in vivo* analysis difficult.

Key findings of this chapter are as follows: (1) NPC assembly is regulated by the Ran-mediated release of pore components from importing β. These data suggest that NPC assembly is regulated by importin β's sequestering of nucleoporins. (2) Interphase assembly can occur *de novo* both *in vitro* and *in vivo*. These findings imply

that a new fusion between the inner and outer nuclear membrane must be form to assemble a new pore. (3) The core Nup107-160 subcomplex is required from both the cytoplasmic and nuclear side for NPC formation. Together with the model of *de novo* formation these data suggest that pore assembly is a coordinated process involving the assembly of proteins on both sides of the nuclear membrane.

How recruitment of subcomplexes of a newly forming NPC is spatially coordinated between the cytoplasm and nuclear surface. It is possible that communication between the INM and ONM is initiated by luminal interactions of transmembrane components of the NPC. One possible candidate, Gp210 contains a long luminal domain that is known to dimerize [166], however Gp210 is not expressed in all cell types making it a less likely candidate to universally initiate NPC assembly [167]. It remains to be seen if there are unidentified transmemrabane nucleoporins that may be involved in the initiation of NPC assembly or if there are proteins that only transiently associate and participate in new pore formation.

Although a detailed study recently characterized the recruitment of nucleoporins to chromatin during nuclear reformation at the end of open mitosis [168], it is not clear if this correlates to the directly to the addition of these proteins to an assembling NPC. It is also possible that post-mitotic pore assembly differs from interphase assemble since the nucleus is not fully closed when pores assemble at the end of mitosis. A modified version of the *in vivo* assay developed to image interphase NPC assembly could prove useful in determining the order of addition of proteins to a

newly forming pore. Such an analysis would lead to a better understanding of the role of each nucleoporin during NPC formation.

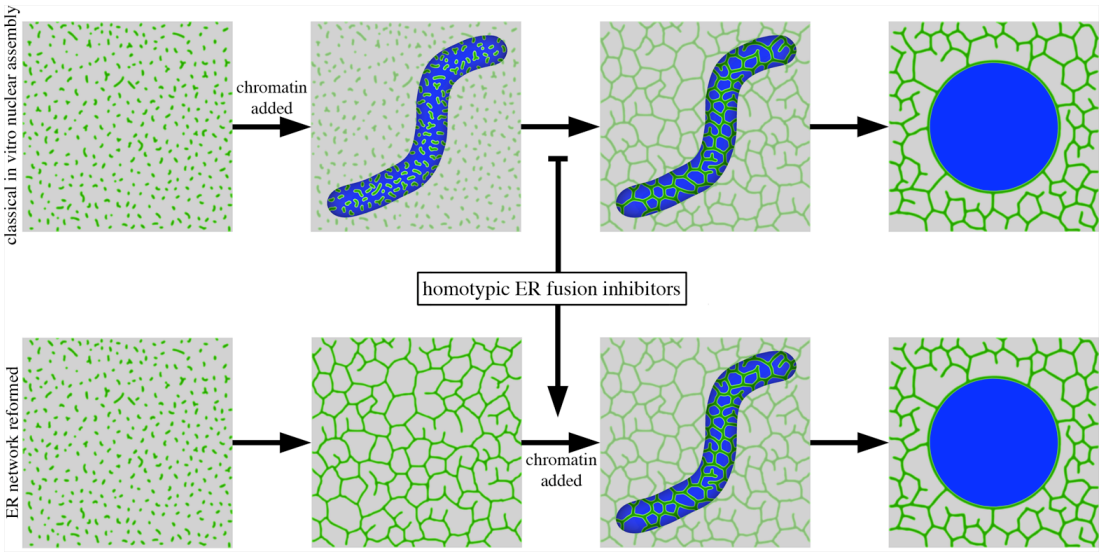

Chapter VI Figure 1

The morphology of the starting membranes dictates the biochemical requirements of cell-free nuclear assembly. Classically, nuclei were formed by mixing membrane fragments with sperm chromatin and cytosol (classical nuclear assembly). In this case, membrane fragments bind to the chromatin surface, fuse into a tubular network and expand to form the NE. Alternatively, when ER fragments are reformed into an ER network prior to chromatin addition, the network binds to chromatin and expands to enclose the chromatin. The addition of homotypic ER fusion inhibitors blocks nuclear assembly when fragmented membranes are mixed with chromatin (classical nuclear assembly). However, when these inhibitors are added after ER network assembly, there is no affect on NE formation.

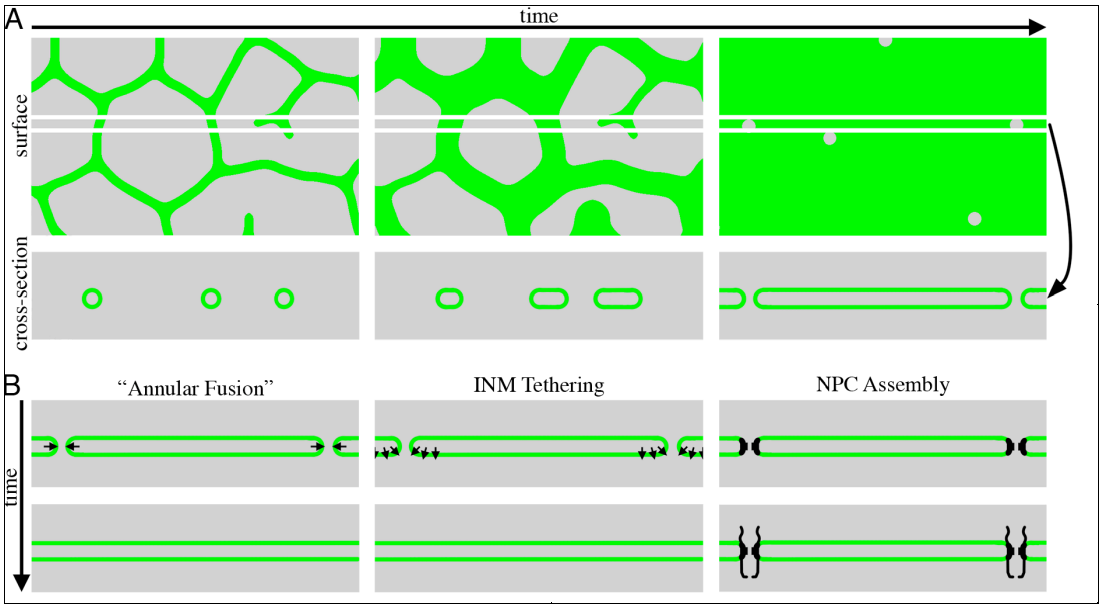

Chapter VI Figure 2

Hole closure is the final step for sealing of the nuclei. (A) After the ER network collapses onto the chromatin surface (left panel), membrane tubules flatten and merge into sheets (center panel). Connections between the INM and ONM in the form of small holes are the result of membrane flattening and merging (right panel). (B) There are three possible mechanisms for closure of the final connecting points between the INM and ONM. Protein-mediated constriction of the membrane hole may lead to fission of the two membrane sheets ("annular fusion"). This step may also be mediated by progressive tethering of the INM to chromatin by DNA-binding NETs (INM tethering). Alternatively, the final holes of NE formation may act as sites of NPC assembly (NPC assembly).

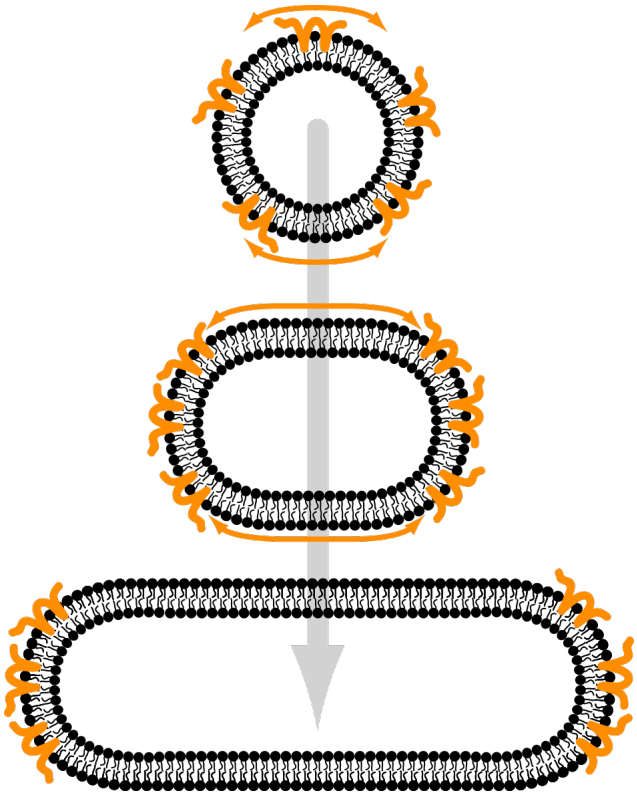

Chapter VI Figure 3
Removal of Reticulons from flattening membrane tubules is important for NE formation. This schematic illustration depicts the cross-section of a membrane tubule as it flattens into a NE. The membrane curving Reticulons (orange) must be displaced from the flattening membrane.

References

1. Callan, H.G., and Tomlin, S.G. (1950). Experimental studies on amphibian oocyte nuclei. I. Investigation of the structure of the nuclear membrane by means of the electron microscope. Proc R Soc Lond B Biol Sci *137*, 367-378.

2. Cohen, M., Tzur, Y.B., Neufeld, E., Feinstein, N., Delannoy, M.R., Wilson, K.L., and Gruenbaum, Y. (2002). Transmission electron microscope studies of the nuclear envelope in Caenorhabditis elegans embryos. J Struct Biol *140*, 232-240.

3. Hetzer, M., Walther, T.C., and Mattaj, I.W. (2005). Pushing the Envelope: Structure, Function, and Dynamics of the Nuclear Periphery. Annual review of cell and developmental biology.

4. Fahrenkrog, B., Koser, J., and Aebi, U. (2004). The nuclear pore complex: a jack of all trades? Trends Biochem Sci *29*, 175-182.

5. Vasu, S.K., and Forbes, D.J. (2001). Nuclear pores and nuclear assembly. Current opinion in cell biology *13*, 363-375.

6. Wente, S.R. (2000). Gatekeepers of the nucleus. Science (New York, N.Y *288*, 1374-1377.

7. Wozniak, R.W., and Lusk, C.P. (2003). Nuclear pore complexes. Curr Biol *13*, R169.

8. Terry, L.J., Shows, E.B., and Wente, S.R. (2007). Crossing the nuclear envelope: hierarchical regulation of nucleocytoplasmic transport. Science *318*, 1412-1416.

9. Stavru, F., Hulsmann, B.B., Spang, A., Hartmann, E., Cordes, V.C., and Gorlich, D. (2006). NDC1: a crucial membrane-integral nucleoporin of metazoan nuclear pore complexes. J Cell Biol *173*, 509-519.

10. Soderqvist, H., and Hallberg, E. (1994). The large C-terminal region of the integral pore membrane protein, POM121, is facing the nuclear pore complex. European journal of cell biology *64*, 186-191.

11. Wozniak, R.W., and Blobel, G. (1992). The single transmembrane segment of gp210 is sufficient for sorting to the pore membrane domain of the nuclear envelope. J Cell Biol *119*, 1441-1449.

12. Voeltz, G.K., Rolls, M.M., and Rapoport, T.A. (2002). Structural organization of the endoplasmic reticulum. EMBO Rep *3*, 944-950.

13. Newport, J.W., and Forbes, D.J. (1987). The nucleus: structure, function, and dynamics. Annu Rev Biochem *56*, 535-565.

14. Gerace, L., and Burke, B. (1988). Functional organization of the nuclear envelope. Annu Rev Cell Biol *4*, 335-374.

15. Apel, E.D., Lewis, R.M., Grady, R.M., and Sanes, J.R. (2000). Syne-1, a dystrophin- and Klarsicht-related protein associated with synaptic nuclei at the neuromuscular junction. J Biol Chem *275*, 31986-31995.

16. Mislow, J.M., Holaska, J.M., Kim, M.S., Lee, K.K., Segura-Totten, M., Wilson, K.L., and McNally, E.M. (2002). Nesprin-1alpha self-associates and binds directly to emerin and lamin A in vitro. FEBS letters *525*, 135-140.

17. Zhang, Q., Skepper, J.N., Yang, F., Davies, J.D., Hegyi, L., Roberts, R.G., Weissberg, P.L., Ellis, J.A., and Shanahan, C.M. (2001). Nesprins: a novel family of spectrin-repeat-containing proteins that localize to the nuclear membrane in multiple tissues. Journal of cell science *114*, 4485-4498.

18. Burke, B., and Stewart, C.L. (2002). Life at the edge: the nuclear envelope and human disease. Nat Rev Mol Cell Biol *3*, 575-585.

19. Gruenbaum, Y., Margalit, A., Goldman, R.D., Shumaker, D.K., and Wilson, K.L. (2005). The nuclear lamina comes of age. Nat Rev Mol Cell Biol *6*, 21-31.

20. Worman, H.J., and Courvalin, J.C. (2000). The inner nuclear membrane. J Membr Biol *177*, 1-11.

21. Lusk, C.P., Blobel, G., and King, M.C. (2007). Highway to the inner nuclear membrane: rules for the road. Nat Rev Mol Cell Biol *8*, 414-420.

22. Foisner, R. (2001). Inner nuclear membrane proteins and the nuclear lamina. Journal of cell science *114*, 3791-3792.

23. Schirmer, E.C., Florens, L., Guan, T., Yates, J.R., 3rd, and Gerace, L. (2003). Nuclear membrane proteins with potential disease links found by subtractive proteomics. Science (New York, N.Y *301*, 1380-1382.

24. Foisner, R., and Gerace, L. (1993). Integral membrane proteins of the nuclear envelope interact with lamins and chromosomes, and binding is modulated by mitotic phosphorylation. Cell *73*, 1267-1279.

25. Taddei, A. (2007). Active genes at the nuclear pore complex. Current opinion in cell biology *19*, 305-310.

26. Akhtar, A., and Gasser, S.M. (2007). The nuclear envelope and transcriptional control. Nat Rev Genet *8*, 507-517.

27. Mounkes, L.C., and Stewart, C.L. (2004). Aging and nuclear organization: lamins and progeria. Current opinion in cell biology *16*, 322-327.

28. Muchir, A., and Worman, H.J. (2004). The nuclear envelope and human disease. Physiology (Bethesda) *19*, 309-314.

29. Worman, H.J., and Courvalin, J.C. (2004). How do mutations in lamins A and C cause disease? J Clin Invest *113*, 349-351.

30. Wilson, K.L. (2000). The nuclear envelope, muscular dystrophy and gene expression. Trends in cell biology *10*, 125-129.

31. Roux, K.J., and Burke, B. (2007). Nuclear envelope defects in muscular dystrophy. Biochim Biophys Acta *1772*, 118-127.

32. Nagano, A., and Arahata, K. (2000). Nuclear envelope proteins and associated diseases. Curr Opin Neurol *13*, 533-539.

33. Mounkes, L., Kozlov, S., Burke, B., and Stewart, C.L. (2003). The laminopathies: nuclear structure meets disease. Curr Opin Genet Dev *13*, 223-230.

34. Pollex, R.L., and Hegele, R.A. (2004). Hutchinson-Gilford progeria syndrome. Clin Genet *66*, 375-381.

35. Heath, B. (1980). Variant mitoses in lower eukaryotes:indicators of evolution of mitosis? Int. Rev. Cytol. *64*, 1-80.

36. Sazer, S. (2005). Nuclear envelope: nuclear pore complexity. Curr Biol *15*, R23-26.

37. De Souza, C.P., Osmani, A.H., Hashmi, S.B., and Osmani, S.A. (2004). Partial nuclear pore complex disassembly during closed mitosis in Aspergillus nidulans. Curr Biol *14*, 1973-1984.

38. Lenart, P., Rabut, G., Daigle, N., Hand, A.R., Terasaki, M., and Ellenberg, J. (2003). Nuclear envelope breakdown in starfish oocytes proceeds by partial NPC disassembly followed by a rapidly spreading fenestration of nuclear membranes. J Cell Biol *160*, 1055-1068.

39. Muhlhausser, P., and Kutay, U. (2007). An in vitro nuclear disassembly system reveals a role for the RanGTPase system and microtubule-dependent steps in nuclear envelope breakdown. J Cell Biol *178*, 595-610.

40. Hetzer, M., Gruss, O.J., and Mattaj, I.W. (2002). The Ran GTPase as a marker of chromosome position in spindle formation and nuclear envelope assembly. Nat Cell Biol *4*, E177-184.

41. Beaudouin, J., Gerlich, D., Daigle, N., Eils, R., and Ellenberg, J. (2002). Nuclear envelope breakdown proceeds by microtubule-induced tearing of the lamina. Cell *108*, 83-96.

42. Galy, V., Antonin, W., Jaedicke, A., Sachse, M., Santarella, R., Haselmann, U., and Mattaj, I. (2008). A role for gp210 in mitotic nuclear-envelope breakdown. Journal of cell science *121*, 317-328.

43. Liu, J., Prunuske, A.J., Fager, A.M., and Ullman, K.S. (2003). The COPI complex functions in nuclear envelope breakdown and is recruited by the nucleoporin Nup153. Dev Cell *5*, 487-498.

44. Gerace, L., and Blobel, G. (1980). The nuclear envelope lamina is reversibly depolymerized during mitosis. Cell *19*, 277-287.

45. Peter, M., Nakagawa, J., Doree, M., Labbe, J.C., and Nigg, E.A. (1990). In vitro disassembly of the nuclear lamina and M phase-specific phosphorylation of lamins by cdc2 kinase. Cell *61*, 591-602.

46. Enoch, T., Peter, M., Nurse, P., and Nigg, E.A. (1991). p34cdc2 acts as a lamin kinase in fission yeast. J Cell Biol *112*, 797-807.

47. Salina, D., Enarson, P., Rattner, J.B., and Burke, B. (2003). Nup358 integrates nuclear envelope breakdown with kinetochore assembly. J Cell Biol *162*, 991-1001.

48. Loiodice, I., Alves, A., Rabut, G., Van Overbeek, M., Ellenberg, J., Sibarita, J.B., and Doye, V. (2004). The entire Nup107-160 complex, including three new members, is targeted as one entity to kinetochores in mitosis. Molecular biology of the cell *15*, 3333-3344.

49. Collas, P., and Poccia, D. (2000). Membrane fusion events during nuclear envelope assembly. Subcell Biochem *34*, 273-302.

50. Ellenberg, J., Siggia, E.D., Moreira, J.E., Smith, C.L., Presley, J.F., Worman, H.J., and Lippincott-Schwartz, J. (1997). Nuclear membrane dynamics and reassembly in living cells: targeting of an inner nuclear membrane protein in interphase and mitosis. J Cell Biol *138*, 1193-1206.

51. Lohka, M.J., and Masui, Y. (1983). Formation in vitro of sperm pronuclei and mitotic chromosomes induced by amphibian ooplasmic components. Science (New York, N.Y *220*, 719-721.

52. Newport, J. (1987). Nuclear reconstitution in vitro: stages of assembly around protein-free DNA. Cell *48*, 205-217.

53. Vigers, G.P., and Lohka, M.J. (1991). A distinct vesicle population targets membranes and pore complexes to the nuclear envelope in Xenopus eggs. J Cell Biol *112*, 545-556.

54. Vigers, G.P., and Lohka, M.J. (1992). Regulation of nuclear envelope precursor functions during cell division. Journal of cell science *102 (Pt 2)*, 273-284.

55. Collas, P., and Poccia, D. (1996). Distinct egg membrane vesicles differing in binding and fusion properties contribute to sea urchin male pronuclear envelopes formed in vitro. Journal of cell science *109 (Pt 6)*, 1275-1283.

56. Sheehan, M.A., Mills, A.D., Sleeman, A.M., Laskey, R.A., and Blow, J.J. (1988). Steps in the assembly of replication-competent nuclei in a cell-free system from Xenopus eggs. J Cell Biol *106*, 1-12.

57. Boman, A.L., Delannoy, M.R., and Wilson, K.L. (1992). GTP hydrolysis is required for vesicle fusion during nuclear envelope assembly in vitro. J Cell Biol *116*, 281-294.

58. Hetzer, M., Meyer, H.H., Walther, T.C., Bilbao-Cortes, D., Warren, G., and Mattaj, I.W. (2001). Distinct AAA-ATPase p97 complexes function in discrete steps of nuclear assembly. Nat Cell Biol *3*, 1086-1091.

59. Goldberg, M.W., and Allen, T.D. (1992). High resolution scanning electron microscopy of the nuclear envelope: demonstration of a new, regular, fibrous lattice attached to the baskets of the nucleoplasmic face of the nuclear pores. J Cell Biol *119*, 1429-1440.

60. Wiese, C., Goldberg, M.W., Allen, T.D., and Wilson, K.L. (1997). Nuclear envelope assembly in Xenopus extracts visualized by scanning EM reveals a transport-dependent 'envelope smoothing' event. Journal of cell science *110 (Pt 13)*, 1489-1502.

61. Yang, L., Guan, T., and Gerace, L. (1997). Integral membrane proteins of the nuclear envelope are dispersed throughout the endoplasmic reticulum during mitosis. J Cell Biol *137*, 1199-1210.

62. Anderson, D.J., and Hetzer, M.W. (2007). Nuclear Envelope Formation by Chromatin-mediated Reorganization of the Endoplasmic Reticulum. Nature Cell Biology *In Press*.

63. Ulbert, S., Platani, M., Boue, S., and Mattaj, I.W. (2006). Direct membrane protein-DNA interactions required early in nuclear envelope assembly. J Cell Biol *173*, 469-476.

64. Segura-Totten, M., Kowalski, A.K., Craigie, R., and Wilson, K.L. (2002). Barrier-to-autointegration factor: major roles in chromatin decondensation and nuclear assembly. J Cell Biol *158*, 475-485.

65. Pyrpasopoulou, A., Meier, J., Maison, C., Simos, G., and Georgatos, S.D. (1996). The lamin B receptor (LBR) provides essential chromatin docking sites at the nuclear envelope. The EMBO journal *15*, 7108-7119.

66. Collas, P., Courvalin, J.C., and Poccia, D. (1996). Targeting of membranes to sea urchin sperm chromatin is mediated by a lamin B receptor-like integral membrane protein. J Cell Biol *135*, 1715-1725.

67. Gorjanacz, M., Klerkx, E.P., Galy, V., Santarella, R., Lopez-Iglesias, C., Askjaer, P., and Mattaj, I.W. (2007). Caenorhabditis elegans BAF-1 and its kinase VRK-1 participate directly in post-mitotic nuclear envelope assembly. Embo J *26*, 132-143.

68. Bengtsson, L., and Wilson, K.L. (2004). Multiple and surprising new functions for emerin, a nuclear membrane protein. Current opinion in cell biology *16*, 73-79.

69. Hirano, Y., Segawa, M., Ouchi, F.S., Yamakawa, Y., Furukawa, K., Takeyasu, K., and Horigome, T. (2005). Dissociation of emerin from barrier-to-autointegration factor is regulated through mitotic phosphorylation of emerin in a xenopus egg cell-free system. J Biol Chem *280*, 39925-39933.

70. Dreier, L., and Rapoport, T.A. (2000). In vitro formation of the endoplasmic reticulum occurs independently of microtubules by a controlled fusion reaction. J Cell Biol *148*, 883-898.

71. Baur, T., Ramadan, K., Schlundt, A., Kartenbeck, J., and Meyer, H.H. (2007). NSF- and SNARE-mediated membrane fusion is required for nuclear envelope formation and completion of nuclear pore complex assembly in Xenopus laevis egg extracts. Journal of cell science *120*, 2895-2903.

72. Antonin, W., Franz, C., Haselmann, U., Antony, C., and Mattaj, I.W. (2005). The Integral Membrane Nucleoporin pom121 Functionally Links Nuclear Pore Complex Assembly and Nuclear Envelope Formation. Molecular cell *17*, 83-92.

73. Drin, G., Casella, J.F., Gautier, R., Boehmer, T., Schwartz, T.U., and Antonny, B. (2007). A general amphipathic alpha-helical motif for sensing membrane curvature. Nat Struct Mol Biol *14*, 138-146.

74. Rasala, B.A., Orjalo, A.V., Shen, Z., Briggs, S., and Forbes, D.J. (2006). ELYS is a dual nucleoporin/kinetochore protein required for nuclear pore assembly and proper cell division. Proc Natl Acad Sci U S A *103*, 17801-17806.

75. Franz, C., Walczak, R., Yavuz, S., Santarella, R., Gentzel, M., Askjaer, P., Galy, V., Hetzer, M., Mattaj, I.W., and Antonin, W. (2007). MEL-28/ELYS is required for the recruitment of nucleoporins to chromatin and postmitotic nuclear pore complex assembly. EMBO Rep *8*, 165-172.

76. Hawryluk-Gara, L.A., Platani, M., Santarella, R., Wozniak, R.W., and Mattaj, I.W. (2008). Nup53 is Required for Nuclear Envelope and Nuclear Pore Complex Assembly. Mol Biol Cell.

77. Franz, C., Askjaer, P., Antonin, W., Iglesias, C.L., Haselmann, U., Schelder, M., de Marco, A., Wilm, M., Antony, C., and Mattaj, I.W. (2005). Nup155 regulates nuclear envelope and nuclear pore complex formation in nematodes and vertebrates. The EMBO journal.

78. Gillespie, P.J., Khoudoli, G.A., Stewart, G., Swedlow, J.R., and Blow, J.J. (2007). ELYS/MEL-28 chromatin association coordinates nuclear pore complex assembly and replication licensing. Curr Biol *17*, 1657-1662.

79. Broers, J.L., Machiels, B.M., van Eys, G.J., Kuijpers, H.J., Manders, E.M., van Driel, R., and Ramaekers, F.C. (1999). Dynamics of the nuclear lamina as monitored by GFP-tagged A-type lamins. Journal of cell science *112 (Pt 20)*, 3463-3475.

80. Moir, R.D., Yoon, M., Khuon, S., and Goldman, R.D. (2000). Nuclear lamins A and B1: different pathways of assembly during nuclear envelope formation in living cells. J Cell Biol *151*, 1155-1168.

81. Sullivan, T., Escalante-Alcalde, D., Bhatt, H., Anver, M., Bhat, N., Nagashima, K., Stewart, C.L., and Burke, B. (1999). Loss of A-type lamin expression compromises nuclear envelope integrity leading to muscular dystrophy. J Cell Biol *147*, 913-920.

82. Liu, J., Ben-Shahar, T.R., Riemer, D., Treinin, M., Spann, P., Weber, K., Fire, A., and Gruenbaum, Y. (2000). Essential roles for Caenorhabditis elegans lamin gene in nuclear organization, cell cycle progression, and spatial organization of nuclear pore complexes. Molecular biology of the cell *11*, 3937-3947.

83. Steen, R.L., Beullens, M., Landsverk, H.B., Bollen, M., and Collas, P. (2003). AKAP149 is a novel PP1 specifier required to maintain nuclear envelope integrity in G1 phase. Journal of cell science *116*, 2237-2246.

84. Steen, R.L., and Collas, P. (2001). Mistargeting of B-type lamins at the end of mitosis: implications on cell survival and regulation of lamins A/C expression. J Cell Biol *153*, 621-626.

85. Chaudhary, N., and Courvalin, J.C. (1993). Stepwise reassembly of the nuclear envelope at the end of mitosis. J Cell Biol *122*, 295-306.

86. Daigle, N., Beaudouin, J., Hartnell, L., Imreh, G., Hallberg, E., Lippincott-Schwartz, J., and Ellenberg, J. (2001). Nuclear pore complexes form immobile networks and have a very low turnover in live mammalian cells. J Cell Biol *154*, 71-84.

87. Reddy, K.L., Zullo, J.M., Bertolino, E., and Singh, H. (2008). Transcriptional repression mediated by repositioning of genes to the nuclear lamina. Nature.

88. Maul, G.G., Maul, H.M., Scogna, J.E., Lieberman, M.W., Stein, G.S., Hsu, B.Y., and Borun, T.W. (1972). Time sequence of nuclear pore formation in phytohemagglutinin-stimulated lymphocytes and in HeLa cells during the cell cycle. J Cell Biol *55*, 433-447.

89. Hinshaw, J.E., and Milligan, R.A. (2003). Nuclear pore complexes exceeding eightfold rotational symmetry. J Struct Biol *141*, 259-268.

90. Ohba, T., Schirmer, E.C., Nishimoto, T., and Gerace, L. (2004). Energy- and temperature-dependent transport of integral proteins to the inner nuclear membrane via the nuclear pore. J Cell Biol *167*, 1051-1062.

91. King, M.C., Lusk, C.P., and Blobel, G. (2006). Karyopherin-mediated import of integral inner nuclear membrane proteins. Nature *442*, 1003-1007.

92. D'Angelo, M.A., and Hetzer, M.W. (2006). The role of the nuclear envelope in cellular organization. Cell Mol Life Sci *63*, 316-332.

93. Burke, B., and Ellenberg, J. (2002). Remodelling the walls of the nucleus. Nat Rev Mol Cell Biol *3*, 487-497.

94. Terasaki, M. (2000). Dynamics of the endoplasmic reticulum and golgi apparatus during early sea urchin development. Molecular biology of the cell *11*, 897-914.

95. Zaal, K.J., Smith, C.L., Polishchuk, R.S., Altan, N., Cole, N.B., Ellenberg, J., Hirschberg, K., Presley, J.F., Roberts, T.H., Siggia, E., et al. (1999). Golgi membranes are absorbed into and reemerge from the ER during mitosis. Cell *99*, 589-601.

96. Porter, K.R., and Machado, R.D. (1960). Studies on the endoplasmic reticulum. IV. Its form and distribution during mitosis in cells of onion root tip. J Biophys Biochem Cytol *7*, 167-180.

97. Lohka, M.J., and Masui, Y. (1983). The germinal vesicle material required for sperm pronuclear formation is located in the soluble fraction of egg cytoplasm. Exp Cell Res *148*, 481-491.

98. Gant, T.M., and Wilson, K.L. (1997). Nuclear assembly. Annual review of cell and developmental biology *13*, 669-695.

99. D'Angelo, M.A., Anderson, D.J., Richard, E., and Hetzer, M.W. (2006). Nuclear pores form de novo from both sides of the nuclear envelope. Science *312*, 440-443.

100. Hetzer, M., Bilbao-Cortes, D., Walther, T.C., Gruss, O.J., and Mattaj, I.W. (2000). GTP hydrolysis by Ran is required for nuclear envelope assembly. Molecular cell *5*, 1013-1024.

101. Shibata, Y., Voeltz, G.K., and Rapoport, T.A. (2006). Rough sheets and smooth tubules. Cell *126*, 435-439.

102. Voeltz, G.K., Prinz, W.A., Shibata, Y., Rist, J.M., and Rapoport, T.A. (2006). A class of membrane proteins shaping the tubular endoplasmic reticulum. Cell *124*, 573-586.

103. Forbes, D.J., Kirschner, M.W., and Newport, J.W. (1983). Spontaneous formation of nucleus-like structures around bacteriophage DNA microinjected into Xenopus eggs. Cell *34*, 13-23.

104. Onischenko, E.A., Gubanova, N.V., Kieselbach, T., Kiseleva, E.V., and Hallberg, E. (2004). Annulate lamellae play only a minor role in the storage of excess nucleoporins in Drosophila embryos. Traffic (Copenhagen, Denmark) *5*, 152-164.

105. Walther, T.C., Askjaer, P., Gentzel, M., Habermann, A., Griffiths, G., Wilm, M., Mattaj, I.W., and Hetzer, M. (2003). RanGTP mediates nuclear pore complex assembly. Nature *424*, 689-694.

106. Philpott, A., and Leno, G.H. (1992). Nucleoplasmin remodels sperm chromatin in Xenopus egg extracts. Cell *69*, 759-767.

107. Burke, B. (2001). The nuclear envelope: filling in gaps. Nat Cell Biol *3*, E273-274.

108. Heald, R., Tournebize, R., Blank, T., Sandaltzopoulos, R., Becker, P., Hyman, A., and Karsenti, E. (1996). Self-organization of microtubules into bipolar spindles around artificial chromosomes in Xenopus egg extracts. Nature *382*, 420-425.

109. Powell, K.S., and Latterich, M. (2000). The making and breaking of the endoplasmic reticulum. Traffic (Copenhagen, Denmark) *1*, 689-694.

110. Fagarasanu, A., Fagarasanu, M., and Rachubinski, R.A. (2007). Maintaining peroxisome populations: a story of division and inheritance. Annual review of cell and developmental biology *23*, 321-344.

111. Worman, H.J., and Gundersen, G.G. (2006). Here come the SUNs: a nucleocytoskeletal missing link. Trends in cell biology *16*, 67-69.

112. Stewart, C.L., Roux, K.J., and Burke, B. (2007). Blurring the boundary: the nuclear envelope extends its reach. Science (New York, N.Y *318*, 1408-1412.

113. Yang, Y.S., and Strittmatter, S.M. (2007). The reticulons: a family of proteins with diverse functions. Genome biology *8*, 234.

114. Shibata, Y., Voss, C., Rist, J.M., Hu, J., Rapoport, T.A., Prinz, W.A., and Voeltz, G.K. (2008). The reticulon and DP1/Yop1p proteins form immobile oligomers in the tubular endoplasmic reticulum. J Biol Chem.

115. Margalit, A., Vlcek, S., Gruenbaum, Y., and Foisner, R. (2005). Breaking and making of the nuclear envelope. Journal of cellular biochemistry *95*, 454-465.

116. Lenart, P., and Ellenberg, J. (2003). Nuclear envelope dynamics in oocytes: from germinal vesicle breakdown to mitosis. Current opinion in cell biology *15*, 88-95.

117. Puhka, M., Vihinen, H., Joensuu, M., and Jokitalo, E. (2007). Endoplasmic reticulum remains continuous and undergoes sheet-to-tubule transformation during cell division in mammalian cells. J Cell Biol *179*, 895-909.

118. Ellenberg, J., and Lippincott-Schwartz, J. (1999). Dynamics and mobility of nuclear envelope proteins in interphase and mitotic cells revealed by green fluorescent protein chimeras. Methods *19*, 362-372.

119. Anderson, D.J., and Hetzer, M.W. (2007). Nuclear envelope formation by chromatin-mediated reorganization of the endoplasmic reticulum. Nat Cell Biol *9*, 1160-1166.

120. Shaner, N.C., Campbell, R.E., Steinbach, P.A., Giepmans, B.N., Palmer, A.E., and Tsien, R.Y. (2004). Improved monomeric red, orange and yellow fluorescent proteins derived from Discosoma sp. red fluorescent protein. Nat Biotechnol *22*, 1567-1572.

121. Mora-Bermudez, F., Gerlich, D., and Ellenberg, J. (2007). Maximal chromosome compaction occurs by axial shortening in anaphase and depends on Aurora kinase. Nat Cell Biol *9*, 822-831.

122. Ribbeck, K., and Gorlich, D. (2001). Kinetic analysis of translocation through nuclear pore complexes. The EMBO journal *20*, 1320-1330.

123. Hu, J., Shibata, Y., Voss, C., Shemesh, T., Li, Z., Coughlin, M., Kozlov, M.M., Rapoport, T.A., and Prinz, W.A. (2008). Membrane proteins of the endoplasmic reticulum induce high-curvature tubules. Science (New York, N.Y *319*, 1247-1250.

124. Crisp, M., Liu, Q., Roux, K., Rattner, J.B., Shanahan, C., Burke, B., Stahl, P.D., and Hodzic, D. (2006). Coupling of the nucleus and cytoplasm: role of the LINC complex. J Cell Biol *172*, 41-53.

125. Maul, G.G. (1977). Nuclear pore complexes. Elimination and reconstruction during mitosis. J Cell Biol *74*, 492-500.

126. Mattaj, I.W. (2004). Sorting out the nuclear envelope from the endoplasmic reticulum. Nat Rev Mol Cell Biol *5*, 65-69.

127. Audhya, A., Desai, A., and Oegema, K. (2007). A role for Rab5 in structuring the endoplasmic reticulum. J Cell Biol *178*, 43-56.

128. Anderson, D.J., and Hetzer, M.W. (2008). The life cycle of the metazoan nuclear envelope. Current opinion in cell biology.

129. Olsen, J.V., Blagoev, B., Gnad, F., Macek, B., Kumar, C., Mortensen, P., and Mann, M. (2006). Global, in vivo, and site-specific phosphorylation dynamics in signaling networks. Cell *127*, 635-648.

130. Rabut, G., Doye, V., and Ellenberg, J. (2004). Mapping the dynamic organization of the nuclear pore complex inside single living cells. Nat Cell Biol *6*, 1114-1121.

131. Anderson, D.J., and Hetzer, M.W. (2008). Shaping the endoplasmic reticulum into the nuclear envelope. Journal of cell science *121*, 137-142.

132. Cai, M., Huang, Y., Ghirlando, R., Wilson, K.L., Craigie, R., and Clore, G.M. (2001). Solution structure of the constant region of nuclear envelope protein LAP2 reveals two LEM-domain structures: one binds BAF and the other binds DNA. The EMBO journal *20*, 4399-4407.

133. Gant, T.M., Harris, C.A., and Wilson, K.L. (1999). Roles of LAP2 proteins in nuclear assembly and DNA replication: truncated LAP2beta proteins alter lamina assembly, envelope formation, nuclear size, and DNA replication efficiency in Xenopus laevis extracts. J Cell Biol *144*, 1083-1096.

134. Haraguchi, T., Koujin, T., Hayakawa, T., Kaneda, T., Tsutsumi, C., Imamoto, N., Akazawa, C., Sukegawa, J., Yoneda, Y., and Hiraoka, Y. (2000). Live fluorescence imaging reveals early recruitment of emerin, LBR, RanBP2, and Nup153 to reforming functional nuclear envelopes. Journal of cell science *113 (Pt 5)*, 779-794.

135. Anderson, D.J., and Hetzer, M.W. (2008). Reshaping of the endoplasmic reticulum limits the rate for nuclear envelope formation. J Cell Biol *182*, 911-924.

136. Dultz, E., Zanin, E., Wurzenberger, C., Braun, M., Rabut, G., Sironi, L., and Ellenberg, J. (2008). Systematic kinetic analysis of mitotic dis- and reassembly of the nuclear pore in living cells. J Cell Biol *180*, 857-865.

137. Prufert, K., Winkler, C., Paulin-Levasseur, M., and Krohne, G. (2004). The lamina-associated polypeptide 2 (LAP2) genes of zebrafish and chicken: no LAP2alpha isoform is synthesised by non-mammalian vertebrates. European journal of cell biology *83*, 403-411.

138. Schild-Prufert, K., Giegerich, M., Schafer, M., Winkler, C., and Krohne, G. (2006). Structural and functional characterization of the zebrafish lamin B receptor. European journal of cell biology *85*, 813-824.

139. Lin, F., Blake, D.L., Callebaut, I., Skerjanc, I.S., Holmer, L., McBurney, M.W., Paulin-Levasseur, M., and Worman, H.J. (2000). MAN1, an inner nuclear membrane protein that shares the LEM domain with lamina-associated polypeptide 2 and emerin. J Biol Chem *275*, 4840-4847.

140. Ye, Q., and Worman, H.J. (1996). Interaction between an integral protein of the nuclear envelope inner membrane and human chromodomain proteins homologous to Drosophila HP1. J Biol Chem *271*, 14653-14656.

141. Furukawa, K., Fritze, C.E., and Gerace, L. (1998). The major nuclear envelope targeting domain of LAP2 coincides with its lamin binding region but is distinct from its chromatin interaction domain. J Biol Chem *273*, 4213-4219.

142. Mansfeld, J., Guttinger, S., Hawryluk-Gara, L.A., Pante, N., Mall, M., Galy, V., Haselmann, U., Muhlhausser, P., Wozniak, R.W., Mattaj, I.W., et al. (2006). The conserved transmembrane nucleoporin NDC1 is required for nuclear pore complex assembly in vertebrate cells. Molecular cell *22*, 93-103.

143. Ketema, M., Wilhelmsen, K., Kuikman, I., Janssen, H., Hodzic, D., and Sonnenberg, A. (2007). Requirements for the localization of nesprin-3 at the nuclear envelope and its interaction with plectin. Journal of cell science *120*, 3384-3394.

144. Snapp, E.L., Hegde, R.S., Francolini, M., Lombardo, F., Colombo, S., Pedrazzini, E., Borgese, N., and Lippincott-Schwartz, J. (2003). Formation of stacked ER cisternae by low affinity protein interactions. J Cell Biol *163*, 257-269.

145. Stick, R., Angres, B., Lehner, C.F., and Nigg, E.A. (1988). The fates of chicken nuclear lamin proteins during mitosis: evidence for a reversible redistribution of lamin B2 between inner nuclear membrane and elements of the endoplasmic reticulum. J Cell Biol *107*, 397-406.

146. Manilal, S., Nguyen, T.M., and Morris, G.E. (1998). Colocalization of emerin and lamins in interphase nuclei and changes during mitosis. Biochemical and biophysical research communications *249*, 643-647.

147. Somech, R., Gal-Yam, E.N., Shaklai, S., Geller, O., Amariglio, N., Rechavi, G., and Simon, A.J. (2007). Enhanced expression of the nuclear envelope LAP2 transcriptional repressors in normal and malignant activated lymphocytes. Annals of hematology *86*, 393-401.

148. Gorlich, D., and Kutay, U. (1999). Transport between the cell nucleus and the cytoplasm. Annual review of cell and developmental biology *15*, 607-660.

149. Maul, G.G., Deaven, L.L., Freed, J.J., Campbell, G.L., and Becak, W. (1980). Investigation of the determinants of nuclear pore number. Cytogenet Cell Genet *26*, 175-190.

150. Winey, M., Yarar, D., Giddings, T.H., Jr., and Mastronarde, D.N. (1997). Nuclear pore complex number and distribution throughout the Saccharomyces cerevisiae cell cycle by three-dimensional reconstruction from electron micrographs of nuclear envelopes. Molecular biology of the cell *8*, 2119-2132.

151. Bodoor, K., Shaikh, S., Enarson, P., Chowdhury, S., Salina, D., Raharjo, W.H., and Burke, B. (1999). Function and assembly of nuclear pore complex proteins. Biochem Cell Biol *77*, 321-329.

152. Rabut, G., Lenart, P., and Ellenberg, J. (2004). Dynamics of nuclear pore complex organization through the cell cycle. Current opinion in cell biology *16*, 314-321.

153. Davis, L.I., and Blobel, G. (1987). Nuclear pore complex contains a family of glycoproteins that includes p62: glycosylation through a previously unidentified cellular pathway. Proc Natl Acad Sci U S A *84*, 7552-7556.

154. Dasso, M. (2002). The Ran GTPase: theme and variations. Curr Biol *12*, R502-508.

155. Klebe, C., Prinz, H., Wittinghofer, A., and Goody, R.S. (1995). The kinetic mechanism of Ran--nucleotide exchange catalyzed by RCC1. Biochemistry *34*, 12543-12552.

156. Finlay, D.R., Meier, E., Bradley, P., Horecka, J., and Forbes, D.J. (1991). A complex of nuclear pore proteins required for pore function. J Cell Biol *114*, 169-183.

157. Harel, A., Chan, R.C., Lachish-Zalait, A., Zimmerman, E., Elbaum, M., and Forbes, D.J. (2003). Importin beta negatively regulates nuclear membrane fusion and nuclear pore complex assembly. Molecular biology of the cell *14*, 4387-4396.

158. Bischoff, F.R., Klebe, C., Kretschmer, J., Wittinghofer, A., and Ponstingl, H. (1994). RanGAP1 induces GTPase activity of nuclear Ras-related Ran. Proc Natl Acad Sci U S A *91*, 2587-2591.

159. Klebe, C., Bischoff, F.R., Ponstingl, H., and Wittinghofer, A. (1995). Interaction of the nuclear GTP-binding protein Ran with its regulatory proteins RCC1 and RanGAP1. Biochemistry *34*, 639-647.

160. Gorlich, D. (1997). Nuclear protein import. Current opinion in cell biology *9*, 412-419.

161. Harel, A., Orjalo, A.V., Vincent, T., Lachish-Zalait, A., Vasu, S., Shah, S., Zimmerman, E., Elbaum, M., and Forbes, D.J. (2003). Removal of a single pore subcomplex results in vertebrate nuclei devoid of nuclear pores. Molecular cell *11*, 853-864.

162. Walther, T.C., Alves, A., Pickersgill, H., Loiodice, I., Hetzer, M., Galy, V., Hulsmann, B.B., Kocher, T., Wilm, M., Allen, T., et al. (2003). The conserved Nup107-160 complex is critical for nuclear pore complex assembly. Cell *113*, 195-206.

163. Macaulay, C., and Forbes, D.J. (1996). Assembly of the nuclear pore: biochemically distinct steps revealed with NEM, GTP gamma S, and BAPTA. J Cell Biol *132*, 5-20.

164. Antonin, W., and Mattaj, I.W. (2005). Nuclear pore complexes: Round the bend? Nat Cell Biol *7*, 10-12.

165. Martins, S., Eikvar, S., Furukawa, K., and Collas, P. (2003). HA95 and LAP2 beta mediate a novel chromatin-nuclear envelope interaction implicated in initiation of DNA replication. J Cell Biol *160*, 177-188.

166. Favreau, C., Bastos, R., Cartaud, J., Courvalin, J.C., and Mustonen, P. (2001). Biochemical characterization of nuclear pore complex protein gp210 oligomers. Eur J Biochem *268*, 3883-3889.

167. Olsson, M., Scheele, S., and Ekblom, P. (2004). Limited expression of nuclear pore membrane glycoprotein 210 in cell lines and tissues suggests cell-type specific nuclear pores in metazoans. Exp Cell Res *292*, 359-370.

168. Antonin, W., Ellenberg, J., and Dultz, E. (2008). Nuclear pore complex assembly through the cell cycle: regulation and membrane organization. FEBS letters *582*, 2004-2016.